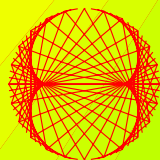


2010, VOLUME 2

# PROGRESS IN PHYSICS

**“All scientists shall have the right to present their scientific research results, in whole or in part, at relevant scientific conferences, and to publish the same in printed scientific journals, electronic archives, and any other media.” — Declaration of Academic Freedom, Article 8**



ISSN 1555-5534

# PROGRESS IN PHYSICS

A quarterly issue scientific journal, registered with the Library of Congress (DC, USA). This journal is peer reviewed and included in the abstracting and indexing coverage of: Mathematical Reviews and MathSciNet (AMS, USA), DOAJ of Lund University (Sweden), Zentralblatt MATH (Germany), Scientific Commons of the University of St. Gallen (Switzerland), Open-J-Gate (India), Referativnyi Zhurnal VINITI (Russia), etc.

---

To order printed issues of this journal, contact the Editors. Electronic version of this journal can be downloaded free of charge:  
<http://www.ptep-online.com>

## Editorial Board

Dmitri Rabounski, Editor-in-Chief  
rabounski@ptep-online.com  
Florentin Smarandache, Assoc. Editor  
smarand@unm.edu  
Larissa Borissova, Assoc. Editor  
borissova@ptep-online.com

## Postal address

Department of Mathematics and Science,  
University of New Mexico,  
200 College Road,  
Gallup, NM 87301, USA

## Copyright © *Progress in Physics*, 2010

All rights reserved. The authors of the articles do hereby grant *Progress in Physics* non-exclusive, worldwide, royalty-free license to publish and distribute the articles in accordance with the Budapest Open Initiative: this means that electronic copying, distribution and printing of both full-size version of the journal and the individual papers published therein for non-commercial, academic or individual use can be made by any user without permission or charge. The authors of the articles published in *Progress in Physics* retain their rights to use this journal as a whole or any part of it in any other publications and in any way they see fit. Any part of *Progress in Physics* howsoever used in other publications must include an appropriate citation of this journal.

This journal is powered by  $\text{\LaTeX}$

A variety of books can be downloaded free from the Digital Library of Science:  
<http://www.gallup.unm.edu/~smarandache>

ISSN: 1555-5534 (print)  
ISSN: 1555-5615 (online)

Standard Address Number: 297-5092  
Printed in the United States of America

APRIL 2010

VOLUME 2

## CONTENTS

<b>Minasyan V. and Samoilo V.</b> Two New Type Surface Polaritons Excited into Nanoholes in Metal Films .....	3
<b>Seshavatharam U. V. S.</b> Physics of Rotating and Expanding Black Hole Universe .....	7
<b>Daywitt W. C.</b> The Radiation Reaction of a Point Electron as a Planck Vacuum Response Phenomenon .....	15
<b>Daywitt W. C.</b> A Massless-Point-Charge Model for the Electron .....	17
<b>Stone R. A. Jr.</b> Quark Confinement and Force Unification .....	19
<b>Christianto V. and Smarandache F.</b> A Derivation of Maxwell Equations in Quaternion Space .....	23
<b>Smarandache F. and Christianto V.</b> On Some Novel Ideas in Hadron Physics. Part II ..	28
<b>Cahill R. T.</b> Lunar Laser-Ranging Detection of Light-Speed Anisotropy and Gravitational Waves .....	31
<b>Zhang T. X.</b> Fundamental Elements and Interactions of Nature: A Classical Unification Theory .....	36
<b>Borisova L. B.</b> A Condensed Matter Model of the Sun: The Sun's Space Breaking Meets the Asteroid Strip .....	43
<b>Marquet P.</b> The Matter-Antimatter Concept Revisited .....	48
<b>Harney M. and Haranas I. I.</b> A Derivation of $\pi(n)$ Based on a Stability Analysis of the Riemann-Zeta Function .....	55
<b>Comay E.</b> On the Significance of the Upcoming Large Hadron Collider Proton-Proton Cross Section Data .....	56
<b>Minasyan V. and Samoilo V.</b> The Intensity of the Light Diffraction by Supersonic Longitudinal Waves in Solid .....	60
<b>Quznetsov G.</b> Oscillations of the Chromatic States and Accelerated Expansion of the Universe .....	64

## LETTERS

<b>Rabounski D.</b> Smarandache Spaces as a New Extension of the Basic Space-Time of General Relativity .....	L1
---	----

---

## Information for Authors and Subscribers

*Progress in Physics* has been created for publications on advanced studies in theoretical and experimental physics, including related themes from mathematics and astronomy. All submitted papers should be professional, in good English, containing a brief review of a problem and obtained results.

All submissions should be designed in  $\text{\LaTeX}$  format using *Progress in Physics* template. This template can be downloaded from *Progress in Physics* home page <http://www.ptep-online.com>. Abstract and the necessary information about author(s) should be included into the papers. To submit a paper, mail the file(s) to the Editor-in-Chief.

All submitted papers should be as brief as possible. We accept brief papers, no larger than 8 typeset journal pages. Short articles are preferable. Large papers can be considered in exceptional cases to the section *Special Reports* intended for such publications in the journal. Letters related to the publications in the journal or to the events among the science community can be applied to the section *Letters to Progress in Physics*.

All that has been accepted for the online issue of *Progress in Physics* is printed in the paper version of the journal. To order printed issues, contact the Editors.

This journal is non-commercial, academic edition. It is printed from private donations. (Look for the current author fee in the online version of the journal.)

---

# Two New Type Surface Polaritons Excited into Nanoholes in Metal Films

Vahan Minasyan and Valentin Samoïlov

Scientific Center of Applied Research, JINR, Dubna, 141980, Russia

E-mails: mvahan@scar.jinr.ru; scar@off-serv.jinr.ru

We argue that the smooth metal-air interface should be regarded as a distinct dielectric medium, the skin of the metal. Here we present quantized Maxwell's equations for electromagnetic field in an isotropic homogeneous medium, allowing us to solve the absorption anomaly property of these metal films. The results imply the existence of light quasi-particles with spin one and effective mass  $m = 2.5 \times 10^{-5} m_e$  which in turn provide the presence of two type surface polaritons into nanoholes in metal films.

## 1 Introduction

There have been many studies of optical light transmission through individual nanometer-sized holes in opaque metal films in recent years [1–3]. These experiments showed highly unusual transmission properties of metal films perforated with a periodic array of subwavelength holes, because the electric field is highly localized inside the grooves (around 300-1000 times larger than intensity of incoming optical light). Here we analyze the absorption anomalies for light in the visible to near-infrared range observed into nanoholes in metal films. These absorption anomalies for optical light as seen as enhanced transmission of optical light in metal films, and attributed to surface plasmons (collective electron density waves propagating along the surface of the metal films) excited by light incident on the hole array [4]. The enhanced transmission of optical light is then associated with surface plasmon (SP) polaritons. Clearly, the definition of surface metal-air region is very important factor, since this is where the surface plasmons are excited. In contrast to this surface plasmon theory, in which the central role is played by collective electron density waves propagating along the surface of metal films in a free electron gas model, the authors of paper [5] propose that the surface metal-air medium should be regarded as a metal skin and that the ideas of the Richardson-Dushman effect of thermionic emission are crucial [6]. Some of the negatively charged electrons are thermally excited from the metal, and these evaporated electrons are attracted by positively charged lattice of metal to form a layer at the metal-air interface. However, it is easy to show that the thermal Richardson-Dushman effect is insufficient at room temperature  $T \simeq 300K$  because the exponent  $\exp^{-\frac{\phi}{kT}}$  with a value of the work function  $\phi \simeq 1 \text{ eV} - 10 \text{ eV}$  leads to negligible numbers of such electrons.

In this letter, we shall regard the metal skin as a distinct dielectric medium consisting of neutral molecules at the metal surface. Each molecule is considered as a system consisting of an electron coupled to an ion, creating of dipole. The electron and ion are linked by a spring which in turn defines the frequency  $\omega_0$  of electron oscillation in the dipole. Obviously, such dipoles are discussed within elementary dispersion theory [7]. Further, we shall examine the quantiza-

tion scheme for local electromagnetic field in the vacuum, as first presented by Planck for in his black body radiation studies. In this context, the classic Maxwell equations lead to appearance of the so-called ultraviolet catastrophe; to remove this problem, Planck proposed modelled the electromagnetic field as an ideal Bose gas of massless photons with spin one. However, Dirac [8] showed the Planck photon-gas could be obtained through a quantization scheme for the local electromagnetic field, presenting a theoretical description of the quantization of the local electromagnetic field in vacuum by use of a model Bose-gas of local plane electromagnetic waves, propagated by speed  $c$  in vacuum. An investigation of quantization scheme for the local electromagnetic field [9] predicted the existence of light quasi-particles with spin one and finite effective mass  $m = 2.5 \times 10^{-5} m_e$  (where  $m_e$  is the mass of electron) by introducing quantized Maxwell equations. In this letter, we present properties of photons which are excited in clearly dielectric medium, and we show existence of two new type surface polaritons into nanoholes in metal films.

## 2 Quantized Maxwell equations

We now investigate Maxwells equations for dielectric medium [7] by quantum theory field [8]

$$\text{curl } \vec{H} - \frac{1}{c} \frac{d\vec{D}}{dt} = 0, \quad (1)$$

$$\text{curl } \vec{E} + \frac{1}{c} \frac{d\vec{B}}{dt} = 0, \quad (2)$$

$$\text{div } \vec{D} = 0, \quad (3)$$

$$\text{div } \vec{B} = 0, \quad (4)$$

where  $\vec{B} = \vec{B}(\vec{r}, t)$  and  $\vec{D} = \vec{D}(\vec{r}, t)$  are, respectively, the local magnetic and electric induction depending on space coordinate  $\vec{r}$  and time  $t$ ;  $\vec{H} = \vec{H}(\vec{r}, t)$  and  $\vec{E} = \vec{E}(\vec{r}, t)$  are, respectively, the magnetic and electric field vectors, and  $c$  is the velocity of light in vacuum. The further equations are

$$\vec{D} = \epsilon \vec{E}, \quad (5)$$

$$\vec{B} = \mu \vec{H}, \quad (6)$$

where  $\varepsilon > 1$  and  $\mu = 1$  are, respectively, the dielectric and the magnetic susceptibilities of the dielectric medium.

The Hamiltonian of the radiation field  $\hat{H}_R$  is

$$\hat{H}_R = \frac{1}{8\pi} \int (\varepsilon E^2 + \mu H^2) dV. \quad (7)$$

We now wish to solve a problem connected with a quantized electromagnetic field, and begin from the quantized equations of Maxwell. We search for a solution of (1)–(6), in an analogous manner to that presented in [9]

$$\vec{E} = -\frac{\alpha}{c} \frac{d\vec{H}_0}{dt} + \beta \vec{E}_0 \quad (8)$$

and

$$\vec{H} = \alpha \text{curl} \vec{H}_0 + \beta \vec{H}_0, \quad (9)$$

where  $\alpha = \frac{\hbar\sqrt{2\pi}}{\sqrt{m}}$  and  $\beta = c\sqrt{2m\pi}$  are the constants obtained in [9]. Thus  $\vec{E}_0 = \vec{E}_0(\vec{r}, t)$  and  $\vec{H}_0 = \vec{H}_0(\vec{r}, t)$  are, respectively, vectors of electric and magnetic field for one Bose-light-particle of electromagnetic field with spin one and finite effective mass  $m$ . The vectors of local electric  $\vec{E}_0$  and magnetic  $\vec{H}_0$  fields, presented by equations (8) and (9), satisfy to equations of Maxwell in dielectric medium

$$\text{curl} \vec{H}_0 - \frac{\varepsilon}{c} \frac{d\vec{E}_0}{dt} = 0, \quad (10)$$

$$\text{curl} \vec{E}_0 + \frac{1}{c} \frac{d\vec{H}_0}{dt} = 0, \quad (11)$$

$$\text{div} \vec{E}_0 = 0, \quad (12)$$

$$\text{div} \vec{H}_0 = 0. \quad (13)$$

By using of (10), we can rewrite (9) as

$$\vec{H} = \frac{\alpha\varepsilon}{c} \frac{d\vec{E}_0}{dt} + \beta \vec{H}_0. \quad (14)$$

The equations (10)–(13) lead to a following wave-equations:

$$\nabla^2 \vec{E}_0 - \frac{\varepsilon}{c^2} \frac{d^2 \vec{E}_0}{dt^2} = 0 \quad (15)$$

and

$$\nabla^2 \vec{H}_0 - \frac{\varepsilon}{c^2} \frac{d^2 \vec{H}_0}{dt^2} = 0 \quad (16)$$

which in turn have the following solutions

$$\vec{E}_0 = \frac{1}{V} \sum_{\vec{k}} \left( \vec{E}_{\vec{k}}^+ e^{i(\vec{k}\vec{r} + \frac{kc t}{\sqrt{\varepsilon}})} + \vec{E}_{\vec{k}}^- e^{-i(\vec{k}\vec{r} + \frac{kc t}{\sqrt{\varepsilon}})} \right), \quad (17)$$

$$\vec{H}_0 = \frac{1}{V} \sum_{\vec{k}} \left( \vec{H}_{\vec{k}}^+ e^{i(\vec{k}\vec{r} + \frac{kc t}{\sqrt{\varepsilon}})} + \vec{H}_{\vec{k}}^- e^{-i(\vec{k}\vec{r} + \frac{kc t}{\sqrt{\varepsilon}})} \right), \quad (18)$$

where  $\vec{E}_{\vec{k}}^+$ ,  $\vec{H}_{\vec{k}}^+$  and  $\vec{E}_{\vec{k}}^-$ ,  $\vec{H}_{\vec{k}}^-$  are, respectively, the second quantization vector wave functions, essentially the vector Bose

“creation” and “annihilation” operators for the Bose quasi-particles of electric and magnetic waves with spin one in dielectric medium. With these new terms  $\vec{E}_0$  and  $\vec{H}_0$ , the radiation Hamiltonian  $\hat{H}_R$  in (7) takes the form

$$\begin{aligned} \hat{H}_R &= \frac{1}{8\pi} \int (\varepsilon E^2 + H^2) dV = \\ &= \frac{1}{8\pi} \int \left[ \varepsilon \left( -\frac{\alpha}{c} \frac{d\vec{H}_0}{dt} + \beta \vec{E}_0 \right)^2 + \right. \\ &\quad \left. + \left( \frac{\alpha\varepsilon}{c} \frac{d\vec{E}_0}{dt} + \beta \vec{H}_0 \right)^2 \right] dV, \end{aligned} \quad (19)$$

where, by substituting into (17) and (18), leads to the reduced form of  $\hat{H}_R$

$$\hat{H}_R = \hat{H}_e + \hat{H}_h, \quad (20)$$

where the operators  $\hat{H}_e$  and  $\hat{H}_h$  are

$$\begin{aligned} \hat{H}_e &= \sum_{\vec{k}} \left( \frac{\hbar^2 k^2 \varepsilon^2}{2m} + \frac{mc^2 \varepsilon}{2} \right) \vec{E}_{\vec{k}}^+ \vec{E}_{\vec{k}}^- - \\ &- \frac{1}{2} \sum_{\vec{k}} \left( \frac{\hbar^2 k^2 \varepsilon^2}{2m} - \frac{mc^2 \varepsilon}{2} \right) \left( \vec{E}_{\vec{k}}^+ \vec{E}_{-\vec{k}}^+ + \vec{E}_{-\vec{k}}^- \vec{E}_{\vec{k}}^- \right) \end{aligned} \quad (21)$$

and

$$\begin{aligned} \hat{H}_h &= \sum_{\vec{k}} \left( \frac{\hbar^2 k^2 \varepsilon}{2m} + \frac{mc^2}{2} \right) \vec{H}_{\vec{k}}^+ \vec{H}_{\vec{k}}^- - \\ &- \frac{1}{2} \sum_{\vec{k}} \left( \frac{\hbar^2 k^2 \varepsilon}{2m} - \frac{mc^2}{2} \right) \left( \vec{H}_{\vec{k}}^+ \vec{H}_{-\vec{k}}^+ + \vec{H}_{-\vec{k}}^- \vec{H}_{\vec{k}}^- \right). \end{aligned} \quad (22)$$

In the letter [9], the boundary wave number  $k_0 = \frac{mc}{\hbar}$  for electromagnetic field in vacuum was appeared by suggestion that the light quasi-particles interact with each other by repulsive potential  $U_{\vec{k}}$  in momentum space

$$U_{\vec{k}} = -\frac{\hbar^2 k^2}{2m} + \frac{mc^2}{2} \geq 0.$$

As result, condition for wave numbers of light quasi-particles  $k \leq k_0$  is appeared.

On other hand, due to changing energetic level into Hydrogen atom, the appearance of photon with energy  $\hbar kc$  is determined by a distance between energetic states for electron going from high level to low one. The ionization energy of the Hydrogen atom  $E_I = \frac{m_e e^4}{2\hbar^2}$  is the maximal one for destruction atom. Therefore, one coincides with energy of free light quasi-particle  $\frac{\hbar^2 k_0^2}{2m}$  which is maximal too because  $k \leq k_0$ . The later represents as radiated photon with energy  $\hbar k_0 c$  in vacuum. This reasoning claims the important condition as  $\frac{m_e e^4}{2\hbar^2} = \hbar k_0 c$  which in turn determines a effective mass of the light quasi-particles  $m = \frac{m_e e^4}{2\hbar^2 c^2} = 2.4 \times 10^{-35}$  kg in vacuum.

In analogy manner, we may find the boundary wave number  $k_\varepsilon = \frac{mc}{\hbar\varepsilon}$  for light quasi-particles of electromagnetic field

in isotropic homogenous medium by suggestion that light quasi-particles in medium interact with each other by repulsive potentials  $U_{E,\vec{k}}$  in (21) and  $U_{H,\vec{k}}$  in (22) which correspond, respectively, to electric and magnetic fields in momentum space

$$U_{E,\vec{k}} = -\frac{\hbar^2 k^2 \varepsilon^2}{2m} + \frac{mc^2 \varepsilon}{2} \geq 0$$

and

$$U_{H,\vec{k}} = -\frac{\hbar^2 k^2 \varepsilon}{2m} + \frac{mc^2}{2} \geq 0.$$

Obviously, the both expressions in above determine wave numbers of light quasi-particles  $k$  satisfying to condition  $k \leq k_\varepsilon$ .

We now apply a new linear transformation of the vector Bose-operators which is a similar to the Bogoliubov transformation [10] for scalar Bose operator, so as to evaluate the energy levels of the operator  $\hat{H}_R$  within diagonal form

$$\vec{E}_{\vec{k}} = \frac{\vec{e}_{\vec{k}} + M_{\vec{k}} \vec{e}_{-\vec{k}}^+}{\sqrt{1 - M_{\vec{k}}^2}} \quad (23)$$

and

$$\vec{H}_{\vec{k}} = \frac{\vec{h}_{\vec{k}} + L_{\vec{k}} \vec{h}_{-\vec{k}}^+}{\sqrt{1 - L_{\vec{k}}^2}}, \quad (24)$$

where  $M_{\vec{k}}$  and  $L_{\vec{k}}$  are the real symmetrical functions of a wave vector  $\vec{k}$ .

The operator Hamiltonian  $\hat{H}_R$  within using of a canonical transformation takes a following form

$$\hat{H}_R = \sum_{\vec{k} \leq k_\varepsilon} \chi_{\vec{k}} \vec{e}_{\vec{k}}^+ \vec{e}_{\vec{k}} + \sum_{\vec{k} \leq k_\varepsilon} \eta_{\vec{k}} \vec{h}_{\vec{k}}^+ \vec{h}_{\vec{k}} \quad (25)$$

Hence, we infer that the Bose-operators  $\vec{e}_{\vec{k}}^+$ ,  $\vec{e}_{\vec{k}}$  and  $\vec{h}_{\vec{k}}^+$ ,  $\vec{h}_{\vec{k}}$  are, respectively, the vector creation and annihilation operators of two types of free photons with energies

$$\begin{aligned} \chi_{\vec{k}} &= \sqrt{\left(\frac{\hbar^2 k^2 \varepsilon^2}{2m} + \frac{mc^2 \varepsilon}{2}\right)^2 - \left(\frac{\hbar^2 k^2 \varepsilon^2}{2m} - \frac{mc^2 \varepsilon}{2}\right)^2} = \\ &= \hbar k v_e \end{aligned} \quad (26)$$

and

$$\begin{aligned} \eta_{\vec{k}} &= \sqrt{\left(\frac{\hbar^2 k^2 \varepsilon}{2m} + \frac{mc^2}{2}\right)^2 - \left(\frac{\hbar^2 k^2 \varepsilon}{2m} - \frac{mc^2}{2}\right)^2} = \\ &= \hbar k v_h. \end{aligned} \quad (27)$$

where  $v_e = c\varepsilon^{\frac{3}{2}}$  and  $v_h = c\varepsilon^{\frac{1}{2}}$  are, respectively, velocities of photons excited by the electric and the magnetic field. Thus, we predict the existence of two types photons excited in dielectric medium, with energies  $\chi_{\vec{k}} = \hbar k c \varepsilon^{\frac{3}{2}}$  and  $\eta_{\vec{k}} = \hbar k c \varepsilon^{\frac{1}{2}}$  that depend on the dielectric response of the homogeneous medium  $\varepsilon$ . The velocities of the two new type photon modes  $v_e = c\varepsilon^{\frac{3}{2}}$  and  $v_h = c\varepsilon^{\frac{1}{2}}$  are more than velocity  $c$  of photon in

vacuum because  $\varepsilon > 1$ . Obviously, the phase velocity of light is given by  $v_p = \frac{c}{\sqrt{\varepsilon}}$ , contradicting the results obtained for  $v_e = c\varepsilon^{\frac{3}{2}}$  and  $v_h = c\varepsilon^{\frac{1}{2}}$ . This is the source of the absorption anomalies in isotropic homogeneous media.

### 3 Skin of metal on the boundary metal-air

A standard model of metal regards it as a gas of free electrons with negative charge  $-e$  in a box of volume  $V$ , together with a background of lattice ions of opposite charge  $e$  to preserve charge neutrality. For the boundary of this metal with the vacuum, we introduce the concept of a metal skin comprising free neutral molecules at the metal surface. The skin then has a thickness similar to the size of the molecule, a small number of Bohr diameter  $a = \frac{2\hbar^2}{m_e^2} = 1 \text{ \AA}$ . We assume  $N_0$  molecules per unit area is  $N_0 = \frac{3}{4\pi r^3}$  (where  $r = \frac{a}{2}$  is the Bohr radius) which in turn determines the dielectric constant of metal's skin  $\varepsilon$  under an electromagnetic field in the visible to near-infrared range with frequency  $\omega \leq \omega_0$ , by the well known formulae

$$\varepsilon = 1 + \frac{4\pi N_0 e^2}{m_e (\omega_0^2 - \omega^2)}. \quad (28)$$

As we show in below, namely, the anomalies property of light is observed near resonance frequency  $\omega_0$ .

### 4 Two new type surface polaritons excited in metal films

We now show that presented theory explains the absorption anomalies such as enhanced transmission of optical light in metal films. We consider the subwavelength sized holes into metal films as cylindrical resonator with partly filled homogeneous medium [11]. The hole contains vacuum which has boundary with metals skin with width  $a = 10^{-4} \mu\text{m}$  but the grooves radius is  $d = 0.75 \mu\text{m}$  as experimental data [2]. The standing electromagnetic wave is excited by incoming light with frequency  $\omega$  related to the frequency of cylindrical resonator  $\omega$  by following system of dispersion equations

$$\left. \begin{aligned} \frac{J_1\left(\frac{\omega d}{c}\right)}{J_0\left(\frac{\omega d}{c}\right)} &= \frac{J_1\left(\frac{\omega \sqrt{\varepsilon} d}{c}\right)}{J_0\left(\frac{\omega \sqrt{\varepsilon} d}{c}\right)} \\ J_0\left(\frac{\omega \sqrt{\varepsilon} (d+a)}{c}\right) &= 0 \end{aligned} \right\}, \quad (29)$$

where  $J_0(z)$  and  $J_1(z)$ , are, respectively, the Bessel functions of zero and one orders.

There is observed a shape resonance in lamellar metallic gratings when frequency  $\omega$  of optical light in the visible to near-infrared range coincides with resonance frequency of dipole  $\omega_0$  in metal's skin because the dielectric response is given by

$$\lim_{\omega \rightarrow \omega_0} \varepsilon \rightarrow \infty.$$

Therefore, the energies of two types of surface polaritons tend to infinity. This result confirms that the electric

field is highly localized inside the grooves because the energy of electric field inside the grooves is 300–1000 times higher than energy incoming optical light in air  $\chi_{\vec{k}} = \eta_{\vec{k}} = \hbar kc$  as  $\varepsilon = 1$  in air. Thus, we have shown the existence of two new type surface polaritons with energies  $\chi_{\vec{k}}$  and  $\eta_{\vec{k}}$  which are excited into nanoholes.

The resonance frequency of dipole  $\omega_0$  in metal's skin is defined from (29), at condition  $\varepsilon \rightarrow \infty$  in the metal skin, which is fulfilled at  $\omega = \omega_0$ . In turn, this leads to following equation:

$$J_1\left(\frac{\omega_0 d}{c}\right) = 0, \quad (30)$$

because second equation in (29) is fulfilled automatically at condition  $\varepsilon \rightarrow \infty$ .

The equation (30) has a root  $\omega_0 = \frac{3.8c}{d}$  which in turn determines the resonance wavelength  $\lambda_0 = \frac{2\pi c}{\omega_0} = 1.24 \mu\text{m}$ . This theoretical result is confirmed by experiment [2], where the zero-order transmission spectra were obtained with a Cary-5 spectrophotometer using of incoherent light sources with a wavelength range  $0.2 \leq \lambda \leq 3.3 \mu\text{m}$ . Thus, the geometry of hole determines the transmission property of light into nanoholes.

In conclusion, we may say that the theory presented above confirms experimental results on metal films, and in turn solves the problem connected with the absorption anomalies in isotropic homogeneous media.

### Acknowledgements

We are particularly grateful to Professor Marshall Stoneham F.R.S. (London Centre for Nanotechnology, and Department of Physics and Astronomy, University College of London, Gower Street, London WC1E 6BT, UK) for valuable scientific support and corrected English.

Submitted on November 11, 2009 / Accepted on November 30, 2009

### References

1. Lopez-Rios T., Mendoza D., Garcia-Vidal F.J., Sanchez-Dehesa J., Panter B. Surface shape resonances in lamellar metallic gratings. *Physical Review Letters*, 1998, v. 81 (3), 665–668.
2. Ghaemi H.F., Grupp D. E., Ebbesen T.W., Lezes H.J. Surface plasmons enhance optical transmission through subwavelength holes. *Physical Review B*, 1998, v. 58 (11), 6779–6782.
3. Sonnichen C., Duch A.C., Steininger G., Koch M., Feldman J. Launching surface plasmons into nanoholes in metal films. *Applied Physics Letters*, 2000, v. 76 (2), 140–142.
4. Raether H. Surface plasmons. Springer-Verlag, Berlin, 1988.
5. Minasyan V.N. et al. New charged spinless bosons at interface between vacuum and a gas of electrons with low density, Preprint E17-2002-96 of JINR, Dubna, Russia, 2002.
6. Modinos A. Field, thermionic and secondary electron emission spectroscopy. Plenum Press, New York and London 1984.
7. Born M. and Wolf E. Principles of optics. Pergamon press, Oxford, 1980.
8. Dirac P.A.M. The principles of Quantum Mechanics. Clarendon press, Oxford, 1958.
9. Minasyan V.N. Light bosons of electromagnetic field and breakdown of relativistic theory. arXiv: 0808.0567.
10. Bogoliubov N.N. On the theory of superfluidity. *Journal of Physics (USSR)*, 1947, v. 11, 23.
11. Minasyan V.N. et al. Calculation of modulator with partly filled by electro-optic crystal. *Journal of Opto-Mechanics Industry (USSR)*, 1988, v. 1, 6.

# Physics of Rotating and Expanding Black Hole Universe

U. V. S. Seshavatharam

Honorary Faculty, Institute of Scientific Research on Vedas (I-SERVE), Hyderabad-35, India  
Email: seshavatharam.uvs@gmail.com

Throughout its journey universe follows strong gravity. By unifying general theory of relativity and quantum mechanics a simple derivation is given for rotating black hole's temperature. It is shown that when the rotation speed approaches light speed temperature approaches Hawking's black hole temperature. Applying this idea to the cosmic black hole it is noticed that there is "no cosmic temperature" if there is "no cosmic rotation". Starting from the Planck scale it is assumed that universe is a rotating and expanding black hole. Another key assumption is that at any time cosmic black hole rotates with light speed. For this cosmic sphere as a whole while in light speed rotation "rate of decrease" in temperature or "rate of increase" in cosmic red shift is a measure of "rate of cosmic expansion". Since 1992, measured CMBR data indicates that, present CMB is same in all directions equal to 2.726 °K, smooth to 1 part in 100,000 and there is no continuous decrease! This directly indicates that, at present rate of decrease in temperature is practically zero and rate of expansion is practically zero. Universe is isotropic and hence static and is rotating as a rigid sphere with light speed. At present galaxies are revolving with speeds proportional to their distances from the cosmic axis of rotation. If present CMBR temperature is 2.726 °K, present value of obtained angular velocity is  $2.17 \times 10^{-18} \frac{\text{rad}}{\text{sec}} \cong 67 \frac{\text{Km}}{\text{sec} \times \text{Mpc}}$ . Present cosmic mass density and cosmic time are fitted with a  $\ln$  (volume ratio) parameter. Finally it can be suggested that dark matter and dark energy are ad-hoc and misleading concepts.

## 1 Introduction

Now as recently reported at the American Astronomical Society a study using the Very Large Array radio telescope in New Mexico and the French Plateau de Bure Interferometer has enabled astronomers to peer within a billion years of the Big Bang and found evidence that black holes were the first that leads galaxy growth [1]. The implication is that the black holes started growing first. Initially astrophysicists attempted to explain the presence of these black holes by describing the evolution of galaxies as gathering mass until black holes form at their center but further observation demanded that the galactic central black hole co-evolved with the galactic bulge plasma dynamics and the galactic arms. This is a fundamental confirmation of N. Hamein's theory [2] described in his papers as a universe composed of "different scale black holes from universal size to atomic size".

This clearly suggests that: (1) Galaxy constitutes a central black hole; (2) The central black hole grows first; (3) Star and galaxy growth goes parallel or later to the central black holes growth. The fundamental questions are: (1) If "black hole" is the result of a collapsing star, how and why a stable galaxy contains a black hole at its center? (2) Where does the central black hole comes from? (3) How the galaxy center will grow like a black hole? (4) How its event horizon exists with growing? If these are the observed and believed facts — not only for the author — this is a big problem for the whole science community to be understood. Any how, the important point to be noted here is that "due to some unknown reasons

galactic central black holes are growing"! This is the key point for the beginning of the proposed expanding or growing cosmic black hole! See this latest published reference [3] for the "black hole universe".

In our daily life generally it is observed that any animal or fruit or human beings (from birth to death) grows with closed boundaries (irregular shapes also can have a closed boundary). An apple grows like an apple. An elephant grows like an elephant. A plant grows like a plant. A human grows like a human. Through out their life time they won't change their respective identities. These are observed facts. From these observed facts it can be suggested that "growth" or "expansion" can be possible with a closed boundary. By any reason if the closed boundary is opened it leads to "destruction" rather than "growth or expansion". Thinking that nature loves symmetry, in a heuristic approach in this paper author assumes that "through out its life time universe is a black hole". Even though it is growing, at any time it is having an event horizon with a closed boundary and thus it retains her identity as a black hole for ever. Note that universe is an independent body. It may have its own set of laws. At any time if universe maintains a closed boundary to have its size minimum at that time it must follow "strong gravity" at that time. If universe is having no black hole structure any massive body (which is bound to the universe) may not show a black hole structure. That is black hole structure may be a subset of cosmic structure. This idea may be given a chance.

Rotation is a universal phenomenon [4, 5, 6]. We know that black holes are having rotation and are not stationary. Re-

cent observations indicates that black holes are spinning close to speed of light [7]. In this paper author made an attempt to give an outline of “expanding and light speed rotating black hole universe” that follows strong gravity from its birth to end of expansion.

Stephen Hawking in his famous book *A Brief History of Time* [8], in Chapter 3 which is entitled *The Expanding Universe*, says: “Friedmann made two very simple assumptions about the universe: that the universe looks identical in which ever direction we look, and that this would also be true if we were observing the universe from anywhere else. From these two ideas alone, Friedmann showed that we should not expect the universe to be static. In fact, in 1922, several years before Edwin Hubble’s discovery, Friedmann predicted exactly what Hubble found... We have no scientific evidence for, or against, the Friedmann’s second assumption. We believe it only on grounds of modesty: it would be most remarkable if the universe looked the same in every direction around us, but not around other points in the universe”. From this statement it is very clear and can be suggested that, the possibility for a “closed universe” and a “flat universe” is 50–50 per cent and one can not completely avoid the concept of a “closed universe”. Clearly speaking, from Hubble’s observations and interpretations in 1929, the possibility of “galaxy receding” and “galaxy revolution” is 50–50 per cent and one can not completely avoid the concept of “rotating universe”.

### 1.1 Need for cosmic constant speed rotation

1. Assume that a planet of mass  $M$  and size  $R$  rotates with angular velocity  $\omega_e$  and linear velocity  $v_e$  in such a way that free or loosely bound particle of mass  $m$  “lying on its equator” gains a kinetic energy equal to its potential energy and linear velocity of planet’s rotation is equal to free particle’s escape velocity. That is without any external power or energy, test particle gains escape velocity by virtue of planet’s rotation

$$\frac{mv_e^2}{2} = \frac{GMm}{R}, \quad (1)$$

$$\omega_e = \frac{v_e}{R} = \sqrt{\frac{2GM}{R^3}}. \quad (2)$$

Using this idea, “black hole radiation” and “origin of cosmic rays” can be understood. Now writing  $M = \frac{4\pi}{3}R^3\rho_e$  and  $\omega_e = \frac{v_e}{R} = \sqrt{\frac{8\pi G\rho_e}{3}}$  it can be written as

$$\omega_e^2 = \frac{8\pi G\rho_e}{3}, \quad (3)$$

where density  $\rho_e$  is

$$\text{density} = \rho_e = \frac{3\omega_e^2}{8\pi G}. \quad (4)$$

In real time this obtained density may or may not be equal to the actual density. But the ratio  $\frac{8\pi G\rho_{real}}{3\omega_e^2}$  may have some

physical meaning. From equation (4) it is clear that proportionality constant being  $\frac{3}{8\pi G}$

$$\text{density} \propto \text{angular velocity}^2. \quad (5)$$

Equation (4) is similar to the “flat model concept” of cosmic “critical density”

$$\rho_0 = \frac{3H_0^2}{8\pi G}. \quad (6)$$

Comparing equations (4) and (6) dimensionally and conceptually  $\rho_e = \frac{3\omega_e^2}{8\pi G}$  and  $\rho_0 = \frac{3H_0^2}{8\pi G}$  one can say that

$$H_0^2 \rightarrow \omega_e^2 \Rightarrow H_0 \rightarrow \omega_e. \quad (7)$$

In any physical system under study, for any one “simple physical parameter” there will not be two different units and there will not be two different physical meanings. This is a simple clue and brings “cosmic rotation” into picture. This is possible in a closed universe only. It is very clear that dimensions of Hubble’s constant must be “radian per second”. Cosmic models that depends on this “critical density” must accept “angular velocity of the universe” in the place of Hubble’s constant. In the sense “cosmic rotation” must be included in the existing models of cosmology. If this idea is rejected without any proper reason, alternatively the subject of cosmology can be studied in a rotating picture where the ratio of existing Hubble’s constant and estimated present cosmic angular velocity will give some valuable information.

2. After the Big Bang, since 5 billion years if universe is “accelerating” and at present dark energy is driving it- right from the point of Big Bang to the visible cosmic boundary in all directions, thermal photon wavelength must be stretched instantaneously and continuously from time to time and cosmic temperature must decrease instantaneously and continuously for every second. This is just like “rate of stretching of a rubber band of infinite length”. Note that photon light speed concept is not involved here. Against to this idea since 1992 from COBE satellite’s CMBR data reveals that cosmic temperature is practically constant at 2.726 °K. This observational clash clearly indicates that something is going wrong with accelerating model. Moreover the standard model predicts that the cosmic background radiation should be cooling by something like one part in  $10^{10}$  per year. This is at least 6 orders of magnitude below observable limits. Such a small decrease in cosmic temperature might be the result of cosmic “slowing down” rather than cosmic acceleration. See this latest published reference for cosmic slowing down [9].

3. If universe is accelerating, just like “rate of stretching of a rubber band of infinite length” CMBR photon wavelength stretches and CMBR temperature decreases. Technically from time to time if we are able to measure the changes in cosmic temperature then rate of decrease in cosmic temperature will give the rate of increase in cosmic expansion

accurately. Even though acceleration began 5 billion years before since all galaxies will move simultaneously from our galaxy “rate of increase” in super novae red shift can not be measured absolutely and accurately. Hence it is reasonable to rely upon “rate of decrease” in cosmic temperature rather than “rate of increase” in galaxy red shift.

4. Based on this analysis if “cosmic constant temperature” is a representation of “isotropy” it can be suggested that at present there is no acceleration and there is no space expansion and thus universe is static. From observations it is also clear that universe is homogeneous in which galaxies are arranged in a regular order and there is no mutual attraction in between any two galaxies. Not only that Hubble’s observations clearly indicates that there exists a linear relation in between galaxy distance and galaxy speed which might be a direct consequence of “cosmic rotation” with “constant speed”. This will be true if it is assumed that “rate of increase in red shift” is a measure of cosmic “rate of expansion”. Instead of this in 1929 Hubble interpreted that “red shift” is a measure of cosmic “expansion”. This is the key point where Einstein’s static universe was discarded with a simple 50–50 percent misinterpretation [10].

5. At present if universe is isotropic and static how can it be stable? The only one solution to this problem is “rotation with constant speed”. If this idea is correct universe seems to follow a closed model. If it is true that universe is started with a big bang, the “Big Bang” is possible only with “big crunch” which is possible only with a closed model.

6. At present if universe rotates as a rigid sphere with constant speed then galaxies will revolve with speeds proportional to their distances from the cosmic axis of rotation. This idea matches with the Hubble’s observations but not matches with the Hubble’s interpretation as “galaxy receding”. From points 2, 3 and 4 it is very clear that at present universe is isotropic and static. Hence the Hubble’s law must be re-interpreted as “at present as galaxy distance increases its revolving speed increases”. If so  $H_0$  will turn out to be the present angular velocity. In this way cosmic stability and homogeneity can be understood.

7. This “constant speed cosmic rotation” can be extended to the Big Bang also. As time passes while in constant speed of rotation some how if the cosmic sphere expands then “galaxy receding” as well as “galaxy revolution” both will come into picture. In the past while in constant speed of rotation at high temperatures if expansion is rapid for any galaxy (if born) receding is rapid and photon from the galaxy travels towards the cosmic center in the opposite direction of space expansion and suffers a continuous fast rate of stretching and there will be a continuous fast rate of increase in red shift. At present at small temperatures if expansion is slow galaxy receding is small and photon suffers continuous but very slow rate of stretching and there will be a continuous but very slow rate of increase in red shift i.e. red shift practically remains constant. From this analysis it can be suggested that rate of

decrease in cosmic temperature or rate of increase in red shift will give the rate of cosmic expansion.

8. In the past we have galaxy receding and at present we can have galaxy revolution. By this time at low temperature and low angular velocity, galaxies are put into stable orbits.

## 1.2 Need for cosmic strong gravity

1. After Big Bang if universe follows “least path of expansion” then at any time “time of action” will be minimum and “size of expansion” will be minimum and its effects are stable and observable.

2. For any astrophysical body its size is minimum if it follows strong gravity. Being an astrophysical body at any time to have a minimum size of expansion universe will follow strong gravity. No other alternative is available.

3. Following a closed model and similar to the growth of an “apple shaped apple” if universe grows in mass and size it is natural to say that as time is passing cosmic black hole is “growing or expanding”.

## 1.3 Need for light speed cosmic rotation and red shift boundary from 0 to 1

1. From Hubble’s observations when the red shift  $z \leq 0.003$ , velocity-distance relation is given by  $v = zc$  and ratio of galaxy distance and red shift is equal to  $\frac{c}{H_0}$ . If  $H_0$  represents the present cosmic angular velocity  $\frac{c}{H_0}$  must be the present size of the universe. Hence it can be guessed that cosmic speed of rotation is  $c$ . Since from Big Bang after a long time, i.e. at present if rotation speed is  $c$ , it means at the time of Big Bang also cosmic rotation speed might be  $c$ . Throughout the cosmic journey cosmic rotation speed [7] is constant at  $c$ . This is a heuristic idea. One who objects this idea must explain — being bound to the cosmic space, why photon travels at only that much of speed. This idea supports the recent observations of light speed rotation of black holes. Universe is an independent body. It is having its own mechanism for this to happen.

2. Galaxies lying on the equator will revolve with light speed and galaxies lying on the cosmic axis will have zero speed. Hence it is reasonable to put the red shift boundary as 0 to 1. Then their distances will be proportional to their red shifts from the cosmic axis of rotation.

## 1.4 Origin of cosmic black hole temperature

1. Following the Hawking’s black hole temperature formula (see subsection 2.1) it is noticed that black hole temperature is directly proportional to its rotational speed. For a stationary or non-rotating black hole its temperature is zero. As the rotational speed increases black hole’s temperature increases and reaches to maximum if its rotational speed approaches to light speed. At any time if we treat universe as black hole when it is stationary its temperature will be zero. Without cosmic black hole rotation there is no cosmic temperature.

2. When the growing cosmic black hole rotates at light speed it attains a maximum temperature corresponding to its mass or angular velocity at that time. As time passes if the cosmic black hole continues to rotate at light speed and expands then rate of decrease in temperature seems to be minimum if rate of increase in size is minimum and thus it always maintains least size of expansion to have minimum drop in temperature.

## 2 The four assumptions

To implement the Planck scale successfully in cosmology, to develop a unified model of cosmology and to obtain the value of present Hubble's constant (without considering the cosmic red shifts), starting from the Planck scale it is assumed that at any time  $t$ : (1) *The universe can be treated as a rotating and growing black hole*; (2) *With increasing mass and decreasing angular velocity universe always rotates with speed of light*; (3A) *Without cosmic rotation there is no "cosmic temperature"*; (3B) *Cosmic temperature follows Hawking black hole temperature formula where mass is equal to the geometric mean of Planck mass  $M_P$  and cosmic mass  $M_i$* ; (4) *Rate of decrease in CMBR temperature is a measure of cosmic rate of expansion*.

### 2.1 Derivation for black hole temperature and base for assumptions 1, 2 and 3

A black hole of mass  $M$  having size  $R$  rotates with an angular velocity  $\omega$  and rotational speed  $v = R\omega$ . Assume that its temperature  $T$  is inversely proportional to its rotational time period  $t$ . Keeping "Law of uncertainty" in view assume that

$$(k_B T) \times t = \frac{\hbar}{2} = \frac{h}{4\pi}. \quad (8)$$

$$T \times t = \frac{\hbar}{2k_B}. \quad (9)$$

where,  $t$  = rotational time period,  $T$  = temperature,  $k_B$  = Boltzmann's radiation constant,  $h$  = Planck's constant and  $\frac{k_B T}{2} + \frac{k_B T}{2} = k_B T$  is the sum of kinetic and potential energies of a particle in any one direction.

Stephen Hawking in Chapter 11 *The Unification of Physics* of his book [8], says: "The main difficulty in finding a theory that unifies gravity with the other forces is that general relativity is a "classical" theory; that is, it does not incorporate the uncertainty principle of quantum mechanics. On the other hand, the other partial theories depend on quantum mechanics in an essential way. A necessary first step, therefore, is to combine general relativity with the uncertainty principle. As we have seen, this can produce some remarkable consequences, such as black holes not being black, and the universe not having any singularities but being completely self-contained and without a boundary". We know that

$$t = \frac{2\pi}{\omega} = \frac{2\pi R}{v} = \frac{4\pi GM}{c^2 v}, \quad (10)$$

$$T = \frac{\hbar c^2 v}{8\pi k_B GM} = \frac{\hbar \omega}{4\pi k_B}, \quad (11)$$

thus if black hole rotational speed  $v$  reaches light speed then its temperature reaches to maximum

$$v \rightarrow v_{max} = c \Rightarrow T \rightarrow T_{max} = \frac{\hbar c^3}{8\pi k_B GM} = \frac{\hbar \omega_{max}}{4\pi k_B}. \quad (12)$$

Note that this idea couples GTR and quantum mechanics successfully. Hawking's black hole temperature formula can be obtained easily. And its meaning is simple and there is no need to consider the pair particle creation for understanding "Hawking radiation". This is the main advantage of this simple derivation. From this idea it is very clear that origin of Hawking radiation is possible in another way also. But it has to be understood more clearly. Information can be extracted from a black hole, if it rotates with light speed. *If a black hole rotates at light speed photons or elementary particles can escape from its "equator only" with light speed and in the direction of black hole rotation and this seems to be a signal of black hole radiation around the black hole equator. With this idea origin of cosmic rays can also be understood.* Note that not only at the black hole equator Hawking radiation can take place at the event horizon of the black hole having a surface area.

This equation (12) is identical to the expression derived by Hawking [11]. From the assumptions and from the obtained expressions it is clear that black hole temperature is directly proportional to the rotational speed of the black hole. Temperature of a stationary black hole is always zero and increases with increasing rotational speed and reaches to maximum at light speed rotation. In this way also GTR and quantum mechanics can be coupled. *But this concept is not the output from Hawking's black hole temperature formula. In any physical system for any physical expression there exists only one true physical meaning. Either Hawking's concept is true or the proposed concept is true. Since the black hole temperature formula is accepted by the whole science community author humbly request the science community to kindly look into this major conceptual clash at utmost fundamental level. Recent observations shows that black holes are spinning close to light speed.* Temperature of any black hole is very small and may not be found experimentally. But this idea can successfully be applied to the universe! By any reason if it is assumed that universe is a black hole then it seems to be surprising that temperature of a stationary cosmic black hole is zero. Its temperature increases with increase in its rotational speed and reaches to maximum if the rotational speed approaches light speed. This is the essence of cosmic black hole rotation. CMBR temperature demands the existence of "cosmic rotation". This is the most important point to be noted here.

Hawking radiation is maintained at event horizon as a (particle and anti particle) pair particle creation. One particle falls into the black hole and the other leaves the black

hole. Since the black hole is situated in a free space and lot of free space is available around the black hole's event horizon this might be possible. But applying this idea to the universe this type of thinking may not be possible. There will be no space for the particle to go out side the cosmic boundary or the cosmic event horizon and there is no scope for the creation of antiparticle also. If so the concept of cosmic black hole radiation and normally believed black hole radiation has to be studied in a different point of view. If there is no particle creation at the cosmic event horizon then there will be no evaporation of the cosmic black hole and hence there is no chance for decay of the cosmic black hole. Due to its internal mechanism it will grow like a black hole.

**2.2 Black hole minimum size, maximum rotation speed and stability**

Here, the fundamental question to be answered is — by birth, is black hole a rigid stationary sphere or a rigid light speed rotating sphere? See the web reference [7]. *Super massive black holes, according to new research, are approaching the speed of light. Nine galaxies were examined by NASA using the Chandra X-ray Observatory, and found each to contain black holes pumping out jets of gas in to the surrounding space. "Extremely fast spin might be very common for large black holes", said co-investigator Richard Bower of Durham University. This might help us explain the source of these incredible jets that we see stretching for enormous distances across space.* This reference indicates that author's idea is correct. Not only that it suggests that there is something new in black hole's spin concepts. Author suggests that [12, 13, 14] force limit  $\frac{c^4}{G}$  keeps the black hole stable or rigid even at light speed rotation. This force can be considered as the "classical limit" of force. It represents the "maximum gravitational force of attraction" and "maximum electromagnetic force". It plays an important role in unification scheme. It is the origin of Planck scale. It is the origin of quantum gravity. Similar to this classical force, classical limit of power can be given by  $\frac{c^5}{G}$ . It plays a crucial role in gravitational radiation. It represents the "maximum limit" of mechanical or electromagnetic or radiation power. The quantity  $\frac{c^4}{G}$  can be derived based on "Newton's law of gravitation and "constancy of speed of light". In solar system force of attraction between sun and planet can be given as

$$F = \left(\frac{m}{M}\right)\left(\frac{v^4}{G}\right), \tag{13}$$

where  $M$  = mass of sun,  $m$  = mass of planet and  $v$  = planet orbital velocity. Since  $\frac{m}{M}$  is a ratio  $\frac{v^4}{G}$  must have the dimensions of force. Following the constancy of speed of light, a force of the form  $\frac{c^4}{G}$  can be constructed. With 3 steps origin of rotating black hole formation can be understood with  $\frac{c^5}{G}$  and  $Mc^2$ , i.e.

$$\text{torque} = \tau \leq Mc^2, \tag{14}$$

$$\text{power} = \tau\omega \leq \left(\frac{c^5}{G}\right), \tag{15}$$

$$\omega \leq \frac{c^3}{GM} \Rightarrow \omega_{max} = \frac{c^3}{GM}. \tag{16}$$

To have maximum angular velocity size should be minimum

$$R_{min} = \frac{c}{\omega_{max}} = \frac{GM}{c^2}. \tag{17}$$

That is, if size is minimum, the black hole can rotate with light speed! Hence the space and matter surrounding its equator can turn at light speed! This is found to be true for many galaxy centers. Acceleration due to gravity at its surface can be given as  $\frac{c^4}{GM}$ . Rotational force can be given as  $MR_{min}\omega_{max}^2 = \frac{c^4}{G}$ . This is the ultimate magnitude of force that keeps the black hole stable even at light speed! This is a natural manifestation of space-time geometry.

Note that here in equation (17) only the coefficient 2 is missing compared with Schwarzschild radius. If the concept of "Schwarzschild radius" is believed [15] to be true, for any rotating black hole of rest mass ( $M$ ) the critical conditions are: (1) *Magnitude of kinetic energy never crosses rest energy*; (2) *Magnitude of torque never crosses potential energy*; (3) *Magnitude of mechanical power never crosses  $\left(\frac{c^5}{G}\right)$ .*

Based on virial theorem, potential energy is twice of kinetic energy and hence,  $\tau \leq 2Mc^2$ . In this way factor 2 can be obtained easily from equations (14), (15) and (16). Not only that special theory of relativity, classical mechanics and general theory of relativity can be studied in a unified way.

**2.3 Planck scale and cosmic black hole temperature**

At any time ( $t$ ) from assumption (1) based on black hole concepts, if mass of the universe is  $M_t$  size of the cosmic event horizon can be given by

$$R_t = \frac{2GM_t}{c^2}. \tag{18}$$

From assumption (2) if cosmic event horizon rotates with light speed then cosmic angular velocity can be given by

$$\omega_t = \frac{c}{R_t} = \frac{c^3}{2GM_t}. \tag{19}$$

From assumptions (3A) and (3B),

$$T_t = \frac{\hbar c^3}{8\pi k_B G \sqrt{M_t M_p}}, \tag{20}$$

where  $M_t \geq M_p$ . From equations (19) and (20)

$$4\pi k_B T_t = \hbar \sqrt{\omega_t \omega_p}. \tag{21}$$

This is a very simple expression for the long lived large scale universe! At any time if temperature  $T_t$  is known

$$\omega_t = \left(\frac{4\pi k_B T_t}{\hbar}\right)^2 \left(\frac{1}{\omega_p}\right). \tag{22}$$

Ultimate gravitational force of attraction between any two Planck particles of mass  $M_P$  separated by a minimum distance  $r_{min}$  can be given as

$$\frac{GM_P M_P}{r_{min}^2} = \frac{c^4}{G}, \quad (23)$$

where  $2\pi r_{min} = \lambda_P = \frac{h}{cM_P} =$  Planck wave length. In this way Planck scale mass and energy can be estimated

$$\text{Pl. mass} = M_P = 2.176 \times 10^{-8} \text{ Kg} = \sqrt{\frac{\hbar c}{G}}, \quad (24)$$

$$\text{Pl. size} = R_P = 3.2325 \times 10^{-35} \text{ meter} = \frac{2GM_P}{c^2}, \quad (25)$$

$$\text{Pl. angl. velocity} = \omega_P = 9.274 \times 10^{42} \frac{\text{rad}}{\text{sec}} = \frac{c^3}{2GM_P}, \quad (26)$$

$$\text{Pl. temperature} = T_P = 5.637 \times 10^{30} \text{ }^\circ\text{K} = \frac{\hbar\omega_P}{4\pi k_B}. \quad (27)$$

Substituting the present cosmic CMBR temperature [16] 2.726 °K in equation (22) we get present cosmic angular velocity as  $\omega_t = 2.169 \times 10^{-18} \frac{\text{rad}}{\text{sec}} \approx 66.93 \frac{\text{Km}}{\text{sec} \times \text{Mpc}}$ . Numerically this obtained value is very close to the measured value of Hubble's constant  $H_0$  [17, 18]. Not only that this proposed unified method is qualitatively and quantitatively simple compared with the "cosmic red shift" and "galactic distance" observations. This procedure is error free and is reliable. *Author requests the science community to kindly look into this kind of rotating and growing universe models. If this procedure is really true and applicable to the expanding universe then accelerating model, dark matter and dark energy are becomes ad-hoc concepts.* At any time it can be shown that

$$M_t R_t \omega_t^2 = M_t c \omega_t = \frac{c^4}{2G}. \quad (28)$$

## 2.4 Cosmic mass density and baryon-photon number density ratio

With this model empirically it is noticed that, mass density

$$\rho_{mass} \approx 3 \ln \left( \frac{R_t}{R_P} \right) \left[ \frac{aT_t^4}{c^2} \right] \approx 6 \ln \left( \frac{T_P}{T_t} \right) \left[ \frac{aT_t^4}{c^2} \right]. \quad (29)$$

If  $T_t = 2.726 \text{ }^\circ\text{K}$ ,  $\omega_t = 2.169 \times 10^{-18} \frac{\text{rad}}{\text{sec}}$ ,  $R_t = \frac{c}{\omega_t} = 1.383 \times 10^{26} \text{ meter}$  and  $R_P = 3.232 \times 10^{-35} \text{ meter}$ , present mass density can be obtained as

$$\rho_{mass} \approx 418.82 \times 4.648 \times 10^{-34} = 1.95 \times 10^{-31} \frac{\text{gram}}{\text{cm}^3}.$$

This is very close to the observed mater density [19] of the universe  $(1.75 \text{ to } 4.1) \times 10^{-31} \frac{\text{gram}}{\text{cm}^3}$ . If this idea is true the proposed term

$$3 \ln \left( \frac{R_t}{R_P} \right) \approx 6 \ln \left( \frac{T_P}{T_t} \right), \quad (30)$$

can be given a chance in modern cosmology. Actually this is the term given as

$$\ln \left( \frac{\text{cosmic volume at time, } t}{\text{Planck volume}} \right) \approx 3 \ln \left( \frac{R_t}{R_P} \right). \quad (31)$$

The interesting idea is that, if  $R_t \rightarrow R_P$ , and  $T_t \rightarrow T_P$ , the term  $3 \ln \left( \frac{R_t}{R_P} \right) \rightarrow 0$  and mass density at Planck time approaches zero. Conceptually this supports the Big Bang assumption that "at the time of Big Bang matter was in the form of radiation". Not only that as cosmic time increases mass density gradually increases and thermal density gradually decreases. Using this term and considering the present CMBR temperature baryon-photon number density ratio can be fitted as follows

$$\frac{N_B}{N_\gamma} \approx 3 \ln \left( \frac{R_t}{R_P} \right) \left[ \frac{2.7k_B T_t}{m_n c^2} \right], \quad (32)$$

Here interesting point is that

$$\left[ \frac{2.7k_B T_t}{m_n c^2} \right] \approx \frac{\text{average energy per photon}}{\text{rest energy of nucleon}}, \quad (33)$$

thus present value can be given as

$$\frac{N_B}{N_\gamma} \approx \frac{1}{3.535 \times 10^9}. \quad (34)$$

## 2.5 The 2 real densities

Since the cosmic black hole always follows closed model and rotates at light speed, at any time size of cosmic black hole is  $\frac{c}{\omega_t}$ . It's density =  $\frac{\text{mass}}{\text{volume}} = \frac{3\omega_t^2}{8\pi G}$ . It is no where connected with "critical density" concepts. From equations (18), (19) and (20) it is noticed that

$$\frac{3\omega_t^2}{8\pi G} = 5760\pi \left[ \frac{aT_t^4}{c^2} \right]. \quad (35)$$

Finally we can have only 2 real densities, one is "thermal energy density" and the second one is "mass density".

## 3 Origin of the cosmic red shift, galaxy receding and galaxy revolution

*As the cosmic sphere is expanding and rotating galaxies receding and revolving from and about the cosmic axis. As time passes photon from the galaxy travels opposite to the direction of expansion and reaches to the cosmic axis or center. Thus photon shows a red shift about the cosmic center. If this idea is true cosmic red shift is a measure of galactic distances from the cosmic axis of rotation or center. Galaxy receding is directly proportional to the rate of expansion of the rotating cosmic sphere as a whole. In this scenario for any galaxy continuous increase in red shift is a measure of rapid expansion and "practically constant red shift" is a measure of very*

slow expansion. That is change in galaxy distance from cosmic axis is practically zero. At any time ( $t$ ) it can be defined as, cosmic red shift

$$z_t = \frac{\Delta\lambda}{\lambda_{measured}} \leq 1. \quad (36)$$

when  $z_t$  is very small this definition is close to the existing red shift definition

$$z = \frac{\Delta\lambda}{\lambda_{emitted}}. \quad (37)$$

At present time relation between equations (36) and (37) can be given as

$$\frac{z}{z+1} \cong z_t. \quad (38)$$

Equation (38) is true only when  $z$  is very small. Note that at Hubble's time the maximum red shift observed was  $z = 0.003$  which is small and value of  $H_0$  was 530 Km/sec/Mpc. By Hubble's time equation (36) might have been defined in place of equation (37). But it not happened so! When rate of expansion is very slow, i.e. at present, based on  $v = r\omega$  concepts

$$v_t \cong z_t c, \quad (39)$$

gives revolving galaxies tangential velocity where increase in red shift is very small and practically remains constant and galaxy's distance from cosmic axis of rotation can be given as

$$r_t \cong \frac{v_t}{\omega_t} \cong z_t \left( \frac{c}{\omega_t} \right). \quad (40)$$

Numerically this idea is similar to Hubble's law [20]. This indicates that there is something odd in Hubble's interpretation of present cosmic red shifts and galaxy moments. By this time even though red shift is high if any galaxy shows a continuous increase in red shift then it can be interpreted that the galaxy is receding fast in the sense this light speed rotating cosmic sphere is expanding at a faster rate. Measured galactic red shift data indicates that, for any galaxy at present there is no continuous increase in their red shifts and are practically constants! This is a direct evidence for the slow rate of expansion of the present light speed rotating universe. When the universe was young i.e. in the past, Hubble's law was true in the sense "red shift was a measure of galaxy receding (if born)" and now also Hubble's law is true in the sense "red shift is a measure of galaxy revolution".

As time is passing "galaxy receding" is gradually stopped and "galaxy revolution" is gradually accomplished. Galaxies lying on the equator will revolve with light speed and galaxies lying on the cosmic axis will have zero speed. Hence it is reasonable to put the red shift boundary as 0 to 1. Then their distances will be proportional to their red shifts from the cosmic axis of rotation.

#### 4 The present cosmic time

(1) Time required to complete one radian is  $\frac{1}{\omega_t}$  where  $\omega_t$  is the angular velocity of the universe at time  $t$ . At any time this is not the cosmic age. If at present  $\omega_t \rightarrow H_0$ , it will not represent the present age of the universe. (2) Time required to complete one revolution is  $\frac{2\pi}{\omega_t}$ . (3) Time required to move from Planck volume to existing volume = present cosmic age.

How to estimate this time? Author suggests a heuristic procedure in the following way. With reference to Big Bang picture present cosmic time can be given as

$$t \cong \ln\left(\frac{T_P}{T_t}\right) \sqrt{\frac{3c^2}{8\pi G a T_t^4}} = 4.33 \times 10^{21} \text{ seconds}. \quad (41)$$

Here  $T_t \leq T_P$ , and interesting idea is that if  $T_t \rightarrow T_P$ , the term  $\ln\left(\frac{T_t}{T_P}\right) \rightarrow 0$ . It indicates that, unlike the Planck time, here in this model cosmic time starts from zero seconds. This idea is very similar to the birth of a living creature. How and why, the living creature has born? This is a fundamental question to be investigated by the present and future mankind. In the similar way, how and why, the "Planck particle" born? has to be investigated by the present and future cosmologists. Proposed time is 9400 times of  $\frac{1}{H_0}$ . With this large time "smooth cosmic expansion" can be possible. Inflation, magnetic monopoles problem and super novae dimming can be understood by a "larger cosmic time and smooth cosmic expansion". Proportionality constant being unity with the following 3 assumptions "cosmic time" can be estimated

$$t \propto 3 \ln\left(\frac{R_t}{R_P}\right), \quad (42)$$

$$t \propto \left[ \frac{M_P c^2}{4\pi k_B T_t} \right], \quad (43)$$

$$t \propto \left[ \frac{\hbar}{k_B T_t} \right]. \quad (44)$$

After simplification, obtained relation can be given as

$$t = \sqrt{\frac{36\pi}{90}} \times \ln\left(\frac{T_P}{T_t}\right) \sqrt{\frac{3c^2}{8\pi G a T_t^4}}, \quad (45)$$

$$t = 1.121 \times \ln\left(\frac{T_P}{T_t}\right) \sqrt{\frac{3c^2}{8\pi G a T_t^4}} = 4.85 \times 10^{21} \text{ sec}. \quad (46)$$

#### 5 Conclusion

The force  $\frac{c^4}{G}$  and power  $\frac{c^5}{G}$  are really the utmost fundamental tools of black hole physics and black hole cosmology. In this paper author presented a biological model for viewing the universe in a black hole picture. In reality its validity has to be studied, understood and confirmed by the science community at utmost fundamental level. At present also regarding the cosmic acceleration some conflicts are there [9].

The concept of dark energy is still facing and raising a number of fundamental problems. If one is able to understand the need and importance of “universe being a black hole for ever”, “CMBR temperature being the Hawking temperature” and “angular velocity of cosmic black hole being the present Hubble’s constant”, a true unified model of “black hole universe” can be developed.

The main advantage of this model is that, it mainly depends on CMBR temperature rather than the complicated red shift observations. From the beginning and up to right now if universe rotates at light speed- “Big Bang nucleosynthesis concepts” can be coupled with the proposed “cosmic black hole concepts”. Clearly speaking, in the past there was no Big Bang. Rotating at light speed for ever high temperature and high RPM (revolution per minute) the “small sized Planck particle” gradually transforms into low temperature and low RPM “large sized massive universe”.

### Acknowledgements

Author is very much grateful to the editors of the journal, Dr. Dimtri Rabounski and Dr. Larissa Borissova, for their kind guidance, discussions, valuable suggestions and accepting this paper for publication. Author is indebted to Institute of Scientific Research on Vedas (I-SERVE, recognized by DSIR as SIRO), Hyderabad, India, for its all-round support in preparing this paper. For considering this paper as poster presentation author is very much thankful to the following organizing committees: “DAE-BRNS HEP 2008, India”, “ISRAMA 2008, India”, “PIRT-CMS 2008, India”, “APSC 2009, India”, “IICFA 2009, India” and “JGRG-19, Japan”. Author is very much thankful to Prof. S. Lakshminarayana, Dept. of Nuclear Physics, Andhra University, Vizag, India, Dr. Sankar Hazra, PIRT-CMS, Kolkata, India, and Dr. José López-Bonilla, Mexico, for their special encouragement and guidance in publishing and giving a life to this paper. Finally author is very much thankful to his brothers B. Vamsi Krishna (software professional) and B. R. Srinivas (Associate Professor) for encouraging, providing technical and financial support.

Submitted on September 16, 2009 / Accepted on December 06, 2009

### References

1. Carilli et al. Black holes lead Galaxy growth, new research shows. Lecture presented to the American Astronomical Society’s meeting in Long Beach, California, 4–8 January 2009, National Radio Astronomy Observatory, Socorro, NM: <http://www.nrao.edu/pr/2009/bhbulge>
2. Hamein N. et al. Scale Unification-A Universal scaling law for organized matter. *Proceedings of the Unified Theories Conference 2008*, Budapest, 2008.
3. Tianxi Zhang. A new cosmological model: black hole Universe. *Progress in Physics*, 2009, v.3.
4. Rabounski D. On the speed of rotation of isotropic space: insight into the redshift problem. *The Abraham Zelmanov Journal*, 2009, v.2, 208–223.
5. Gentry R.V. New cosmic center Universe model matches eight of Big Bang’s major predictions without the F-L paradigm. CERN Electronic Publication EXT-2003-022.
6. Obukhov Y.N. On physical foundations and observational effects of cosmic Rotation. *Colloquium on Cosmic Rotation*, Wissenschaft und Technik Verlag, Berlin, 2000, 23–96.
7. Black holes spinning near the speed of light. <http://www.space.com/scienceastronomy080115-st-massive-black-hole.html>
8. Hawking S.W. A brief history of time. Bantam Dell Publishing Group, 1988.
9. Shafieloo A. et al. Is cosmic acceleration slowing down? *Phys. Rev. D*, 2009, v.80, 101301; arXiv: 0903.5141.
10. Hubble E.P. A relation between distance and radial velocity among extra-galactic nebulae. *PNAS*, 1929, v.15, 168–173.
11. Hawking S.W. Particle creation by black holes. *Commun. Math. Phys.*, 1975, v.43, 199–220.
12. Hamein N. et al. The origin of spin: a consideration of torque and coriolis forces in Einstein’s field equations and Grand Unification Theory. In: *Beyond the Standard Model: Searching for Unity in Physics*, The Noetic Press, 2005, 153–168.
13. Rauscher E.A. A unifying theory of fundamental processes. Lawrence Berkeley National Laboratory Reports UCRL-20808 (June 1971), and *Bull. Am. Phys. Soc.*, 1968, v.13, 1643.
14. Kostro L. Physical interpretations of the coefficients  $c/G$ ,  $c^2/G$ ,  $c^3/G$ ,  $c^4/G$ ,  $c^5/G$  that appear in the equations of General Relativity. In: *Mathematics, Physics and Philosophy in the Interpretations of Relativity Theory*, Budapest, September 4–6, 2009, <http://www.phil-inst.hu/~szekely>
15. Schwarzschild K. Über das Gravitationsfeld eines Massenpunktes nach der Einsteinschen Theorie. *Sitzungsberichte der Königlich Preussischen Akademie der Wissenschaften*, 1916, 189–196 (published in English as: Schwarzschild K. On the gravitational field of a point mass according to Einstein’s theory. *Abraham Zelmanov Journal*, 2008, vol. 1, 10–19).
16. Yao W.-M. et al. Cosmic Microwave Background. *Journal of Physics*, 2006, G33, 1.
17. Kirsner R.P. Hubble’s diagram and cosmic expansion. *PNAS*, 2004, v.101, no.1, 8–13.
18. Huchra J. Estimates of the Hubble constant. Harvard-Smithsonian Center for Astrophysics, 2009, <http://www.cfa.harvard.edu/~huchra/hubble.plot.dat>
19. Copi C.J. et al. Big bang nucleosynthesis and the baryon density of the universe. arXiv: astro-ph/9407006.
20. Rabounski D. Hubble redshift due to the global non-holonomy of space. *The Abraham Zelmanov Journal*, 2009, v.2, 11–28.

## The Radiation Reaction of a Point Electron as a Planck Vacuum Response Phenomenon

William C. Daywitt

National Institute for Standards and Technology (retired), Boulder, Colorado, USA. E-mail: wcdawitt@earthlink.net

The polarizability of the Planck vacuum (PV) transforms the bare Coulomb field  $e_*/r^2$  of a point charge into the observed field  $e/r^2$ , where  $e_*$  and  $e$  are the bare and observed electronic charges respectively [1]. In uniform motion this observed field is transformed into the well-known relativistic electric and magnetic fields [2, p.380] by the interaction taking place between the bare-charge field and the PV continuum. Given the involvement of the PV in both these transformations, it is reasonable to conclude that the negative-energy PV must also be connected to the radiation reaction or damping force of an accelerated point electron. This short paper examines that conclusion by comparing it to an early indication [3] that the point electron problem may involve more than just a massive point charge.

The nonrelativistic damping force

$$\frac{2e^2}{3c^3} \frac{d\ddot{\mathbf{r}}}{dt} \quad (1)$$

is the one experimentally tested fact around which the classical equations of motion for the point electron are constructed. The relativistic version of the equation of motion due to Dirac [3] can be expressed as [4, p.393]

$$m a^\mu = \frac{2e^2}{3c^3} \frac{v^\alpha (v_\alpha \dot{a}^\mu - \dot{a}_\alpha v^\mu)}{c^2} + F^\mu \quad (2)$$

where  $\mu = 0, 1, 2, 3$ ;  $v^\mu$  and  $a^\mu$  are the velocity and acceleration 4-vectors; the dot above the acceleration vectors represents differentiation with respect to the proper time; and  $F^\mu$  is the external 4-force driving the electron. The first term on the right side of (2) is the relativistic damping-force 4-vector that leads to (1) in the nonrelativistic limit. In the derivation of (2) Dirac stayed within the framework of the Maxwell equations; so the  $m$  on the left side is a derived electromagnetic mass for the electron.

In deriving (2) Dirac was not interested in the physical origin of the damping force (1) — he was interested in a covariant expression for the damping force that recovered (1) in the nonrelativistic limit, whatever it took. In the derivation he utilized a radiation-reaction field proportional to the difference between retarded and advanced fields [4, p.399]:

$$\frac{F_{\text{ret}}^{\mu\alpha} - F_{\text{adv}}^{\mu\alpha}}{2} \longrightarrow \frac{2e}{3c^3} \frac{(v^\mu \dot{a}^\alpha - \dot{a}^\mu v^\alpha)}{c} \quad (3)$$

where  $F_{\text{ret}}^{\mu\alpha}$  and  $F_{\text{adv}}^{\mu\alpha}$  are, respectively, the retarded and advanced electromagnetic field tensors for a point charge. The right side of (3) is the left side evaluated at the point electron. It is significant that this field difference is nonsingular at the position of the electron's charge, for the Maxwell equations then imply that the origin of the damping force and the field (3) *must be attributed to charged sources other than the*

*electron charge* since that charge's Coulomb field diverges as  $r \rightarrow 0$ . This conclusion implies that a third entity, in addition to the electron charge and its mass, is the cause of the damping force.

It can be argued that this third entity is the omnipresent PV if it is assumed that the electron charge interacts with the PV in the near neighborhood of the charge to produce the damping force. Under this assumption, the advanced field in (3) represents in a rough way *the reaction field from the PV converging on the charge*. (To the present author's knowledge, there exists no other simple explanation for this convergent field.) Thus the superficial perception of the advanced field in (3) as a cause-and-effect-violating conundrum is changed into that of an acceptable physical effect involving the PV.

The Wheeler-Feynman model for the damping force [5] [4, pp.394–399] comes to a conclusion similar to the preceding result involving the PV. In their case the third entity mentioned above is a completely absorbing shell containing a compact collection of massive point charges that surrounds the point electron. The total force exerted on the electron by the absorber is [4, eqn.(21–91)]

$$e \sum_{i=1}^n \frac{F_{\text{ret } \mu\alpha}^{(i)} v^\alpha}{c} + \frac{2e^2}{3c^3} \frac{(v_\mu \dot{a}_\alpha - \dot{a}_\mu v_\alpha) v^\alpha}{c^2} \quad (4)$$

where  $F_{\text{ret } \mu\alpha}^{(i)}$  is the retarded field tensor due to the  $i$ -th charged particle in an absorber containing  $n$  particles, and where the  $v_{\mu s}$  and  $a_{\mu s}$  are defined in (2). (The reader should note that the index  $i$  on the sum is defined somewhat differently here than in [4].) A central property of the electron-plus-absorber system is that there is no radiation outside that system. That is, the disturbance caused by the accelerated electron is confined to a neighborhood (the electron-plus-absorber) surrounding the electron.

In summary, the importance of the PV theory to (1) and its covariant cousin in the Dirac radiation-reaction equation

(2) is that it explains the advanced field in (3) as a convergent field whose source is the PV. Also, it is interesting to note that the Wheeler-Feynman model for the damping force tends to support the PV model, where the free-space absorber is a rough approximation for the negative-energy PV in the vicinity of the accelerated electron charge.

Submitted on December 01, 2009 / Accepted on December 18, 2010

### References

1. Daywitt W.C. The Planck vacuum. *Progress in Physics*, 2009, v. 1, 20.
  2. Jackson J.D. Classical electrodynamics. John Wiley & Sons Inc., 1st ed., 2nd printing, NY, 1962.
  3. Dirac P.A.M. Classical theory of radiating electrons. *Proc. R. Soc. Lond. A*, 1938, v. 167, 148–169.
  4. Panofsky W.K.H., Phillips M. Classical electricity and magnetism. Addison-Wesley Publ. Co. Inc., Mass. (USA) and London (England), 1962.
  5. Wheeler J.A., Feynman R.P. Interaction with the absorber as the mechanism of radiation. *Rev. Mod. Phys.*, 1945, v. 17, no. 2 and 3, 157.
-

## A Massless-Point-Charge Model for the Electron

William C. Daywitt

National Institute for Standards and Technology (retired), Boulder, Colorado, USA. E-mail: wcdawitt@earthlink.net

“It is rather remarkable that the modern concept of electrodynamics is not quite 100 years old and yet still does not rest firmly upon uniformly accepted theoretical foundations. Maxwell’s theory of the electromagnetic field is firmly ensconced in modern physics, to be sure, but the details of how charged particles are to be coupled to this field remain somewhat uncertain, despite the enormous advances in quantum electrodynamics over the past 45 years. Our theories remain mathematically ill-posed and mired in conceptual ambiguities which quantum mechanics has only moved to another arena rather than resolve. Fundamentally, we still do not understand just what is a charged particle” [1, p.367]. As a partial answer to the preceding quote, this paper presents a new model for the electron that combines the seminal work of Puthoff [2] with the theory of the Planck vacuum (PV) [3], the basic idea for the model following from [2] with the PV theory adding some important details.

The Abraham-Lorentz equation for a point electron can be expressed as [4, p.83]

$$m\dot{\mathbf{r}} = (m_0 + \delta m)\dot{\mathbf{r}} = \frac{2e^2}{3c^3} \frac{d\dot{\mathbf{r}}}{dt} + \mathbf{F}, \quad (1)$$

where

$$\delta m = \frac{4e^2}{3\pi c^2} \int_0^{k_{c*}} dk = \frac{4\alpha m_*}{3\pi^{1/2}} \quad (2)$$

is the electromagnetic mass correction;  $e (= e_* \sqrt{\alpha})$  is the observed electronic charge;  $\alpha$  is the fine structure constant;  $e_*$  is the true or bare electronic charge;  $k_{c*} (= \sqrt{\pi}/r_*)$  is the cutoff wavenumber for the mass correction [2, 5];  $m_*$  and  $r_*$  ( $= e_*^2/m_*c^2$ ) are the mass and Compton radius of the Planck particles in the PV;  $m$  and  $m_0$  are the observed and bare electron masses; and  $\mathbf{F}$  is some external force driving the electron. One of the  $e_*$ s in the product  $e^2 (= \alpha e_*^2)$  comes from the free electronic charge and the other from the charge on the individual Planck particles making up the PV. The bare mass is defined via

$$m_0 = m - \delta m \approx -\alpha m_* \quad (3)$$

the approximation following from (2) and the fact that  $\alpha m_* \gg m$ . In other words, the bare mass is equal to some huge *negative* mass  $\alpha m_*$ , an unacceptable result in any classical or semiclassical context.

The problem with the mass in (1) and (3) stems from assigning, ad hoc, a mass to the point charge to create the point electron, a similar problem showing up in quantum electrodynamics. The PV theory, however, derives the string of Compton relations [5]

$$r_* m_* c^2 = r_c m c^2 = e_*^2 \quad (4)$$

that relate the mass  $m$  and Compton radius  $r_c (= e_*^2/mc^2)$  of the various elementary particles to the mass  $m_*$  and Compton radius  $r_*$  of the Planck particles constituting the negative

energy PV. Since the same bare charge  $e_*$  is associated with the various masses in (4), it is reasonable to suggest that  $e_*$  is massless, implying that the electron charge is also massless. A massless-point-charge electron model is pursued in what follows.

The Puthoff model for a charged particle [2, 5] starts with an equation of motion for the mass  $m_0$

$$m_0 \ddot{\mathbf{r}} = e_* \mathbf{E}_{zp}, \quad (5)$$

where  $m_0$ , considered to be some function of the actual particle mass  $m$ , is eliminated from (5) by substituting the damping constant

$$\Gamma = \frac{2e_*^2}{3c^3 m_0} \quad (6)$$

and the electric dipole moment  $\mathbf{p} = e_* \mathbf{r}$ , where  $\mathbf{r}$  represents the random excursions of the point charge about its average position at  $\langle \mathbf{r} \rangle = 0$ . The force driving the charge is  $e_* \mathbf{E}_{zp}$ , where  $\mathbf{E}_{zp}$  is the zero-point electric field [5, Appendix B]

$$\begin{aligned} \mathbf{E}_{zp}(\mathbf{r}, t) = e_* \text{Re} \sum_{\sigma=1}^2 \int d\Omega_k \int_0^{k_{c*}} dk k^2 \widehat{\mathbf{e}}_{\sigma}(\mathbf{k}) \sqrt{k/2\pi^2} \times \\ \times \exp[i(\mathbf{k} \cdot \mathbf{r} - \omega t + \Theta_{\sigma}(\mathbf{k}))] \end{aligned} \quad (7)$$

and  $\omega = ck$ . The details of the equation are unimportant here, except to note that this free-space stochastic field depends only upon the nature of the PV through the Planck particle charge  $e_*$  and the cutoff wavenumber  $k_{c*}$ .

Inserting (6) into (5) leads to the equation of motion

$$\ddot{\mathbf{p}} = \frac{3c^3 \Gamma}{2} \mathbf{E}_{zp} \quad (8)$$

for the point charge in the massless-charge electron model, where the mass equation of motion (5) is now discarded. The

mass  $m$  of the electron is then defined via the charge's average kinetic energy [2, 5]

$$m \equiv \frac{2e_*^2 \langle \dot{\mathbf{r}}_2^2 \rangle}{3c^3 c^2 \Gamma}, \quad (9)$$

where  $\dot{\mathbf{r}}_2$  represents the planar velocity of the charge normal to its instantaneous propagation vector  $\mathbf{k}$ , and where

$$\langle \dot{\mathbf{r}}_2^2 \rangle = \frac{3c^4 (k_{c*} \Gamma)^2}{2\pi} \quad (10)$$

is the squared velocity averaged over the random fluctuations of the field.

The cutoff wavenumber and damping constant are determined to be [2, 5]

$$k_{c*} = \frac{\sqrt{\pi}}{r_*} \quad (11)$$

and

$$\Gamma = \left( \frac{r_*}{r_c} \right) \frac{r_*}{c} = \left( \frac{1.62 \times 10^{-33}}{3.91 \times 10^{-11}} \right) \frac{r_*}{c} \sim 10^{-66} \text{ [sec]}, \quad (12)$$

where the vanishingly small damping constant is due to the large number ( $\sim 10^{99}$  per  $\text{cm}^3$ ) of agitated Planck particles in the PV contributing their fields simultaneously to the zero-point electric field fluctuations in (7). This damping constant is assumed to be associated with the dynamics taking place within the PV and leading to the free-space vacuum field (7).

Inserting (11) and (12) into (9) and (10) yields

$$\frac{\langle \dot{\mathbf{r}}_2^2 \rangle}{c^2} = \frac{3}{2} \left( \frac{r_*}{r_c} \right)^2 \quad (13)$$

and

$$m = \frac{r_* m_*}{r_c} \quad (14)$$

where the result in (14) agrees with the Compton relations in (4). Equation (13) shows the root-mean-square relative velocity of the massless charge to be

$$\frac{\langle \dot{\mathbf{r}}_2^2 \rangle^{1/2}}{c} = \sqrt{\frac{3}{2}} \left( \frac{r_*}{r_c} \right) \sim 10^{-23} \quad (15)$$

a vanishingly small fraction of the speed of light. The reason for this small rms velocity is the small damping constant (12) that prevents the velocity from building up as the charge is randomly accelerated.

The equation of motion (8) of the point charge can be put in a more transparent form by replacing the zero-point field (7) with [3]

$$\mathbf{E}_{zp} = \sqrt{\frac{\pi}{2}} \frac{e_*}{r_*^2} \mathbf{I}_{zp}, \quad (16)$$

where  $\mathbf{I}_{zp}$  is a random variable of zero mean and unity mean square  $\langle \mathbf{I}_{zp}^2 \rangle = 1$ . Making this substitution leads to

$$\ddot{\mathbf{r}} = \sqrt{\frac{9\pi}{8}} \left( \frac{m}{m_*} \right) \frac{c^2}{r_*} \mathbf{I}_{zp} = \sqrt{\frac{9\pi}{8}} \frac{c^2}{r_c} \mathbf{I}_{zp}, \quad (17)$$

where the factors multiplying  $\mathbf{I}_{zp}$  are the rms acceleration of the point charge. The electron mass  $m$  now appears on the *right side* of the equation of motion, a radical departure from equations of motion similar to (1) and (5) that are modeled around Newton's second law with the mass multiplying the acceleration  $\ddot{\mathbf{r}}$  on the left of the equation. The final expression follows from the Compton relations in (4) and shows that the acceleration is roughly equivalent to a constant force accelerating the charge from zero velocity to the speed of light in the time  $r_c/c$  it takes a photon to travel the electron's Compton radius  $r_c$ .

The overall dynamics of the new electron model can be summarized in the following manner. The zero point agitation of the Planck particles within the degenerate negative-energy PV create zero-point electromagnetic fields that exist in free space [5], the evidence being the  $e_*$  and  $k_{c*}$  in (7), the rms Coulomb field  $e_*/r_*^2$  in (16), and the fact that  $\mathbf{E}_{zp}$  drives the free-space charge  $e_*$ . When the charge is injected into free space (presumably from the PV), the driving force  $e_* \mathbf{E}_{zp}$  generates the electron mass in (9), thereby creating the point electron characterized by its bare point charge  $e_*$ , its derived mass  $m$ , and its Compton radius  $r_c$ . Concerning the point-charge aspect of the model, it should be recalled that, experimentally, the electron appears to have no structure at least down to a radius around  $10^{-20}$  [cm], nine orders of magnitude smaller than the electron's Compton radius in (12).

Submitted on December 23, 2009 / Accepted on January 18, 2010

## References

1. Grandy W.T. Jr. Relativistic quantum mechanics of leptons and fields. Kluwer Academic Publishers, Dordrecht-London, 1991.
2. Puthoff H.E. Gravity as a Zero-Point-Fluctuation Force. *Phys. Rev. A*, 1989, v.39, no.5, 2333–2342.
3. Daywitt W.C. The Planck vacuum. *Progress in Physics*, 2009, v. 1, 20.
4. de la Peña L., Cetto A.M. The quantum dice — an introduction to stochastic electrodynamics. Kluwer Academic Publishers, Boston, 1996. Note that the upper integral limit for  $\delta m$  in (2) of the present paper is different from that in (3.114) on p.83 of reference [4].
5. Daywitt W.C. The source of the quantum vacuum. *Progress in Physics*, 2009, v. 1, 27.

# Quark Confinement and Force Unification

Robert A. Stone Jr.

1313 Connecticut Ave, Bridgeport, CT 06607, USA. E-mail: robert.a.stone.jr@gmail.com

String theory had to adopt a bi-scale approach in order to produce the weakness of gravity. Taking a bi-scale approach to particle physics along with a spin connection produces 1) the measured proton radius, 2) a resolution of the multiplicity of measured weak angle values 3) a correct theoretical value for the  $Z^0$  4) a reason that  $\hbar$  is a constant and 5) a “neutral current” source. The source of the “neutral current” provides 6) an alternate solution to quark confinement, 7) produces an effective  $r$  like potential, and 8) gives a reason for the observed but unexplained Regge trajectory like  $J \sim M^2$  behavior seen in quark composite particle spin families.

## 1 Introduction

One of the successful aspects of String Theory is its ability to produce both atomic type and gravitational type forces within the same mathematical formalism. The problem was that the resultant gravitational force magnitude was not even close.

This problem continued until the string theorists added extra dimension of about  $10^{19}$ th times larger than plank scale dimensions [1, 2]. The weakness of inter-scale gravity is due to the size difference between the two scales.

But a bi-scale approach raises the question; Is there also a “strong” intra-scale gravity force at the scale that produces the other strong particle level forces?

The particle level gravity proposition (e.g. Recami [3] and Salam [4]) is revisited, as the source of the “neutral current”.

Spin in the Standard Model (SM) is not viewed as physical. As shown in [5], it is not the SM mathematics, but the “standard” view of the mathematics that results in the Cosmological Constant Problem while hiding Nature’s mass symmetry, a symmetry in keeping with the cosmological constant and a symmetry that results in a single mass formula for the fundamental particles ( $W^\pm$ ,  $p^\pm$ ,  $e^\mp$ ) and electron generations.

The results of [5] could not have occurred without putting aside the SM “standard” view.

This paper proposes that the particle’s components real spin is the source of a particle level gravity.

## 2 The spin connection

It is proposed that spin is the source of a strong particle level gravity and associated intra-scale induced curvature. A spin torsion connection to a “strong” gravity is not new [6].

An intra-scale induced curvature is different than an inter-scale induced curvature. An inter-scale force is related to the difference between scales making  $G$  a constant.

The proposed intra-scale gravity magnitude is dependent on the frequency of spin. The higher the energy the higher the frequency (e.g. like  $E = h\nu$  used in the development of the Schrödinger equation). The higher the frequency the higher the resultant curvature. Thus this intra-scale gravity value is not a constant.

Given the units of strong particle level gravity ( $sG$ ) are  $\text{gm}^{-1}\text{cm}^3\text{sec}^{-2}$  and spin ( $h$ ) are  $\text{gm}^1\text{cm}^2\text{sec}^{-1}$  the first spin  $\frac{1}{2}\hbar$  particle “ $x$ ” relationship one might propose is

$$C \frac{2 sG_x m_x^2}{c} = \hbar, \quad (1)$$

where  $c$  is the velocity of light,  $C$  is a proportionality constant and the 2 on the lhs comes from the  $\frac{1}{2}$  originally in front of  $\hbar$ .

In [5], a  $4\pi$  definition of Nature’s coupling constants was given for the charged particle weak angle as  $\alpha_{sg} = 2\sqrt{2}(4\pi\varrho)^{-1}$  ( $\sim 0.2344$  vs  $0.2312$  [7]) where  $\varrho = 0.959973785$ .

Equating  $C$  with the  $\alpha_{sg}$  gives

$$\alpha_{sg} \frac{2 sG_x m_x^2}{c} = \hbar. \quad (2)$$

## 3 The proton radius

Using the traditional gravity radius relationship for proof of concept (see §12), i.e.  $R_p = 2 sG_p m_p / c^2$  and the proton mass ( $m_p$  [8]) gives the proton radius of

$$R_p = \frac{2 sG_p m_p}{c^2} = \frac{\hbar}{c m_p \alpha_{sg}} = 8.96978 \times 10^{-14} \text{ cm}. \quad (3)$$

From scattering data, Sick [9] gives a proton radius  $R_p$  of  $8.95 \times 10^{-14} \text{ cm} \pm 0.018$  making (3) 0.221% of Sick’s value and Ezhela [10] gives a proton radius  $R_p$  of  $8.97 \times 10^{-14} \text{ cm} \pm 0.02(\text{exp}) \pm 0.01(\text{norm})$  making (3) 0.0024% of Ezhela’s value.

## 4 A force magnitude unification

The proposed spin frequency strong gravity connection results in the three force distance squared ratios of

$$\alpha_{cs} = 7.2973525310^{-3}, \quad (4)$$

$$\alpha_{cg} = 1.7109648410^{-3}, \quad (5)$$

$$\alpha_{sg} = 0.234463777. \quad (6)$$

Thus the string theory conjecture that Nature’s space-time is bi-scalar and this paper’s conjecture on real spin as the source of a strong particle level gravity curvature results in a unification of forces at the particle level.

## 5 A weak theory puzzle

One recognized puzzle is that there are three statistically different weak angle values (Salam-Weinberg mass ratio SM theoretical value 0.2227 [11],  $\sin^2 \hat{\theta}_W(M_Z) = 0.2312$  [7], neutrino  $s_W^2 = 0.2277$  [11]) rather than a single value as expected by the SM. Note that the conversion between these weak angle forms does not resolve this puzzle.

## 6 A weak theory solution

The puzzle of three different measured weak angles using the present work is no longer a puzzle.

Unlike the SM view, the theoretical definition,  $\alpha_{sg} = 2\sqrt{2}(4\pi\varrho)^{-1}$ , allows for at least two basic weak angle values. When  $\varrho = 1$  the pure theory definition gives  $\alpha_{sg(1)} = 2\sqrt{2}(4\pi)^{-1} \sim 0.2251$ , close to the measured neutrino weak angle (0.2277 [11]). When using the same value of  $\varrho$  used for the fine structure constant definition [5], i.e.  $\varrho = 0.959973785$ , the definition  $\alpha_{sg} = 2\sqrt{2}(4\pi\varrho)^{-1}$  is close to the measured charge particle weak angle ( $\sim 0.2344$  vs 0.2312 [7]).

Thus these two different values,  $s_W^2$  and  $\sin^2 \hat{\theta}_W(M_Z)$ , result from two different spin couplings ( $\varrho = 1$  and  $\varrho = 0.959973785$ ) for two different types of particles, neutrino particles and charged particles.

The resolution for the Salam-Weinberg value in part comes from the recognition that the charged particle weak angle is different from the pure theory value, and that the Salam-Weinberg mass ratio is a pure theory value. The other part comes from the expectation that a true pure theory value would use chargeless particle masses.

Using the PDG  $W$  mass ( $m_W$  [8]) and the new constant  $\alpha_{cg}$  given in [5] to produce the  $W$  particle charge reduced mass value,  $m_W(1 - S\alpha_{cg})$  with  $S=1$ , yields the pure theory Salam-Weinberg bare mass ratio equation

$$1 - \frac{(m_W(1 - \alpha_{cg}))^2}{m_Z^2} = 0.2253 \approx \alpha_{sg(1)} = 0.2251. \quad (7)$$

Note that using the pure theory approach to the Salam-Weinberg mass ratio reduces the number values for the weak angle to two. Now, as theoretically expected, the pure theory charge reduced bare Salam-Weinberg mass ratio numerically matches the pure theory weak angle value.

## 7 A theoretical $Z^0$ mass

Given the theoretical value of the  $W$  mass in [5] and rearranging to give the  $Z^0$  theoretical mass produces the  $m_Z$

$$m_Z = \frac{m_W(1 - \alpha_{cg})}{(1 - \alpha_{sg(1)})^{\frac{1}{2}}} = 91188.64 \text{ MeV}, \quad (8)$$

a value within 0.0011% of the measured PDG value of  $91187.6 \pm 2.1$  [8].

## 8 Confinement and quark's existence

This particle level gravity approach also gives a reason that quarks are only seen inside of particles, but not all particles.

Noting that all quark composite particle masses are greater than the mass symmetry point ( $M_{sp} \sim 21 \text{ MeV}$ ), implies that quark particles are only stable inside the higher curvature (compacted) space-time fabric particles above the mass symmetry point and are not stable inside the low curvature (voided) space-time particles below  $M_{sp}$ .

## 9 Confinement, persistence and Regge trajectories

But if quarks can only exist inside high curvature particles then unstable particle decay may not occur at the quarks base mass but when the curvature is not high enough for the quarks to persist.

This means that the measured quark masses may not be their base mass but their decay point masses.

The two natural postulates, 1) that the enclosure curvature makes quarks stable and 2) that a quark decays before reaching its base mass, imply that a given quark orbital spin configuration will decay at or near some given curvature value. This means that for a specific quark particle spin family (e.g. a  $S = 1/2, 3/2, 5/2$   $J(S\hbar)$  family), all members of the family would decay at or around the same curvature.

That a quark spin family all decay at the same curvature, i.e.  $sG$  is a constant ( $sG = C_{decay}$ ), means that Eq. (2) becomes

$$C' M_x^2 = J(S\hbar). \quad (9)$$

This equation is the Regge trajectory like ( $J \sim M^2$ ) behavior seen in Chew-Fraustchi plots for unstable quark spin families (see [12] for some examples).

Thus the spin strong gravity connection that produces the correct proton radius and the correct weak angle, also gives a reason why quarks do not exist outside of particles and can produce the observed Regge trajectory like behavior.

## 10 The proton and quarks

As indicated by the single quantized mass formula for the electron, proton and  $W$  particle given in [5], the quantization process' spin dominates the proton and thus the (stable) proton is not a typical (unstable) quark composite particle.

Evidence that the proton is not typical also comes from B. G. Sidharth [13]. Sidharth reproduces numerous composite particle masses using the pion as the "base particle". Sidharth states, "Secondly, it may be mentioned that . . . using the proton as the base particle has lead to interesting, but not such comprehensive results".

That the proton is not a quark spin dominated particle may be one of the reasons that QCD has struggled for 40 years, with numerous additions to the model to produce a good proton radius value within 5% and why "solutions", like adding the effect of the  $s$  quarks fails to be supported by experimental evidence consistent with no  $s$  quarks.

The spin connection with the strong gravity approach immediately results in a proton radius value significantly less than 1%.

## 11 A $r$ potential from a $1/r$ potential force

What the data for unstable quark composite particles indicates is that there is an *effective*  $r$  like confining potential.

What the data does not say is how this  $r$  like potential *effect* occurs.

One way of creating this  $r$  potential was found by making a new force nature that requires the QCD “equivalent of the photon”, the gluon, to not only mediate the force as does the photon, but also participates in it (requires glueballs to exist).

However, there is another way that does not require a new force nature nor force form nor particle nature. Note that what follows is for quark (spin dominated) composite particles, not quantization dominated fundamental particles, i.e. the proton, and is a simplification of a complex situation including the frame dragging of quarks.

For quark composite particles the real spin proposition implies that the quark orbital spin angular momentum can be a significant contribution to the strong gravity value.

The particles strong gravity value would not be a constant but fluctuate with the quarks contribution due to their radius and velocity within the strong gravity enclosure.

That is to say, the higher the internal quark real spin angular momentum value, the higher the curvature and the stronger the confinement force. Mathematically this implies a  $C/r$  potential whose “gravitational constant value”  $C$  is not constant, but also a function of constituent quark orbital spin angular momentum.

As the quark orbital spin angular momentum contribution is a function of  $r^2$  ( $C = C'r^2$ ) the resulting effective confining potential ( $V(r)$ ) would be  $V(r) = C/r = C'r^2/r = C'r$ . Thus the quark contribution to the resultant strong gravity confining potential, i.e. *effective behavior*, can act like a  $r$  potential.

Phenomenologically/experimentally the essential requirement is that the *effective* confining behavior, not that the actual potential form, is  $r$  like. Though not rigorous, this shows the potential to produce the *effective*  $r$  like behavior.

## 12 The particle level gravity proposition

The particle level gravity proposition is not new. Back in the early days of the quark strong force conjecture, there also was a particle level gravity conjecture.

Nobel Prize winner Abdus Salam [4] and Recami [3], via two different particle level gravity approaches, show that both asymptotic freedom and confinement can result from this approach. Both of these two approaches lacked a source of or cause and thus were unable to produce any specific values.

As indicated by Ne’eman and Sijacki [12] “Long ago, we noted the existence of a link between Regge trajectories and what we then thought was plain gravity ... In nuclei, ... the quadrupolar nature of the SL(3,R), SU(3) and Eucl(3) sequences ... all of these features again characterize the action of a gravity like spin-2 effective gauge field. Overall the evidence for the existence of such an effective component in

QCD seems overwhelming”.

Note that a particle level gravity theory is a spin torsion intra-scale gravity theory that includes the curvature stress energy tensor. Thus its properties can differ from those associated with traditional inter-scale gravity theory. For example Yilmaz’s [14] attempt at inclusion of a gravity stress energy tensor term appears not to have the intra-scale “hard” event horizon associated with the inter-scale Kerr solution.

With respect to the SM, Sivaram [6] indicates that the Dirac spinor can gain mass via a strong gravity field.

Last but not least, in Sivaram’s paper [6] on the potential of the strong particle level gravity approach, Sivaram states; “It is seen that the form of the universal spin-spin contact interaction ... bears a striking resemblance to that of the familiar four-fermion contact interaction of Fermi’s theory of weak interactions. This suggests the possibility of identifying the coupling of spin and torsion to the vierbein strong gravitational field as the origin of the weak interaction”.

Sivaram’s association of Fermi’s weak theory with the coupling of spin and strong gravity is in keeping with Eq. (2) and the proposition in [5] that  $\alpha_{sg}$  is a theoretical definition of the SM charged particle weak mixing angle.

## 13 Why $h$ is constant and its value source

In particle physics,  $h$  is a constant of spin. However, the Standard Model does not answer the question, “Why does particle physics have the spin constant  $h$ ?”.

The answer naturally results from the real spin extent connection to strong gravity.

The spin extent is limited by the size of the particle. As real spin angular momentum energy is added to the particle, the coupling requires the particle size to contract resulting in extent contraction and resultant increase in frequency to conserve angular momentum, i.e. a spin constant. Field acceleration to a higher spin frequency results in extent contraction to match the higher spin frequency, i.e. a spin constant.

This is the observed Frequency Lorentzian nature of the photon, i.e energy dilation, (wave)length contraction and frequency dilation.

Thus the gravitational curvature constant constrains the spin constant via the coupling value of spin to strong gravity as given in Eq. (2).

## 14 Summary

To produce gravity’s weak value, string theory requires a bi-scale approach where gravity is an inter-scale property. This leads to the conjecture that there is also an intra-scale gravity at the same scale as the other particle forces.

There is also the additional proposition that there is a real spin strong particle level gravity relationship.

If this spin particle level gravity connection is correct then one would expect that it would produce the correct proton radius and it does.

One would also expect that either the  $\alpha_{sg}$  value or the  $\alpha_{cg}$  value should be a value within the Standard Model.

Not only does  $\alpha_{sg}$  match the charged particle weak angle, the pure theory  $\alpha_{sg(1)}$  matches the neutrino weak angle.

These propositions resolve the problem of the NuTeV [11] neutrino results being  $2.5\sigma$  from the SM  $\sin^2 \theta_W^{(on-shell)}$  value. The true  $\sin^2 \theta_W^{(on-shell)}$  is the Salam-Weinberg bare mass ratio which is near the NuTeV result and almost exactly  $\alpha_{sg(1)}$ .

As shown in [15] the FSC definition ( $\alpha_{cs}$ ) of this electro-gravitic approach matches an Einstein-Cartan FSC definition.

In keeping with [5], neither the quantization proposition nor the strong particle level gravity proposition are in conflict with the existence of quarks.

This particle level gravity approach does not require a new force form for the confinement of quarks and due to the spin strong gravity connection, can result in an *effective r* potential force for quark spin dominated unstable particles.

A strong gravity confinement source indicates that quarks can only exist inside high curvature particles thus giving a reason why quarks are not seen as free particles. The high curvature quark connection and the quark mass pattern indicates that the “measured” quark masses are not their base “invariant” mass values but decay point mass values. This proposition results in Regge trajectory like behavior.

Though the SM has had great numerical and behavioral success, its propositions (Higgs, QCD, etc.) result in fundamental problems like the Cosmological Constant Problem ( $10^{34+}$  off) and no excepted solution to the Matter Only Universe Problem, while not addressing the integration of gravity. Thus despite its numerical success, the SM has not solved the particle puzzle in all of its parts.

In [5], taking a non-standard view of the fundamental particle masses, the quantization proposition not only results in a single mass formula for the  $W$ ,  $p$ ,  $e$  and electron generations, it can solve the Cosmological Constant Problem and the Matter Only Universe Problem.

In this paper, the proposition of a real spin connection to the strong particle level gravity gives a source for the weak angle. This makes strong particle level gravity the “neutral current” and the foundation for the particle nature of particles.

These papers produce values for the  $W^\pm$  and  $Z^0$  mass and proton radius that are within the uncertainty in the measured values, naturally results in two weak angle values as experimentally observed, matches these values and explains why Nature has a spin angular momentum constant and thus show this approach potential. Also indicated is the potential of a bi-scalar approach to Nature which can solve the Hierarchy Problem and produce a particle scale Unification of Forces.

Submitted on January 12, 2009 / Accepted on January 18, 2010

## References

1. Antoniadis I., Arkani-Hamed N., Dimopoulos S., and Dvali G. New dimensions at a millimeter to a fermi and superstrings at a TeV. *Phys. Lett.*, 1998, v. B436, 257–263.
2. Arkani-Hamed N., Dimopoulos S., and Dvali G. The hierarchy problem and new dimensions at a millimeter. *Phys. Lett.*, 1998, v. B429, 263–272.
3. Recami E. and Tonin-Zanchin V. The strong coupling constant: its theoretical derivation from a geometric approach to hadron structure. *Found. Phys. Lett.*, 1994, v. 7(1), 85–92.
4. Salam A. and Sivaram C. Strong Gravity Approach to QCD and Confinement. *Mod. Phys. Lett.*, 1993, v. A8(4), 321–326.
5. Stone R.A. Is Fundamental Particle Mass  $4\pi$  Quantized? *Progress in Physics*, 2010, v. 1, 11–13.
6. Sivaram C. and Sinha K.P. Strong spin-two interactions and general relativity. *Phys. Rep.*, 1979, v. 51, 113–187 (p.152).
7. Particle Data Group, Physical Constants 2009. <http://pdg.lbl.gov/2009/constants/rpp2009-phys-constants.pdf>
8. Particle Data Group, Particle Listings, 2009. <http://pdg.lbl.gov/2009/listings/rpp2009-list-p.pdf>, [rpp2009-list-z-boson.pdf](http://pdg.lbl.gov/2009/listings/rpp2009-list-z-boson.pdf), [rpp2009-list-w-boson.pdf](http://pdg.lbl.gov/2009/listings/rpp2009-list-w-boson.pdf)
9. Sick I. On the rms-radius of the proton. *Phys. Lett.*, 2003, v. B576(1), 62–67; also arXiv: nucl-ex/0310008.
10. Ezhela V. and Polishchuk B. Reanalysis of e-p Elastic Scattering Data in Terms of Proton Electromagnetic Formfactors. arXiv: hep-ph/9912401.
11. Zeller G.P. et al. (NuTeV Collaboration) Precise Determination of Electroweak Parameters in Neutrino-Nucleon Scattering. *Phys. Rev. Lett.*, 2002, v. 88, 091802.
12. Ne’eman Y. and Sijacki Dj. Proof of pseudo-gravity as QCD approximation for the hadron IR region and  $J \sim M^2$  Regge trajectories. *Phys. Lett.*, 1992, v. B276(1), 173–178.
13. Sidharth B.G. A QCD generated mass spectrum. arXiv: physics/0309037.
14. Yilmaz H. Toward a Field Theory of Gravitation. *Il Nuovo Cimento*, 1992, v. B8, 941–959.
15. Stone R.A. An Einstein-Cartan Fine Structure Constant definition. *Progress in Physics*, 2010, v. 1, L8.

# A Derivation of Maxwell Equations in Quaternion Space

Vic Christianto\* and Florentin Smarandache†

\*Present address: Institute of Gravitation and Cosmology, PFUR, Moscow, 117198, Russia. E-mail: vxianto@yahoo.com

†Department of Mathematics, University of New Mexico, Gallup, NM 87301, USA. E-mail: smarand@unm.edu

Quaternion space and its respective Quaternion Relativity (it also may be called as Rotational Relativity) has been defined in a number of papers, and it can be shown that this new theory is capable to describe relativistic motion in elegant and straightforward way. Nonetheless there are subsequent theoretical developments which remains an open question, for instance to derive Maxwell equations in Q-space. Therefore the purpose of the present paper is to derive a consistent description of Maxwell equations in Q-space. First we consider a simplified method similar to the Feynman's derivation of Maxwell equations from Lorentz force. And then we present another derivation method using Dirac decomposition, introduced by Gersten (1998). Further observation is of course recommended in order to refute or verify some implication of this proposition.

## 1 Introduction

Quaternion space and its respective Quaternion Relativity (it also may be called as Rotational Relativity) has been defined in a number of papers including [1], and it can be shown that this new theory is capable to describe relativistic motion in elegant and straightforward way. For instance, it can be shown that the Pioneer spacecraft's Doppler shift anomaly can be explained as a relativistic effect of Quaternion Space [2]. The Yang-Mills field also can be shown to be consistent with Quaternion Space [1]. Nonetheless there are subsequent theoretical developments which remains an open issue, for instance to derive Maxwell equations in Q-space [1].

Therefore the purpose of the present article is to derive a consistent description of Maxwell equations in Q-space. First we consider a simplified method similar to the Feynman's derivation of Maxwell equations from Lorentz force. Then we present another method using Dirac decomposition, introduced by Gersten [6]. In the first section we will shortly review the basics of Quaternion space as introduced in [1].

Further observation is of course recommended in order to verify or refute the propositions outlined herein.

## 2 Basic aspects of Q-relativity physics

In this section, we will review some basic definitions of quaternion number and then discuss their implications to quaternion relativity (Q-relativity) physics [1].

Quaternion number belongs to the group of "very good" algebras: of real, complex, quaternion, and octonion, and normally defined as follows [1]

$$Q \equiv a + bi + cj + dk. \quad (1)$$

Where  $a, b, c, d$  are real numbers, and  $i, j, k$  are imaginary quaternion units. These Q-units can be represented either via  $2 \times 2$  matrices or  $4 \times 4$  matrices. There is quaternionic multiplication rule which acquires compact form [1]

$$1q_k = q_k1 = q_k, \quad q_jq_k = -\delta_{jk} + \epsilon_{jkn}q_n. \quad (2)$$

Where  $\delta_{kn}$  and  $\epsilon_{jkn}$  represents 3-dimensional symbols of Kronecker and Levi-Civita, respectively.

In the context of Quaternion Space [1], it is also possible to write the dynamics equations of classical mechanics for an inertial observer in constant Q-basis.  $SO(3, R)$ -invariance of two vectors allow to represent these dynamics equations in Q-vector form [1]

$$m \frac{d^2}{dt^2} (x_k q_k) = F_k q_k. \quad (3)$$

Because of antisymmetry of the connection (generalised angular velocity) the dynamics equations can be written in vector components, by conventional vector notation [1]

$$m (\ddot{\vec{a}} + 2\vec{\Omega} \times \dot{\vec{v}} + \vec{\Omega} \times \vec{r} + \dot{\vec{\Omega}} \times (\vec{\Omega} \times \vec{r})) = \vec{F}. \quad (4)$$

Therefore, from equation (4) one recognizes known types of classical acceleration, i.e. linear, coriolis, angular, centripetal.

From this viewpoint one may consider a generalization of Minkowski metric interval into biquaternion form [1]

$$dz = (dx_k + idt_k) q_k. \quad (5)$$

With some novel properties, i.e.:

- time interval is defined by imaginary vector;
- space-time of the model appears to have six dimensions (6D model);
- vector of the displacement of the particle and vector of corresponding time change must always be normal to each other, or

$$dx_k dt_k = 0. \quad (6)$$

One advantage of this Quaternion Space representation is that it enables to describe rotational motion with great clarity.

After this short review of Q-space, next we will discuss a simplified method to derive Maxwell equations from Lorentz force, in a similar way with Feynman's derivation method using commutative relation [3, 4].

### 3 An intuitive approach from Feynman's derivative

A simplified derivation of Maxwell equations will be discussed here using similar approach known as Feynman's derivation [3–5].

We can introduce now the Lorentz force into equation (4), to become

$$m \left( \frac{d\vec{v}}{dt} + 2\vec{\Omega} \times \vec{v} + \vec{\Omega} \times \vec{r} + \vec{\Omega} \times (\vec{\Omega} \times \vec{r}) \right) = q_{\otimes} \left( \vec{E} + \frac{1}{c} \vec{v} \times \vec{B} \right), \quad (7)$$

or

$$\left( \frac{d\vec{v}}{dt} \right) = \frac{q_{\otimes}}{m} \left( \vec{E} + \frac{1}{c} \vec{v} \times \vec{B} \right) - 2\vec{\Omega} \times \vec{v} - \vec{\Omega} \times \vec{r} - \vec{\Omega} \times (\vec{\Omega} \times \vec{r}). \quad (8)$$

We note here that  $q$  variable here denotes electric charge, not quaternion number.

Interestingly, equation (4) can be compared directly to equation (8) in [3]

$$m\ddot{x} = F - m \left( \frac{d\vec{v}}{dt} \right) + m\vec{r} \times \vec{\Omega} + m2\dot{x} \times \vec{\Omega} + m\vec{\Omega} \times (\vec{r} \times \vec{\Omega}). \quad (9)$$

In other words, we find an exact correspondence between quaternion version of Newton second law (3) and equation (9), i.e. the equation of motion for particle of mass  $m$  in a frame of reference whose origin has linear acceleration  $a$  and an angular velocity  $\vec{\Omega}$  with respect to the reference frame [3].

Since we want to find out an “electromagnetic analogy” for the inertial forces, then we can set  $F = 0$ . The equation of motion (9) then can be derived from Lagrangian  $L = T - V$ , where  $T$  is the kinetic energy and  $V$  is a velocity-dependent generalized potential [3]

$$V(x, \dot{x}, t) = ma \cdot x - m\dot{x} \cdot \vec{\Omega} \times x - \frac{m}{2} (\vec{\Omega} \times x)^2, \quad (10)$$

Which is a linear function of the velocities. We now may consider that the right hand side of equation (10) consists of a scalar potential [3]

$$\phi(x, t) = ma \cdot x - \frac{m}{2} (\vec{\Omega} \times x)^2, \quad (11)$$

and a vector potential

$$A(x, t) \equiv m\dot{x} \cdot \vec{\Omega} \times x, \quad (12)$$

so that

$$V(x, \dot{x}, t) = \phi(x, t) - \dot{x} \cdot A(x, t). \quad (13)$$

Then the equation of motion (9) may now be written in Lorentz form as follows [3]

$$m\ddot{x} = E(x, t) + x \times H(x, t) \quad (14)$$

with

$$E = -\frac{\partial A}{\partial t} - \nabla\phi = -m\Omega \times x - ma + m\Omega \times (x \times \Omega) \quad (15)$$

and

$$H = \nabla \times A = 2m\Omega. \quad (16)$$

At this point we may note [3, p. 303] that Maxwell equations are satisfied by virtue of equations (15) and (16). The correspondence between Coriolis force and magnetic force, is known from Larmor method. What is interesting to remark here, is that the same result can be expected directly from the basic equation (3) of Quaternion Space [1]. The aforementioned simplified approach indicates that it is indeed possible to find out Maxwell equations in Quaternion space, in particular based on our intuition of the direct link between Newton second law in Q-space and Lorentz force (We can remark that this parallel between classical mechanics and electromagnetic field appears to be more profound compared to simple similarity between Coulomb and Newton force).

As an added note, we can mention here, that the aforementioned Feynman's derivation of Maxwell equations is based on commutator relation which has classical analogue in the form of Poisson bracket. Then there can be a plausible way to extend directly this “classical” dynamics to quaternion extension of Poisson bracket, by assuming the dynamics as element of the type:  $r \in H \wedge H$  of the type:  $r = ai \wedge j + bi \wedge k + cj \wedge k$ , from which we can define Poisson bracket on  $H$ . But in the present paper we don't explore yet such a possibility.

In the next section we will discuss more detailed derivation of Maxwell equations in Q-space, by virtue of Gersten's method of Dirac decomposition [6].

### 4 A new derivation of Maxwell equations in Quaternion Space by virtue of Dirac decomposition

In this section we present a derivation of Maxwell equations in Quaternion space based on Gersten's method to derive Maxwell equations from one photon equation by virtue of Dirac decomposition [6]. It can be noted here that there are other methods to derive such a “quantum Maxwell equations” (i.e. to find link between photon equation and Maxwell equations), for instance by Barut quite a long time ago (see ICTP preprint no. IC/91/255).

We know that Dirac deduces his equation from the relativistic condition linking the Energy  $E$ , the mass  $m$  and the momentum  $p$  [7]

$$(E^2 - c^2 \vec{p}^2 - m^2 c^4) I^{(4)} \Psi = 0, \quad (17)$$

where  $I^{(4)}$  is the  $4 \times 4$  unit matrix and  $\Psi$  is a 4-component column (bispinor) wavefunction. Dirac then decomposes equation (17) by assuming them as a quadratic equation

$$(A^2 - B^2) \Psi = 0, \quad (18)$$

where

$$A = E, \quad (19)$$

$$B = c\vec{p} + mc^2. \quad (20)$$

The decomposition of equation (18) is well known, i.e.  $(A + B)(A - B) = 0$ , which is the basic of Dirac's decomposition method into  $2 \times 2$  unit matrix and Pauli matrix [6].

By virtue of the same method with Dirac, Gersten [6] found in 1998 a decomposition of one photon equation from relativistic energy condition (for massless photon [7])

$$\left(\frac{E^2}{c^2} - \vec{p}^2\right) I^{(3)} \Psi = 0, \quad (21)$$

where  $I^{(3)}$  is the  $3 \times 3$  unit matrix and  $\Psi$  is a 3-component column wavefunction. Gersten then found [6] equation (21) decomposes into the form

$$\left[\frac{E}{c} I^{(3)} - \vec{p} \cdot \vec{S}\right] \left[\frac{E}{c} I^{(3)} + \vec{p} \cdot \vec{S}\right] \vec{\Psi} - \begin{pmatrix} p_x \\ p_y \\ p_z \end{pmatrix} (\vec{p} \cdot \vec{\Psi}) = 0 \quad (22)$$

where  $\vec{S}$  is a spin one vector matrix with components [6]

$$S_x = \begin{pmatrix} 0 & 0 & 0 \\ 0 & 0 & -i \\ 0 & -i & 0 \end{pmatrix}, \quad (23)$$

$$S_y = \begin{pmatrix} 0 & 0 & i \\ 0 & 0 & 0 \\ -i & 0 & 0 \end{pmatrix}, \quad (24)$$

$$S_z = \begin{pmatrix} 0 & -i & 0 \\ -i & 0 & 0 \\ 0 & 0 & 0 \end{pmatrix}, \quad (25)$$

and with the properties

$$\left. \begin{aligned} [S_x, S_y] &= iS_z, & [S_x, S_z] &= iS_y \\ [S_y, S_z] &= iS_x, & \vec{S}^2 &= 2I^{(3)} \end{aligned} \right\}. \quad (26)$$

Gersten asserts that equation (22) will be satisfied if the two equations [6]

$$\left[\frac{E}{c} I^{(3)} + \vec{p} \cdot \vec{S}\right] \vec{\Psi} = 0, \quad (27)$$

$$\vec{p} \cdot \vec{\Psi} = 0 \quad (28)$$

are simultaneously satisfied. The Maxwell equations [8] will be obtained by substitution of  $E$  and  $p$  with the ordinary quantum operators (see for instance Bethe, *Field Theory*)

$$E \rightarrow i\hbar \frac{\partial}{\partial t} \quad (29)$$

and

$$p \rightarrow -i\hbar \nabla \quad (30)$$

and the wavefunction substitution

$$\vec{\Psi} = \vec{E} - i\vec{B}, \quad (31)$$

where  $E$  and  $B$  are electric and magnetic fields, respectively. With the identity

$$(\vec{p} \cdot \vec{S}) \vec{\Psi} = \hbar \nabla \times \vec{\Psi}, \quad (32)$$

then from equation (27) and (28) one will obtain

$$i \frac{\hbar}{c} \frac{\partial (\vec{E} - i\vec{B})}{\partial t} = -\hbar \nabla \times (\vec{E} - i\vec{B}), \quad (33)$$

$$\nabla \cdot (\vec{E} - i\vec{B}) = 0, \quad (34)$$

which are the Maxwell equations if the electric and magnetic fields are real [6, 7].

We can remark here that the combination of  $E$  and  $B$  as introduced in (31) is quite well known in literature [9, 10]. For instance, if we use positive signature in (31), then it is known as Bateman representation of Maxwell equations  $\text{div } \vec{\epsilon} = 0$ ,  $\text{rot } \vec{\epsilon} = \frac{\partial \epsilon}{\partial t}$ ,  $\epsilon = \vec{E} + i\vec{B}$ . But the equation (31) with negative signature represents the *complex nature* of electromagnetic fields [9], which indicates that these fields can also be represented in quaternion form.

Now if we represent in other form  $\vec{\epsilon} = \vec{E} - i\vec{B}$  as more conventional notation, then equation (33) and (34) will get a quite simple form

$$i \frac{\hbar}{c} \frac{\partial \vec{\epsilon}}{\partial t} = -\hbar \nabla \times \vec{\epsilon}, \quad (35)$$

$$\nabla \cdot \vec{\epsilon} = 0. \quad (36)$$

Now to consider quaternionic expression of the above results from Gersten [6], one can begin with the same linearization procedure just as in equation (5)

$$dz = (dx_k + idt_k) q_k, \quad (37)$$

which can be viewed as the quaternionic square root of the metric interval  $dz$

$$dz^2 = dx^2 - dt^2. \quad (38)$$

Now consider the relativistic energy condition (for massless photon [7]) similar to equation (21)

$$E^2 = p^2 c^2 \Rightarrow \left(\frac{E^2}{c^2} - \vec{p}^2\right) = k^2. \quad (39)$$

It is obvious that equation (39) has the same form with (38), therefore we may find its quaternionic square root too, then we find

$$k = (E_{qk} + i\vec{p}_{qk}) q_k, \quad (40)$$

where  $q$  represents the quaternion unit matrix. Therefore the linearized quaternion root decomposition of equation (21) can be written as follows [6]

$$\left[\frac{E_{qk} q_k}{c} I^{(3)} + i\vec{p}_{qk} q_k \cdot \vec{S}\right] \left[\frac{E_{qk} q_k}{c} I^{(3)} + i\vec{p}_{qk} q_k \cdot \vec{S}\right] \vec{\Psi} - \begin{pmatrix} p_x \\ p_y \\ p_z \end{pmatrix} (i\vec{p}_{qk} q_k \cdot \vec{\Psi}) = 0. \quad (41)$$

Accordingly, equation (41) will be satisfied if the two equations

$$\left[ \frac{E_{qk} q_k}{c} I^{(3)} + i \vec{p}_{qk} q_k \cdot \vec{S} \right] \vec{\Psi}_k = 0, \quad (42)$$

$$i \vec{p}_{qk} q_k \cdot \vec{\Psi}_k = 0 \quad (43)$$

are simultaneously satisfied. Now we introduce similar wavefunction substitution, but this time in quaternion form

$$\vec{\Psi}_{qk} = \vec{E}_{qk} - i \vec{B}_{qk} = \vec{\epsilon}_{qk}. \quad (44)$$

And with the identity

$$(\vec{p}_{qk} q_k \cdot \vec{S}) \vec{\Psi}_k = \hbar \nabla_k \times \vec{\Psi}_k. \quad (45)$$

Then from equations (42) and (43) one will obtain the *Maxwell equations in Quaternion-space* as follows

$$i \frac{\hbar}{c} \frac{\partial \vec{\epsilon}_{qk}}{\partial t} = -\hbar \nabla_k \times \vec{\epsilon}_{qk}, \quad (46)$$

$$\nabla_k \cdot \vec{\epsilon}_{qk} = 0. \quad (47)$$

Now the remaining question is to define quaternion differential operator in the right hand side of (46) and (47).

In this regards one can choose some definitions of quaternion differential operator, for instance the Moisil-Theodoresco operator [11]

$$D[\varphi] = \text{grad } \varphi = \sum_{k=1}^3 i_k \partial_k \varphi = i_1 \partial_1 \varphi + i_2 \partial_2 \varphi + i_3 \partial_3 \varphi. \quad (48)$$

where we can define  $i_1 = i$ ;  $i_2 = j$ ;  $i_3 = k$  to represent  $2 \times 2$  quaternion unit matrix, for instance. Therefore the differential of equation (44) now can be expressed in similar notation of (48)

$$D[\vec{\Psi}] = D[\vec{\epsilon}] = i_1 \partial_1 E_1 + i_2 \partial_2 E_2 + i_3 \partial_3 E_3 - i(i_1 \partial_1 B_1 + i_2 \partial_2 B_2 + i_3 \partial_3 B_3), \quad (49)$$

This expression indicates that both electric and magnetic fields can be represented in unified manner in a biquaternion form.

Then we define quaternion differential operator in the right-hand-side of equation (46) by an extension of the conventional definition of curl

$$\nabla \times A_{qk} = \begin{vmatrix} i & j & k \\ \frac{\partial}{\partial x} & \frac{\partial}{\partial y} & \frac{\partial}{\partial z} \\ A_x & A_y & A_z \end{vmatrix}. \quad (50)$$

To become its quaternion counterpart, where  $i, j, k$  represents quaternion matrix as described above. This quaternionic extension of curl operator is based on the known relation of

multiplication of two arbitrary complex quaternions  $q$  and  $b$  as follows

$$q \cdot b = q_0 b_0 - \langle \vec{q}, \vec{b} \rangle + [\vec{q} \times \vec{b}] + q_0 \vec{b} + b_0 \vec{q}, \quad (51)$$

where

$$\langle \vec{q}, \vec{b} \rangle := \sum_{k=1}^3 q_k b_k \in C, \quad (52)$$

and

$$[\vec{q} \times \vec{b}] := \begin{vmatrix} i & j & k \\ q_1 & q_2 & q_3 \\ b_1 & b_2 & b_3 \end{vmatrix}. \quad (53)$$

We can note here that there could be more rigorous approach to define such a quaternionic curl operator [10].

In the present paper we only discuss derivation of Maxwell equations in Quaternion Space using the decomposition method described by Gersten [6]. Further extension to Proca equations in Quaternion Space seems possible too using the same method [7], but it will not be discussed here.

In the next section we will discuss some physical implications of this new derivation of Maxwell equations in Quaternion Space.

## 5 A few implications: de Broglie's wavelength and spin

In the foregoing section we derived a consistent description of Maxwell equations in Q-Space by virtue of Dirac-Gersten's decomposition. Now we discuss some plausible implications of the new proposition.

First, in accordance with Gersten, we submit the viewpoint that the Maxwell equations yield wavefunctions which can be used as guideline for interpretation of Quantum Mechanics [6]. The one-to-one correspondence between classical and quantum wave interpretation actually can be expected not only in the context of Feynman's derivation of Maxwell equations from Lorentz force, but also from known exact correspondence between commutation relation and Poisson bracket [3,5]. Furthermore, the proposed quaternion yields to a novel viewpoint of both the wavelength, as discussed below, and also mechanical model of spin.

The equation (39) implies that momentum and energy could be expressed in quaternion form. Now by introducing de Broglie's wavelength  $\lambda_{DB} = \frac{\hbar}{p} \rightarrow p_{DB} = \frac{\hbar}{\lambda}$ , then one obtains an expression in terms of wavelength

$$k = (E_k + i \vec{p}_k) q_k = (E_k q_k + i \vec{p}_k q_k) = \left( E_k q_k + i \frac{\hbar}{\lambda_k^{DB}} q_k \right). \quad (54)$$

In other words, now we can express de Broglie's wavelength in a consistent Q-basis

$$\lambda_{DB-Q} = \frac{\hbar}{\sum_{k=1}^3 (p_k) q_k} = \frac{\hbar}{v_{group} \sum_{k=1}^3 (m_k) q_k}, \quad (55)$$

therefore the above equation can be viewed as an extended De Broglie wavelength in Q-space. This equation means that

the mass also can be expressed in Q-basis. In the meantime, a quite similar method to define quaternion mass has also been considered elsewhere, but it has not yet been expressed in Dirac equation form as presented here.

Further implications of this new proposition of quaternion de Broglie requires further study, and therefore it is excluded from the present paper.

## 6 Concluding remarks

In the present paper we derive a consistent description of Maxwell equations in Q-space. First we consider a simplified method similar to the Feynman's derivation of Maxwell equations from Lorentz force. And then we present another method to derive Maxwell equations by virtue of Dirac decomposition, introduced by Gersten [6].

In accordance with Gersten, we submit the viewpoint that the Maxwell equations yield wavefunctions which can be used as guideline for interpretation of quantum mechanics. The one-to-one correspondence between classical and quantum wave interpretation asserted here actually can be expected not only in the context of Feynman's derivation of Maxwell equations from Lorentz force, but also from known exact correspondence between commutation relation and Poisson bracket [3, 6].

A somewhat unique implication obtained from the above results of Maxwell equations in Quaternion Space, is that it suggests that the De Broglie wavelength will have quaternionic form. Its further implications, however, are beyond the scope of the present paper.

In the present paper we only discuss derivation of Maxwell equations in Quaternion Space using the decomposition method described by Gersten [6]. Further extension to Proca equations in Quaternion Space seems possible too using the same method [7], but it will not be discussed here.

This proposition, however, deserves further theoretical considerations. Further observation is of course recommended in order to refute or verify some implications of this result.

## Acknowledgements

One of the authors (VC) wishes to express his gratitude to Profs. A. Yefremov and M. Fil'chenkov for kind hospitality in the Institute of Gravitation and Cosmology, PFUR. Special thanks also to Prof. V. V. Kassandrov for excellent guide to Maxwell equations, and to Prof. Y. P. Rybakov for discussions on the interpretation of de Broglie's wavelength.

Submitted on December 11, 2009 / Accepted on January 02, 2010

## References

1. Yefremov A. Quaternions: algebra, geometry and physical theories. *Hypercomplex Numbers in Geometry and Physics*, 2004, v. 1(1), 105; arXiv: math-ph/0501055.
2. Smarandache F. and Christianto V. Less mundane explanation of Pioneer anomaly from Q-relativity. *Progress in Physics*, 2007, v. 3, no.1.
3. Hughes R.J. On Feynman's proof of the Maxwell equations. *Am. J. Phys.*, 1991, v. 60(4), 301.
4. Silagadze Z.K. Feynman's derivation of Maxwell equations and extra dimensions. *Annales de la Fondation Louis de Broglie*, 2002, v.27, no.2, 241.
5. Kauffmann L.H. Non-commutative worlds. arXiv: quant-ph/0403012.
6. Gersten A. Maxwell equations as the one photon quantum equation. *Found. Phys. Lett.*, 1998, v. 12, 291–298.
7. Gondran M. Proca equations derived from first principles. arXiv: quant-ph/0901.3300.
8. Terletsky Y.P., and Rybakov Y.P. *Electrodynamics*. 2nd. Ed., Vysshaya Skola, Moscow, 1990.
9. Kassandrov V.V. Singular sources of Maxwell fields with self-quantized electric charge. arXiv: physics/0308045.
10. Sabadini I., Struppa D.C. Some open problems on the analysis of Cauchy-Fueter system in several variables. A lecture given at Prof. Kawai's *Workshop Exact WKB Analysis and Fourier Analysis in Complex Domain*.
11. Kravchenko V. Quaternionic equation for electromagnetic fields in inhomogenous media. arXiv: math-ph/0202010.

## On Some Novel Ideas in Hadron Physics. Part II

Florentin Smarandache\* and Vic Christianto†

\*Department of Mathematics, University of New Mexico, Gallup, NM 87301, USA. E-mail: smarand@unm.edu

†Present address: Institute of Gravitation and Cosmology, PFUR, Moscow, 117198, Russia. E-mail: vxianto@yahoo.com

As a continuation of the preceding section, we shortly review a series of novel ideas on the physics of hadrons. In the present paper, emphasis is given on some different approaches to the hadron physics, which may be called as “programs” in the sense of Lakatos. For clarity, we only discuss geometrization program, symmetries/unification program, and phenomenology of inter-quark potential program.

### 1 Introduction

We begin the present paper by reiterating that given the extent and complexity of hadron and nuclear phenomena, any attempt for an exhaustive review of new ideas is outright unpractical. Therefore in this second part, we limit our short review on a number of scientific programs (in the sense of Lakatos). Others of course may choose different schemes or categorization. The main idea for this scheme of approaches was attributed to an article by Lipkin on hadron physics. accordingly, we describe the approaches as follows:

1. The geometrization approach, which was based on analogy between general relativity as strong field and the hadron physics;
2. Models inspired by (generalization of) symmetry principles;
3. Various composite hadron models;
4. The last section discusses phenomenological approach along with some kind of inter-quark QCD potential.

To reiterate again, the selection of topics is clearly incomplete, and as such it may not necessarily reflect the prevalent opinion of theorists working in this field (for more standard review the reader may wish to see [1]). Here the citation is far from being complete, because we only cite those references which appear to be accessible and also interesting to most readers.

Our intention here is to simply stimulate a healthy exchange of ideas in this active area of research, in particular in the context of discussions concerning possibilities to explore elementary particles beyond the Standard Model (as mentioned in a number of papers in recent years).

### 2 Geometrization approach

In the preceding section we have discussed a number of hadron or particle models which are essentially based on geometrical theories, for instance Kerr-Schild model or Topological Geometrical Dynamics [1].

However, we can view these models as part of more general approach which can be called “geometrization” program. The rationale of this approach can be summarized as follows (to quote Bruchholz): “The deeper reason is that the standard

model is based on Special Relativity while gravitation is the principal item of General Relativity” [2].

Therefore, if we follow this logic, then it should be clear that the Standard Model which is essentially based on Quantum Electrodynamics and Dirac equation, is mostly special relativistic in nature, and it only explains the weak field phenomena (because of its linearity). And if one wishes to extend these theories to explain the physical phenomena corresponding to the strong field effects (like hadrons), then one should consider the nonlinear effects, and therefore one begins to introduce nonlinear Dirac-Hartree-Fock equation or nonlinear Klein-Gordon equation (we mentioned this approach in the preceding section).

Therefore, for instance, if one wishes to include a consistent general relativistic approach as a model of strong fields, then one should consider the general covariant generalization of Dirac equation [3]

$$(i\gamma^k(x)\bar{\nabla}_k - m)\psi(x) = 0. \quad (1)$$

Where the gamma matrices are related to the 4-vector relative to General Coordinate Transformations (GCT). Then one can consider the interaction of the Dirac field with a scalar external field  $U$  which models a self-consistent quark system field (by virtue of changing  $m \rightarrow m + U$ ) [3].

Another worth-mentioning approach in this context has been cited by Bruchholz [2], i.e. the Geilhaupt’s theory which is based on some kind of Higgs field from GTR and Quantum Thermodynamics theory.

In this regards, although a book has been written discussing some aspects of the strong field (see Grib et al. [3]), actually this line of thought was recognized not so long ago, as cited in Jackson and Okun [4]: “The close mathematical relation between non-Abelian gauge fields and general relativity as connections in fiber bundles was not generally realized until much later”.

Then began the plethora of gauge theories, both including or without gravitational field. The essential part of these GTR-like theories is to start with the group of General Coordinate Transformations (GCT). It is known then that the finite dimensional representations of GCT are characterized by the corresponding ones of the  $SL(4, \mathbb{R})$  which belongs to  $GL(4, \mathbb{R})$  [5]. In this regards, Ne’eman played the pioneering

role in clarifying some aspects related to double covering of  $SL(n, R)$  by  $GL(n, R)$ , see for instance [6]. It can also be mentioned here that spinor  $SL(2, C)$  representation of GTR has been discussed in standard textbooks on General Relativity, see for instance Wald (1983). The  $SL(2, C)$  gauge invariance of Weyl is the most well-known, although others may prefer  $SL(6, C)$ , for instance Abdus Salam et al. [7].

Next we consider how in recent decades the progress of hadron physics was mostly driven by symmetries consideration.

### 3 Symmetries approach

Perhaps it is not quite an exaggeration to remark here that most subsequent developments in both elementary particle physics and also hadron physics were advanced by Yang-Mills' effort to generalize the gauge invariance [8]. And then Ne'eman and Gell-Mann also described hadrons into octets of  $SU(3)$  flavor group.

And therefore, it becomes apparent that there are numerous theories have been developed which intend to generalize further the Yang-Mills theories. We only cite a few of them as follows.

We can note here, for instance, that Yang-Mills field somehow can appear more or less quite naturally if one uses quaternion or hypercomplex numbers as basis. Therefore, it has been proved elsewhere that Yang-Mills field can be shown to appear naturally in Quaternion Space too [8].

Further generalization of Yang-Mills field has been discussed by many authors, therefore we do not wish to reiterate all of them here. Among other things, there are efforts to describe elementary particles (and hadrons) using the most generalized groups, such as  $E_8$  or  $E_{11}$ , see for instance [9].

Nonetheless, it can be mentioned in this regards, that there are other symmetries which have been considered (beside the  $SL(6, C)$  mentioned above), for instance  $U(12)$  which has been considered by Ishida and Ishida, as generalizations of  $SU(6)$  of Sakata, Gursey et al. [10].

One can note here that Gursey's approach was essentially to extend Wigner's idea to elementary particle physics using  $SU(2)$  symmetry. Therefore one can consider that Wigner has played the pioneering role in the use of groups and symmetries in elementary particles physics, although the mathematical aspects have been presented by Weyl and others.

### 4 Composite model of hadrons

Beside the group and symmetrical approach in Standard Model, composite model of quarks and leptons appear as an equivalent approach, as this method can be traced back to Fermi-Yang in 1949, Sakata in 1956, and of course the Gell-Mann-Ne'eman [10]. Nonetheless, it is well known that at that time quark model was not favorite, compared to the geometrical-unification program, in particular for the reason that the quarks have not been observed.

With regards to quarks, Sakata has considered in 1956 three basic hadrons (proton, neutron, and alphaparticle) and three basic leptons (electron, muon, neutrino). This Nagoya School was quite influential and the Sakata model was essentially transformed into the quark model of Gell-Mann, though with more abstract interpretation. It is perhaps more interesting to remark here, that Pauling's closed-packed spheron model is also composed of three sub-particles.

The composite models include but not limited to superconductor models inspired by BCS theory and NJL (Nambu-Jona-Lasinio theory). In this context, we can note that there are hadron models as composite bosons, and other models as composite fermions. For instance, hadron models based on BCS theory are essentially composite fermions. In developing his own models of composite hadron, Nambu put forward a scheme for the theory of the strong interactions which was based on and has resemblance with the BCS theory of superconductivity, where free electrons in superconductivity becomes hypothetical fermions with small mass; and energy gap of superconductor becomes observed mass of the nucleon. And in this regards, gauge invariance of superconductivity becomes chiral invariance of the strong interaction. Nambu's theory is essentially non-relativistic.

It is interesting to remark here that although QCD is the correct theory for the strong interactions it cannot be used to compute at all energy and momentum scales. For many purposes, the original idea of Nambu-Jona-Lasinio works better.

Therefore, one may say that the most distinctive aspect between geometrization program to describe hadron models and the composite models (especially Nambu's BCS theory), is that the first approach emphasizes its theoretical correspondence to the General Relativity, metric tensors etc., while the latter emphasizes analogies between hadron physics and the strong field of superconductors [3].

In the preceding section we have mentioned another composite hadron models, for instance the nuclear string and Brightsen cluster model. The relativistic wave equation for the composite models is of course rather complicated (compared to the 1-entity model of particles) [10].

### 5 Phenomenology with Inter-Quark potential

While nowadays most physicists prefer not to rely on the phenomenology to build theories, it is itself that has its own virtues, in particular in studying hadron physics. It is known that theories of electromagnetic fields and gravitation are mostly driven by some kind of geometrical principles. But to describe hadrons, one does not have much choices except to take a look at experiments data before begin to start theorizing, this is perhaps what Gell-Mann meant while emphasizing that physicists should sail between Scylla and Charybdis. Therefore one can observe that hadron physics are from the beginning affected by the plentitude of analogies with human senses, just to mention a few: strangeness, flavor and colour.

In other words one may say that hadron physics are more or less phenomenology-driven, and symmetries consideration comes next in order to explain the observed particles zoo.

The plethora of the aforementioned theories actually boiled down to either relativistic wave equation (Klein-Gordon) or non-relativistic wave equation, along with some kind of inter-quark potential. The standard picture of course will use the QCD linear potential, which can be derived from Maxwell equations.

But beside this QCD linear potential, there are other types of potentials which have been considered in the literature, to mention a few of them:

- a. Trigonometric Rosen-Morse potential [11]

$$v_r(|z|) = -2b \cot |z| + a(a+1)^2 \csc |z|, \quad (2)$$

where  $z = \frac{r}{a}$ ;

- b. PT-Symmetric periodic potential [12];  
 c. An Interquark qq-potential from Yang-Mills theory has been considered in [13];  
 d. An alternative PT-Symmetric periodic potential has been derived from radial biquaternion Klein-Gordon equation [14]. Interestingly, we can note here that a recent report by Takahashi et al. indicates that periodic potential could explain better the cluster deuterium reaction in Pd/PdO/ZrO<sub>2</sub> nanocomposite-samples in a joint research by Kobe University in 2008. This experiment in turn can be compared to a previous excellent result by Arata-Zhang in 2008 [15]. What is more interesting here is that their experiment also indicates a drastic mesoscopic effect of D(H) absorption by the Pd-nanocomposite-samples.

Of course, there is other type of interquark potentials which have not been mentioned here.

## 6 Concluding note

We extend a bit the preceding section by considering a number of approaches in the context of hadron theories. In a sense, they are reminiscent of the plethora of formulations that have been developed over the years on classical gravitation: many seemingly disparate approaches can be effectively used to describe and explore the same physics.

It can be expected that those different approaches of hadron physics will be advanced further, in particular in the context of possibility of going beyond Standard Model.

## Acknowledgements

One of the authors (VC) wishes to express his gratitude to Profs. A. Yefremov and M. Fil'chenkov for kind hospitality in the Institute of Gravitation and Cosmology, PFUR. Special thanks to Prof. A. Takahashi for discussion of his experimental results of Pd lattice with his team.

Submitted on December 10, 2009 / Accepted on January 01, 2010

## References

- Georgi H. Effective field theory, HUTP-93/A003. *Ann. Rev. Nucl. and Particle Sci.*, 1993, v.43.
- Bruchholz U.E. Key notes on a Geometric Theory of Fields. *Progress in Physics*, 2009, v.2, 107.
- Grib A., et al. Quantum vacuum effects in strong fields. Friedmann Lab. Publishing, St. Petersburg, 1994, pp.24–25.
- Jackson J.D. and Okun L.B. Historical roots of gauge invariance. *Rev. Mod. Phys.*, 2001, v.73, 676–677.
- Sijacki D.J. World spinors revisited. *Acta Phys. Polonica B*, 1998, v.29, no.4, 1089–1090.
- Ne'eman Y. Gravitational interactions of hadrons: band spinor representations of GL(n,R). *Proc. Natl. Acad. Sci. USA*, 1977, v.74, no.10, 4157–4159.
- Isham C.J., Salam A., and Strathdee J. SL(6,C) gauge invariance of Einstein-like Lagrangians. Preprint ICTP no.IC/72/123, 1972.
- Ch'yla J. From Hermann Weyl to Yang and Mills to Quantum Chromodynamics. *Nucl. Phys. A*, 2005, v.749, 23–32.
- Lisi A.G. An exceptionally simple theory of everything. arXiv: hep-th/0711.0770.
- Ishida S. and Ishida M. U(12): a new symmetry possibly realizing in hadron spectroscopy. arXiv: hep-ph/0203145.
- Compean C. and Kirchbach M. Trigonometric quark confinement potential of QCD traits. arXiv: hep-ph/0708.2521; nucl-th/0610001, quant-ph/0509055.
- Shalaby A.M. arXiv: hep-th/0712.2521.
- Zarembo K. arXiv: hep-th/9806150.
- Christianto V. and Smarandache F. Numerical solution of radial biquaternion Klein-Gordon equation. *Progress in Physics*, 2008, v.1.
- Takahashi A., et al. Deuterium gas charging experiments with Pd powders for excess heat evolution: discussion of experimental result. Abstract to JCF9, 2009.

# Lunar Laser-Ranging Detection of Light-Speed Anisotropy and Gravitational Waves

Reginald T. Cahill

School of Chemical and Physical Sciences, Flinders University, Adelaide 5001, Australia

E-mail: Reg.Cahill@flinders.edu.au

The Apache Point Lunar Laser-ranging Operation (APOLLO), in NM, can detect photon bounces from retroreflectors on the moon surface to 0.1ns timing resolution. This facility enables not only the detection of light speed anisotropy, which defines a local preferred frame of reference — only in that frame is the speed of light isotropic, but also fluctuations/turbulence (gravitational waves) in the flow of the dynamical 3-space relative to local systems/observers. So the APOLLO facility can act as an effective “gravitational wave” detector. A recently published small data set from November 5, 2007, is analysed to characterise both the average anisotropy velocity and the wave/turbulence effects. The results are consistent with some 13 previous detections, with the last and most accurate being from the spacecraft earth-flyby Doppler-shift NASA data.

## 1 Introduction

Light speed anisotropy has been repeatedly detected over more than 120 years, beginning with the Michelson-Morley experiment in 1887 [1]. Contrary to the usual claims, that experiment gave a positive result, and not a null result, and when the data was first analysed, in 2002, using a proper calibration theory for the detector [2, 3] an anisotropy speed, projected onto the plane of the gas-mode interferometer, in excess of 300 km/s was obtained. The problem was that Michelson had used Newtonian physics to calibrate the interferometer. When the effects of a gas in the light path and Lorentz contraction of the arms are taken into account the instrument turns out to be nearly 2000 times less sensitive than Michelson had assumed. In vacuum-mode the Michelson interferometer is totally insensitive to light speed anisotropy, which is why vacuum-mode resonant cavity experiments give a true null result [4]. These experiments demonstrate, in conjunction with the various non-null experiments, that the Lorentz contraction is a real contraction of physical objects, not that light speed is invariant. The anisotropy results of Michelson and Morley have been replicated in numerous experiments [5–15], using a variety of different experimental techniques. The most comprehensive early experiment was by Miller [5], and the direction of the anisotropy velocity obtained via his gas-mode Michelson interferometer has been recently confirmed, to within  $5^\circ$ , using [15] spacecraft earth-flyby Doppler shift data [16]. The same result is obtained using the range data — from spacecraft bounce times.

It is usually argued that light speed anisotropy would be in conflict with the successes of Special Relativity (SR), which supposedly is based upon the invariance of speed of light. However this claim is false because in SR the space and time coordinates are explicitly chosen to make the speed of light invariant wrt these coordinates. In a more natural choice of space and time coordinates the speed of light is anisotropic,

as discussed in [18]. Therein the new exact mapping between the Einstein-Minkowski coordinates and the natural space and time coordinates is given. So, rather than being in conflict with SR, the anisotropy experiments have revealed a deeper explanation for SR effects, namely physical consequences of the motion of quantum matter/radiation wrt a structured and dynamical 3-space. In 1890 Hertz [17] gave the form for the Maxwell equations for observers in motion wrt the 3-space, using the more-natural choice of space and time coordinates [18]. Other laboratory experimental techniques are being developed, such as the use of a Fresnel-drag anomaly in RF coaxial cables, see Fig. 6e in [15]. These experimental results, and others, have lead to a new theory of space, and consequently of gravity, namely that space is an observable system with a known and tested dynamical theory, and with gravity an emergent effect from the refraction of quantum matter and EM waves in an inhomogeneous and time-varying 3-space velocity field [19, 20]. As well all of these experiments show fluctuation effects, that is, the speed and direction of the anisotropy fluctuates over time [15, 20] — a form of turbulence. These are “gravitational waves”, and are very much larger than expected from General Relativity (GR). The observational data [15] determines that the solar system is in motion through a dynamical 3-space at an average speed of some 486 km/s in the direction  $RA = 4.29^h$ ,  $Dec = -75^\circ$ , essentially known since Miller’s extraordinary experiments in 1925/26 atop Mount Wilson. This is the motion of the solar system wrt a detected local preferred frame of reference (FoR) — an actual dynamical and structured system. This FoR is different to and unrelated to the FoR defined by the CMB radiation dipole, see [15].

Here we report an analysis of photon travel time data from the Apache Point Lunar Laser-ranging Operation (APOLLO) facility, Murphy *et al.* [21], for photon bounces from retroreflectors on the moon. This experiment is very similar to the spacecraft Doppler shift observations, and the results are con-

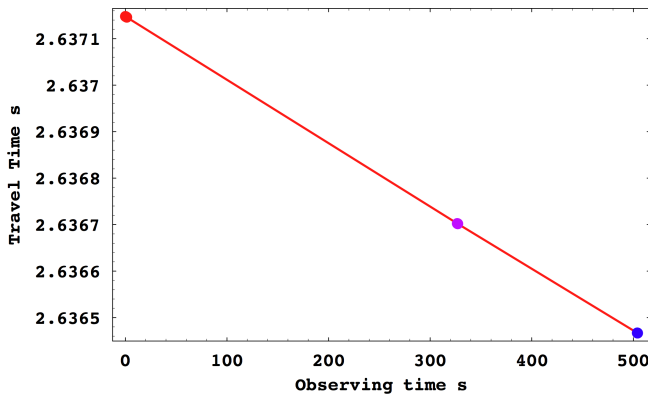


Fig. 1: Total photon travel times, in seconds, for moon bounces from APO, November 5, 2007, plotted against observing time, in seconds, after 1st shot at UTC = 0.5444 hrs. Shots 1–5 shown as 1st data point (size of graphic point unrelated to variation in travel time within each group of shots, typically  $\pm 20$  ns as shown in Fig. 2, shots 1100–1104 shown as middle point, and shots 2642–2636 shown in last graphic point. Data from Murphy [21], and tabulated in Gezari [22] (Table 1 therein). Straight line reveals linear time variation of bounce time vs observer time, over the observing period of some 500 s. Data reveals that distance travelled decreased by 204 m over that 500 s, caused mainly by rotation of earth. Data from shots 1000–1004 not used due to possible misprints in [22]. Expanded data points, after removal of linear trend, and with false zero for 1st shot in each group, are shown in Fig. 2. The timing resolution for each shot is 0.1 ns.

sistent with the anisotropy results from the above mentioned experiments, though some subtleties are involved, and also the presence of turbulence/ fluctuation effects are evident.

## 2 APOLLO lunar ranging data

Light pulses are launched from the APOLLO facility, using the 3.5-meter telescope at Apache Point Observatory (APO), NM. The pulses are reflected by the AP15RR retroreflector, placed on the moon surface during the Apollo 15 mission, and detected with a time resolution of 0.1 ns at the APOLLO facility. The APOLLO facility is designed to study fundamental physics. Recently Gezari [22] has published some bounce-time\* data, and performed an analysis of that data. The analysis and results herein are different from those in [22], as are the conclusions. The data is the bounce time recorded from 2036 bounces, beginning at UTC = 0.54444 hrs and ending at UTC = 0.55028 hrs on November 5, 2007†. Only a small subset of the data from these 2036 bounces is reported in [22], and the bounce times for 15 bounces are shown in Fig. 1, and grouped into 3 bunches‡. The bounce times, at the plot time resolution, show a linear time variation of bounce time vs observer time, presumably mainly caused by changing dis-

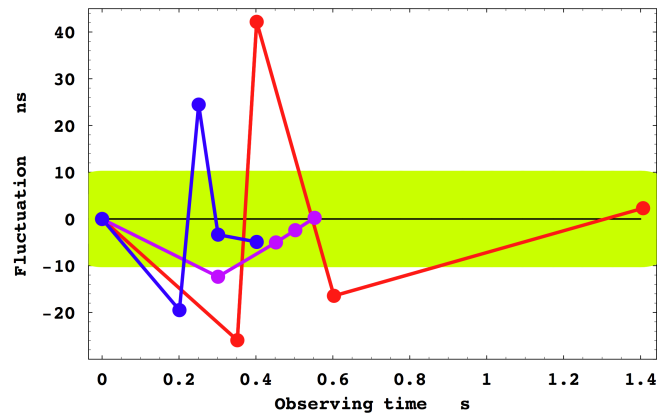


Fig. 2: Fluctuations in bounce time, in ns, within each group of shots, shown as one data point in Fig. 1, and plotted against time, in s, from time of 1st bounce in each group, and after removing the best-fit linear drift in each group, essentially the straight line in Fig. 1. The fluctuations are some  $\pm 20$  ns. Shaded region shows fluctuation range expected from dynamical 3-space and using spacecraft earth-flyby Doppler-shift NASA data [16] for 3-space velocity [15], and using a fluctuation in RA angle of, for example,  $3.4^\circ$  and a 3-space speed of 490 km/s. Fluctuations in only speed or declination of 3-space produce no measurable effect, because of orientation of 3-space flow velocity to APO-moon direction during these shots. These fluctuations suggest turbulence or wave effects in the 3-space flow. These are essentially “gravitational waves”, and have been detected repeatedly since the Michelson-Morley experiment in 1887; see [20] for plots of that fringe shift data.

tance between APO and retroreflector, which is seen to be decreasing over time of observation. Herein we consider only these bounce times, and not the distance modellings, which are based on the assumption that the speed of light is invariant, and so at best are pseudo-ranges.

Of course one would also expect that the travel times would be affected by the changing orientation of the APO-moon photon propagation directions wrt the light speed anisotropy direction. However a bizarre accident of date and timing occurred during these observations. The direction of the light-speed anisotropy on November 5 may be estimated from the spacecraft earth-flyby analysis, and from Fig. 11 of [15] we obtain  $RA=6.0^h$ ,  $Dec=-76^\circ$ , and with a speed  $\approx 490$  km/s. And during these APOLLO observations the direction of the photon trajectories was  $RA=11^h40'$ ,  $Dec=0^\circ3'$ . Remarkably these two directions are almost at right angles to each other ( $88.8^\circ$ ), and then the speed of 490 km/s has a projection onto the photon directions of a mere  $v_p = 11$  km/s.

From the bounce times, alone, it is not possible to extract the anisotropy velocity vector, as the actual distance to the retroreflector is not known. To do that a detailed modelling of the moon orbit is required, but one in which the invariance of the light speed is not assumed. In the spacecraft earth-flyby Doppler shift analysis a similar problem arose, and the resolution is discussed in [15] and [16], and there the asymptotic velocity of motion, wrt the earth, of the spacecraft changed

\*Total travel time to moon and back.

†The year of the data is not given in [22], but only in 2007 is the moon in the position reported therein at these UTC times.

‡An additional 5 shots (shot #1000-1004) are reported in [22] — but appear to have identical launch and travel times, and so are not used herein.

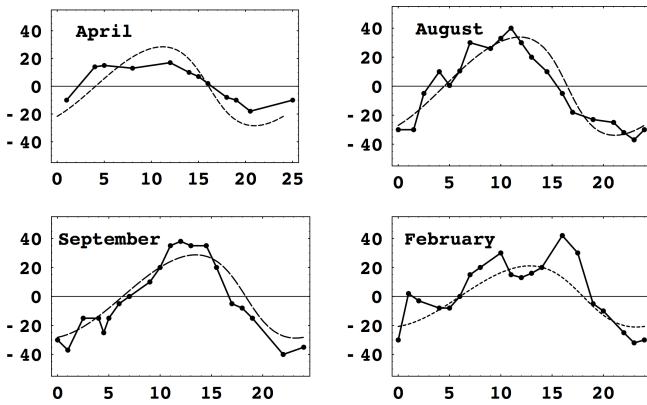


Fig. 3: Azimuth, in degrees, of 3-space flow velocity vs local sidereal time, in hrs, detected by Miller [5] using a gas-mode Michelson interferometer atop Mt Wilson in 1925/26. Each composite day is a collection of results from various days in each indicated month. In August, for example, the RA for the flow being NS (zero azimuth — here measured from S) is  $\approx 5$  hrs and  $\approx 17$  hrs. The dotted curves show expected results for the RA, determined in [19], for each of these months — these vary due to changing direction of orbital speed of earth and of sun-inflow speed, relative to cosmic speed of solar system, but without wave effects. The data shows considerable fluctuations, at the time resolution of these observations ( $\approx 1$  hr). These fluctuations are larger than the errors, given as  $\pm 2.5^\circ$  in [5].

from before to after the flyby, and as well there were various spacecraft with different orbits, and so light-speed anisotropy directional effects could be extracted.

### 3 Bounce-time data analysis

Herein an analysis of the bounce-time data is carried out to try and characterise the light speed anisotropy velocity. If the 3-space flow-velocity vector has projection  $v_p$  onto the photon directions, then the round-trip travel time, between co-moving source/reflector/detector system, shows a 2nd order effect in  $v_p/c$ , see Appendix,

$$t = \frac{2L}{c} + \frac{L v_p^2}{c^2} + \dots \quad (1)$$

where  $L$  is the actual 3-space distance travelled. The last term is the change in net travel time if the photons have speed  $c \pm v_p$ , relative to the moving system. There is also a 1st order effect in  $v_p/c$  caused by the relative motion of the APO site and the retroreflector, but this is insignificant, again because of the special orientation circumstance. These effects are partially hidden by moon orbit modelling if the invariance of light speed is assumed in that modelling. To observe these  $v_p$  effects one would need to model the moon orbit taking into account the various gravity effects, and then observing anomalies in net travel times over numerous orientations of the APO-moon direction, and sampled over a year of observations. However a more subtle effect is used now to extract some characterisation of the anisotropy velocity. In Fig. 2 we have extracted the travel time variations within each group

of 5 shots, by removing a linear drift term, and also using a false zero. We see that the net residual travel times fluctuate by some  $\pm 20$  ns. Such fluctuations are expected, because of the 3-space wave/turbulence effects that have been detected many times, although typically with much longer resolution times. These fluctuations arise from changes in the 3-space velocity, which means fluctuations in the speed, RA and Dec. Changes in speed and declination happen to produce insignificant effects for the present data, because of the special orientation situation noted above, but changes in RA do produce an effect. In Fig. 2 the shaded region shows the variations of 20 ns (plotted as  $\pm 10$ ns because of false zero) caused by a actual change in RA direction of  $+3.4^\circ$ . This assumes a 3-space speed of 490 km/s. Fig. 3 shows fluctuations in RA in the anisotropy vector from the Miller experiment [5]. We see fluctuations of some  $\pm 2$  hrs in RA ( $\equiv \pm 7.3^\circ$  at Dec  $= -76^\circ$ ), observed with a timing resolution of an hour or so. Other experiments show similar variations in RA from day to day, see Fig. 6 in [15], so the actual RA of  $6^h$  in November is not steady, from day to day, and the expected APOLLO time fluctuations are very sensitive to the RA. A fluctuation of  $+3^\circ$  is not unexpected, even over 3 s. So this fluctuation analysis appear to confirm the anisotropy velocity extracted from the earth-flyby Doppler-shift NASA data. However anisotropy observations have never been made over time intervals of the order of 1sec, as in Fig. 2, although the new 1st order in  $v_p/c$  coaxial cable RF gravitational wave detector under construction can collect data at that resolution.

### 4 Conclusions

The APOLLO lunar laser-ranging facility offers significant potential for observing not only the light speed anisotropy effect, which has been detected repeatedly since 1887, with the best results from the spacecraft earth-flyby Doppler-shift NASA data, but also wave/turbulence effects that have also been repeatedly detected, as has been recently reported, and which are usually known as “gravitational waves”\*. These wave effects are much larger than those putatively suggested within GR. Both the anisotropy effect and its fluctuations show that a dynamical and structured 3-space exists, but which has been missed because of two accidents in the development of physics, (i) that the Michelson interferometer is very insensitive to light speed anisotropy, and so the original small fringe shifts were incorrectly taken as a “null effect”, (ii) this in turn lead to the development of the 1905 Special Relativity formalism, in which the speed of light was forced to be invariant, by a peculiar choice of space and time coordinates, which together formed the spacetime construct. Maxwell’s EM equations use these coordinates, but Hertz as early as 1890 gave the more transparent form which use more

\*It may be shown that a dynamical 3-space velocity field may be mapped into a non-flat spacetime metric  $g_{\mu\nu}$  formalism, in that both produce the same matter acceleration, but that metric does not satisfy the GR equations [19,20]

natural space and time coordinates, and which explicitly takes account of the light-speed anisotropy effect, which was of course unknown, experimentally, to Hertz. Hertz had been merely resolving the puzzle as to why Maxwell's equations did not specify a preferred frame of reference effect when computing the speed of light relative to an observer. In the analysis of the small data set from APOLLO from November 5, 2007, the APO-moon photon direction just happened to be at  $90^\circ$  to the 3-space velocity vector, but in any case determination, in general, by APOLLO of that velocity requires subtle and detailed modelling of the moon orbit, taking account of the light speed anisotropy. Then bounce-time data over a year will show anomalies, because the light speed anisotropy vector changes due to motion of the earth about the sun, as 1st detected by Miller in 1925/26, and called the ‘‘apex aberration’’ by Miller, see [15]. An analogous technique resolved the earth-flyby spacecraft Doppler-shift anomaly [16]. Nevertheless the magnitude of the bounce-time fluctuations can be explained by changes in the RA direction of some  $3.4^\circ$ , but only if the light speed anisotropy speed is some 490 km/s. So this is an indirect confirmation of that speed. Using the APOLLO facility as a gravitational wave detector would not only confirm previous detections, but also provide time resolutions down to a few seconds, as the total travel time of some 2.64 s averages the fluctuations over that time interval. Comparable time resolutions will be possible using a laboratory RF coaxial cable wave/turbulence detector, for which a prototype has already been successfully operated. Vacuum-mode laboratory Michelson interferometers are of course insensitive to both the light speed anisotropy effect and its fluctuations, because of a subtle cancellation effect — essentially a design flaw in the interferometer, which fortunately Michelson, Miller and others avoided by using the detector in gas-mode (air) but without that understanding.

## Appendix

Fig. 4 shows co-moving Earth-Moon-Earth photon bounce trajectories in reference frame of 3-space. Define  $t_{AB} = t_B - t_A$  and  $t_{BC} = t_C - t_B$ . The distance AB is  $vt_{AB}$  and distance BC is  $vt_{BC}$ . Total photon-pulse travel time is  $t_{AC} = t_{AB} + t_{BC}$ . Applying the cosine theorem to triangles  $ABB'$  and  $CBB'$  we obtain

$$t_{AB} = \frac{vL \cos(\theta) + \sqrt{v^2 L^2 \cos^2(\theta) + L^2(c^2 - v^2)}}{(c^2 - v^2)}, \quad (2)$$

$$t_{BC} = \frac{-vL \cos(\theta) + \sqrt{v^2 L^2 \cos^2(\theta) + L^2(c^2 - v^2)}}{(c^2 - v^2)}. \quad (3)$$

Then to  $O(v^2/c^2)$

$$t_{AC} = \frac{2L}{c} + \frac{Lv^2(1 + \cos^2(\theta))}{c^3} + \dots \quad (4)$$

However the travel times are measured by a clock, located at the APO, travelling at speed  $v$  wrt the 3-space, and so undergoes a clock-slowdown effect. So  $t_{AC}$  in (4) must be reduced by the factor

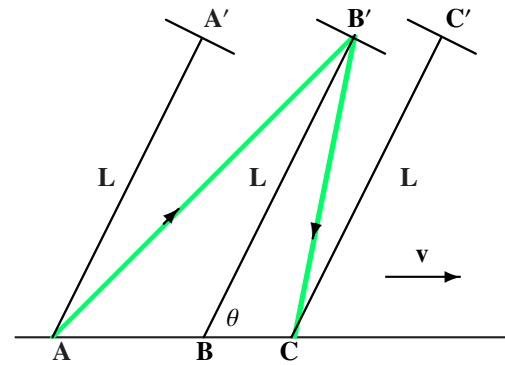


Fig. 4: Co-moving Earth-Moon-Earth photon bounce trajectories in reference frame of 3-space, so speed of light is  $c$  in this frame. Earth (APO) and Moon (retroreflector) here taken to have common velocity  $v$  wrt 3-space. When APO is at locations A,B,C, at times  $t_A, t_B, t_C, \dots$  the moon retroreflector is at corresponding locations  $A', B', C', \dots$  at same respective times  $t_A, t_B, t_C, \dots$ . Earth-Moon separation distance  $L$ , at same times, has angle  $\theta$  wrt velocity  $v$ , and shown at three successive times: (i) when photon pulse leaves APO at A (ii) when photon pulse is reflected at retroreflector at  $B'$ , and (iii) when photon pulse returns to APO at C.

$\sqrt{1 - v^2/c^2}$ , giving

$$t_{AC} = \frac{2L}{c} + \frac{Lv^2 \cos^2(\theta)}{c^3} + \dots = \frac{2L}{c} + \frac{Lv_P^2}{c^3} + \dots \quad (5)$$

where  $v_P$  is the velocity projected onto  $L$ . Note that there is no Lorentz contraction of the distance  $L$ . However if there was a solid rod separating  $AA'$  etc, as in one arm of a Michelson interferometer, then there would be a Lorentz contraction of that rod, and in the above we need to make the replacement  $L \rightarrow L \sqrt{1 - v^2 \cos^2(\theta)/c^2}$ , giving  $t_{AC} = 2L/c + O(v^2/c^2)$ . And then there is no dependence of the travel time on orientation or speed  $v$  to  $O(v^2/c^2)$ .

Applying the above to a laboratory vacuum-mode Michelson interferometer, as in [4], implies that it is unable to detect light-speed anisotropy because of this design flaw. The ‘‘null’’ results from such devices are usually incorrectly reported as proof of the invariance of the speed of light in vacuum. This design flaw can be overcome by using a gas or other dielectric in the light paths, as first reported in 2002 [2].

Submitted on January 14, 2010 / Accepted on January 25, 2010

## References

1. Michelson A.A. and Morley E.W. *Am. J. Sc.*, 1887, v.34, 333–345.
2. Cahill R.T. and Kitto K. Michelson-Morley experiments revisited. *Apeiron*, 2003, v.10(2), 104–117.
3. Cahill R.T. The Michelson and Morley 1887 experiment and the discovery of absolute motion. *Progress in Physics*, 2005, v.3, 25–29.
4. Braxmaier C. *et al. Phys. Rev. Lett.*, 2002, v.88, 010401; Müller H. *et al. Phys. Rev. D*, 2003, v.68, 116006-1-17; Müller H. *et al. Phys. Rev. D*, 2003, v.67, 056006; Wolf P. *et al. Phys. Rev. D*, 2004, v.70, 051902-1-4; Wolf P. *et al. Phys. Rev. Lett.*, 2003, v.90, no.6, 060402; Lipa J.A., *et al. Phys. Rev. Lett.*, 2003, v.90, 060403; Eisele Ch. *et al. Phys. Rev. Lett.*, 2009, v.103, 090401.
5. Miller D.C. *Rev. Mod. Phys.*, 1933, v.5, 203–242.
6. Illingworth K.K. *Phys. Rev.*, 1927, v.3, 692–696.

7. Joos G. *Ann. d. Physik*, 1930, v.7, 385.
8. Jaseja T.S. *et al. Phys. Rev. A*, 1964, v.133, 1221.
9. Torr D.G. and Kolen P. In *Precision Measurements and Fundamental Constants*, Taylor B.N. and Phillips W.D. eds., Natl. Bur. Stand. (U.S.), Special Publ., 1984, 617 and 675.
10. Krisher T.P., Maleki L., Lutes G.F., Primas L.E., Logan R.T., Anderson J.D. and Will C.M. Test of the isotropy of the one-way speed of light using hydrogen-maser frequency standards. *Phys. Rev. D*, 1990, v.42, 731–734.
11. Cahill R.T. The Roland DeWitte 1991 experiment. *Progress in Physics*, 2006, v.3, 60–65.
12. Cahill R.T. A new light-speed anisotropy experiment: absolute motion and gravitational waves detected. *Progress in Physics*, 2006, v.4, 73–92.
13. Munéra H.A., *et al.* In *Proceedings of SPIE*, 2007, v.6664, K1–K8, eds. Roychoudhuri C. *et al.*
14. Cahill R.T. Resolving spacecraft Earth-flyby anomalies with measured light speed anisotropy. *Progress in Physics*, 2008, v.4, 9–15.
15. Cahill R.T. Combining NASA/JPL one-way optical-fiber light-speed data with spacecraft Earth-flyby Doppler-shift data to characterise 3-space flow. *Progress in Physics*, 2009, v.4, 50–64.
16. Anderson J.D., Campbell J.K., Ekelund J.E., Ellis J. and Jordan J.F. Anomalous orbital-energy changes observed during spacecraft flybys of Earth. *Phys. Rev. Lett.*, 2008, v.100, 091102.
17. Hertz H. On the fundamental equations of electro-magnetics for bodies in motion. *Wiedemann's Ann.*, 1890, v.41, 369; also in: *Electric Waves, Collection of Scientific Papers*, Dover Publ., New York, 1962.
18. Cahill R.T. Unravelling Lorentz covariance and the spacetime formalism. *Progress in Physics*, 2008, v.4, 19–24.
19. Cahill R.T. Process physics: from information theory to quantum space and matter. Nova Science Publ., New York, 2005.
20. Cahill R.T. Dynamical 3-space: a review. In: *Ether Space-Time and Cosmology: New Insights into a Key Physical Medium*, Duffy M. and Lévy J., eds., Apeiron, 2009, p.135–200.
21. Murphy T.W. Jr., Adelberger E.G., Battat J.B.R., Carey L.N., Hoyle C.D., LeBlanc P., Michelsen E.L., Nordtvedt K., Orin A.E., Strasburg J.D., Stubbs C.W., Swanson H.E. and Williams E. APOLLO: the Apache Point Observatory Lunar laser-ranging operation: instrument description and first detections. *Publ. Astron. Soc. Pac.*, 2008, v.120, 20–37.
22. Gezari D.Y. Lunar laser ranging test of the invariance of  $c$ . arXiv: 0912.3934.

# Fundamental Elements and Interactions of Nature: A Classical Unification Theory

Tianxi Zhang

Department of Physics, Alabama A & M University, Normal, Alabama, USA. E-mail: tianxi.zhang@aamu.edu

A classical unification theory that completely unifies all the fundamental interactions of nature is developed. First, the nature is suggested to be composed of the following four fundamental elements: mass, radiation, electric charge, and color charge. All known types of matter or particles are a combination of one or more of the four fundamental elements. Photons are radiation; neutrons have only mass; protons have both mass and electric charge; and quarks contain mass, electric charge, and color charge. The nature fundamental interactions are interactions among these nature fundamental elements. Mass and radiation are two forms of real energy. Electric and color charges are considered as two forms of imaginary energy. All the fundamental interactions of nature are therefore unified as a single interaction between complex energies. The interaction between real energies is the gravitational force, which has three types: mass-mass, mass-radiation, and radiation-radiation interactions. Calculating the work done by the mass-radiation interaction on a photon derives the Einsteinian gravitational redshift. Calculating the work done on a photon by the radiation-radiation interaction derives a radiation redshift, which is much smaller than the gravitational redshift. The interaction between imaginary energies is the electromagnetic (between electric charges), weak (between electric and color charges), and strong (between color charges) interactions. In addition, we have four imaginary forces between real and imaginary energies, which are mass-electric charge, radiation-electric charge, mass-color charge, and radiation-color charge interactions. Among the four fundamental elements, there are ten (six real and four imaginary) fundamental interactions. This classical unification theory deepens our understanding of the nature fundamental elements and interactions, develops a new concept of imaginary energy for electric and color charges, and provides a possible source of energy for the origin of the universe from nothing to the real world.

## 1 Introduction

In the ancient times, the nature was ever considered to have five elements: space, wind, water, fire, and earth. In traditional Chinese Wu Xing (or five-element) theory, the space and wind are replaced by metal and wood. All the natural phenomena are described by the interactions of the five elements. There are two cycles of balances: generating (or sheng in Chinese) and overcoming (or ke in Chinese) cycles. The generating cycle includes that wood feeds fire, fire creates earth (or ash), earth bears metal, metal carries water, and water nourishes wood; while the overcoming cycle includes that wood parts earth, earth absorbs water, water quenches fire, fire melts metal, and metal chops wood.

According to the modern scientific view, how many elements does the nature have? How do these fundamental elements interact with each other? It is well known that there have been four fundamental interactions found in the nature. They are the gravitational, electromagnetic, weak, and strong interactions. The gravitational interaction is an interaction between masses. The electromagnetic interaction is an interaction between electric charges. The strong interaction is an interaction between color charges. What is the weak interaction? Elementary particles are usually classified into two

categories: hadrons and leptons. Hadrons participate in both strong and weak interactions, but leptons can only participate in the weak interaction. If the weak interaction is an interaction between weak charges, what is the weak charge? How many types of weak charges? Are the weak charges in hadrons different from those in leptons? Do we really need weak charges for the weak interaction? All of these are still unclear although the weak interaction has been extensively investigated for many decades. Some studies of particular particles show that the weak charges might be proportional to electric charges.

In this paper, we suggest that the nature has four fundamental elements, which are: mass  $M$ , radiation  $\gamma$ , electric charge  $Q$ , and color charge  $C$ . Any type of matter or particle contains one or more of these four elements. For instances, a neutron has mass only; a photon is just a type of radiation, which is massless; a proton contains both mass and electric charge; and a quark combines mass, electric charge, and color charge together. Mass and radiation are well understood as two forms of real energy. Electric charge is a property of some elementary particles such as electrons and protons and has two varieties: positive and negative. Color charge is a property of quarks, which are sub-particles of hadrons, and has three varieties: red, green, and blue. The nature funda-

mental interactions are the forces among these fundamental elements. The weak interaction is considered as an interaction between color charges and electric charges.

Recently, Zhang has considered the electric charge to be a form of imaginary energy [1]. With this consideration, the energy of an electrically charged particle is a complex number. The real part is proportional to the mass as the Einsteinian mass-energy expression represents, while the imaginary part is proportional to the electric charge. The energy of an antiparticle is given by conjugating the energy of its corresponding particle. Newton's law of gravity and Coulomb's law of electric force were classically unified into a single expression of the interaction between the complex energies of two electrically charged particles. Interaction between real energies (including both mass and radiation) is the gravitational force, which has three types: mass-mass, mass-radiation, and radiation-radiation interactions. Calculating the work done by the mass-radiation interaction on a photon, we derived the Einsteinian gravitational redshift. Calculating the work done by the radiation-radiation interaction on a photon, we obtained a radiation redshift, which is negligible in comparison with the gravitational redshift. Interaction between imaginary energies (or between electric charges) is the electromagnetic force.

In this study, we further consider the color charge to be another form of imaginary energy. Therefore, the nature is a system of complex energy and the four fundamental elements of nature are described as a complex energy. The real part includes the mass and radiation, while the imaginary part includes the electric and color charges. All the fundamental interactions can be classically unified into a single interaction between complex energies. The interaction between real energies is gravitational interaction. By including the massless radiation, we have three types of gravitational forces. The interaction between imaginary energies are electromagnetic (between electric charges), weak (between electric and color charges), and strong (between color charges) interactions. In addition, we have four types of imaginary forces (between real and imaginary energies): mass-electric charge interaction, radiation-electric charge interaction, mass-color charge interaction, and radiation-color charge interaction. Among the four fundamental elements, we have in total ten (six real and four imaginary) fundamental interactions.

## 2 Fundamental elements of Nature

### 2.1 Mass — a form of real energy

It is well known that mass is a fundamental property of matter, which directly determines the gravitational interaction via Newton's law of gravity [2]. Mass  $M$  is a quantity of matter [3], and the inertia of motion is solely dependent upon mass [4]. A body experiences an inertial force when it accelerates relative to the center of mass of the entire universe. In short, mass there affects inertia here.

According to Einstein's energy-mass expression (or Einstein's first law) [5], mass is also understood as a form of real energy. A rest object or particle with mass  $M$  has real energy given by

$$E^M = Mc^2, \quad (1)$$

where  $c$  is the speed of light. The real energy is always positive. It cannot be destroyed or created but can be transferred from one form to another.

### 2.2 Radiation — a form of real energy

Radiation  $\gamma$  refers to the electromagnetic radiation (or light). In the quantum physics, radiation is described as radiation photons, which are massless quanta of real energy [6]. The energy of a photon is given by

$$E^\gamma = h\nu, \quad (2)$$

where  $h = 6.6 \times 10^{-34} \text{ J}\cdot\text{s}$  is the Planck constant [7] and  $\nu$  is the radiation frequency from low frequency (e.g.,  $10^3 \text{ Hz}$ ) radio waves to high frequency (e.g.,  $10^{20} \text{ Hz}$ )  $\gamma$ -rays. Therefore, we can generally say that the radiation is also a form of real energy.

### 2.3 Electric charge — a form of imaginary energy

Electric charge is another fundamental property of matter, which directly determines the electromagnetic interaction via Coulomb's law of electric force [8], which is generalized to the Lorentz force expression for moving charged particles. Electric charge has two varieties of either positive or negative. It appears or is observed always in association with mass to form positive or negative electrically charged particles with different amount of masses. The interaction between electric charges, however, is completely independent of mass. Positive and negative charges can annihilate or cancel each other and produce in pair with the total electric charges conserved. Therefore, electric charge should have its own meaning of physics.

Recently, Zhang has considered the electric charge  $Q$  to be a form of imaginary energy [1]. The amount of imaginary energy is defined as

$$E^Q = \frac{Q}{\sqrt{G}}c^2, \quad (3)$$

where  $G$  is the gravitational constant. The imaginary energy has the same sign as the electric charge. Then, for an electrically charged particle, the total energy is

$$E = E^M + iE^Q = (1 + i\alpha)Mc^2. \quad (4)$$

Here,  $i = \sqrt{-1}$  is the imaginary number,  $\alpha$  is the charge-mass ratio defined by

$$\alpha = \frac{Q}{\sqrt{GM}}, \quad (5)$$

in the cgs unit system. Including the electric charge, we have modified Einstein's first law Eq. (1) into Eq. (4). In other words, electric charge is represented as an imaginary mass. For an electrically charged particle, the absolute value of  $\alpha$  is a big number. For instance, proton's  $\alpha$  is about  $10^{18}$  and electron's  $\alpha$  is about  $-2 \times 10^{21}$ . Therefore, an electrically charged particle holds a large amount of imaginary energy in comparison with its real or rest energy. A neutral particle such as a neutron, photon, or neutrino has only a real energy. Weinberg suggested that electric charges come from the fifth-dimension [9], a compact circle space in the Kaluza-Klein theory [10–12]. Zhang has shown that electric charge can affect light and gravity [13].

The energy of an antiparticle [14, 15] is naturally obtained by conjugating the energy of the corresponding particle [1]

$$E^* = (E^M + iE^Q)^* = E^M - iE^Q. \quad (6)$$

The only difference between a particle and its corresponding antiparticle is that their imaginary energies (thus their electric charges) have opposite signs. A particle and its antiparticle have the same real energy but have the sign-opposite imaginary energy. In a particle-antiparticle annihilation process, their real energies completely transfer into radiation photon energies and their imaginary energies annihilate or cancel each other. Since there are no masses to adhere, the electric charges come together due to the electric attraction and cancel each other (or form a positive-negative electric charge pair (+, -)). In a particle-antiparticle pair production process, the radiation photon energies transfer to rest energies with a pair of imaginary energies, which combine with the rest energies to form a particle and an antiparticle.

To describe the energies of all particles and antiparticles, we can introduce a two-dimensional energy space. It is a complex space with two axes denoted by the real energy  $E^M$  and the imaginary energy  $iE^Q$ . There are two phases in this two-dimensional energy space because the real energy is positive. In phase I, both real and imaginary energies are positive, while, in phase II, the imaginary energy is negative. Neutral particles including massless radiation photons are located on the real energy axis. Electrically charged particles are distributed between the real and imaginary energy axes. A particle and its antiparticle cannot be located in the same phase of the energy space. They distribute in two phases symmetrically with respect to the real energy axis.

The imaginary energy is quantized because the electric charge is so. Each electric charge quantum  $e$  has the following imaginary energy  $E_e = ec^2/\sqrt{G} \sim 10^{27}$  eV, which is about  $10^{18}$  times greater than proton's real energy (or the energy of proton's mass). Dividing the size of proton by the imaginary-real energy ratio ( $10^{18}$ ), we obtain a scale length  $l_Q = 10^{-33}$  cm, the size of the fifth-dimension in the Kaluza-Klein theory. In addition, this amount of energy is equivalent to a temperature  $T = 2E_e/k_B \sim 2.4 \times 10^{31}$  K with  $k_B$  the Boltzmann constant. In the epoch of big bang, the universe could

Names	Symbols	Masses	Electric Charge ( $e$ )
up	u	2.4 MeV	2/3
down	d	4.8 MeV	-1/3
charm	c	1.27 GeV	2/3
strange	s	104 MeV	-1/3
top	t	171.2 GeV	2/3
bottom	b	4.2 GeV	-1/3

Table 1: Properties of quarks: names, symbols, masses, and electric charges.

reach this high temperature. Therefore, big bang of the universe from nothing to a real world, if really occurred, might be a process that transfers a certain amount of imaginary energy to real energy. In the recently proposed black hole universe model, however, the imaginary-real energy transformation could not occur because of low temperature [16].

#### 2.4 Color charge — a form of imaginary energy

In the particle physics, all elementary particles can be categorized into two types: hadrons and leptons, in accord with whether they experience the strong interaction or not. Hadrons participate in the strong interaction, while leptons do not. All hadrons are composed of quarks. There are six types of quarks denoted as six different flavors: up, down, charm, strange, top, and bottom. The basic properties of these six quarks are shown in Table 1.

Color charge (denoted by  $C$ ) is a fundamental property of quarks [17], which has analogies with the notion of electric charge of particles. There are three varieties of color charges: red, green, and blue. An antiquark's color is antired, antigreen, or antiblue. Quarks and antiquarks also hold electric charges but the amount of electric charges are fractional such as  $\pm e/3$  or  $\pm 2e/3$ . An elementary particle is usually composed by two or more quarks or antiquarks and colorless with electric charge to be a multiple of  $e$ . For instance, a proton is composed by two up quarks and one down quarks ( $uud$ ); a neutron is composed by one up quark and two down quarks ( $udd$ ); a pion,  $\pi^+$ , is composed by one up quark and one down antiquark ( $u\bar{d}$ ); a charmed sigma,  $\Sigma_c^{++}$ , is composed by two up quarks and one charm quark ( $uu\bar{c}$ ); and so on.

Similar to electric charge  $Q$ , we can consider color charge  $C$  to be another form of imaginary energy. The amount of imaginary energy can be defined by

$$E^C = \frac{C}{\sqrt{G}} c^2. \quad (7)$$

Then, for a quark with mass  $M$ , electric charge  $Q$ , and color charge  $C$ , the total energy of the quark is

$$E = E^M + iE^Q + iE^C = [1 + i(\alpha + \beta)] Mc^2, \quad (8)$$

where  $\beta$  is given by

$$\beta = \frac{C}{\sqrt{GM}}. \quad (9)$$

The total energy of a quark is a complex number.

The energy of an antiquark is naturally obtained by conjugating the energy of the corresponding quark

$$\begin{aligned} E^* &= (E^M + iE^Q + iE^C)^* = E^M - iE^Q - iE^C = \\ &= [1 - i(\alpha + \beta)] Mc^2. \end{aligned} \quad (10)$$

The only difference between a quark and its corresponding antiquark is that their imaginary energies (thus their electric and color charges) have opposite signs. A quark and its antiquark have the same real energy and equal amount of imaginary energy but their signs are opposite. The opposite of the red, green, and blue charges are antired, antigreen, and antiblue charges.

To describe the energies of all particles and antiparticles including quarks and antiquarks, we can introduce a three-dimensional energy space. It is a complex space with three axes denoted by the real energy  $E^M$ , the electric imaginary energy  $iE^Q$ , and the color imaginary energy  $iE^C$ . There are four phases in this three-dimensional energy space. In phase I, all real and imaginary energies are positive; in phase II, the imaginary energy of electric charge is negative; in phase III, the imaginary energies of both electric and color charges are negative; and in phase IV, the imaginary energy of color charge is negative. Neutral particles including massless radiation photons are located on the real-energy axis. Electrically charged particles are distributed on the plane composed of the real-energy axis and the electric charge imaginary-energy axis. Quarks are distributed in all four phases. Particles and their antiparticles are distributed on the plane of the real-energy axis and the electric charge imaginary-energy axis symmetrically with respect to the real-energy axis. Quarks and their antiquarks are distributed in different phases by symmetrically with respect to the real-energy axis and separated by the plane of the real and electric imaginary energy axes.

### 3 Fundamental interactions of Nature

Fundamental interactions of nature are all possible interactions between the four fundamental elements of nature. Each of the four fundamental elements is a form of energy (either real or imaginary), the fundamental interactions can be unified as a single interaction between complex energies given by

$$\vec{F}_{EE} = -G \frac{E_1 E_2}{c^4 r^2} \hat{r}, \quad (11)$$

where  $E_1$  and  $E_2$  are the complex energy given by

$$E_1 = E_1^M + E_1^\gamma + i(E_1^Q + E_1^C), \quad (12)$$

$$E_2 = E_2^M + E_2^\gamma + i(E_2^Q + E_2^C). \quad (13)$$

Replacing  $E_1$  and  $E_2$  by using the energy expression (12) and (13), we obtain

$$\vec{F}_{EE} = \vec{F}_{RR} + \vec{F}_{II} + i\vec{F}_{RI} =$$

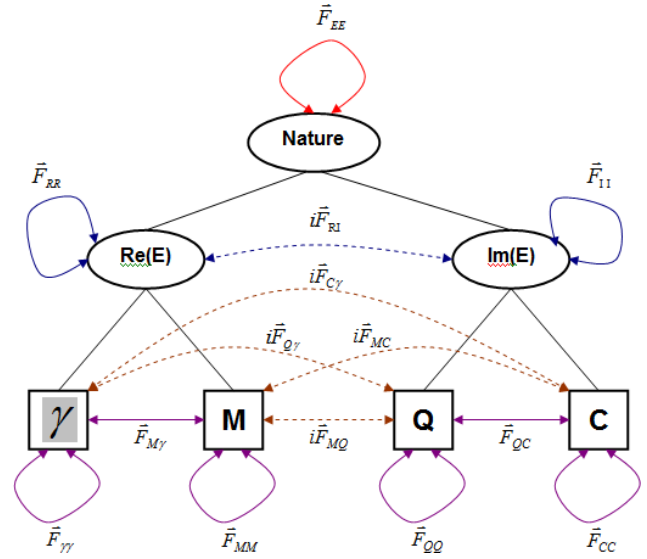


Fig. 1: Fundamental interactions among four fundamental elements of nature: mass, radiation, electric charge and color charge. Mass and radiation are real energies, while electric and color charges are imaginary energies. The nature is a system of complex energy and all the fundamental interactions of nature are classically unified into a single interaction between complex energies. There are six real and four imaginary interactions among the four fundamental elements.

$$\begin{aligned} &= -G \frac{M_1 M_2}{r^2} \hat{r} - G \frac{M_1 h\nu_2 + M_2 h\nu_1}{c^2 r^2} \hat{r} - G \frac{h\nu_1 h\nu_2}{c^4 r^2} \hat{r} + \\ &+ \frac{Q_1 Q_2}{r^2} \hat{r} + \frac{Q_1 C_2 + Q_2 C_1}{r^2} \hat{r} + \frac{C_1 C_2}{r^2} \hat{r} - \\ &- i\sqrt{G} \frac{M_1 Q_2 + M_2 Q_1}{r^2} \hat{r} - i\sqrt{G} \frac{M_1 C_2 + M_2 C_1}{r^2} \hat{r} - \\ &- i\sqrt{G} \frac{h\nu_1 Q_2 + h\nu_2 Q_1}{c^2 r^2} \hat{r} - i\sqrt{G} \frac{h\nu_1 C_2 + h\nu_2 C_1}{c^2 r^2} \hat{r} \equiv \\ &\equiv \vec{F}_{MM} + \vec{F}_{M\gamma} + \vec{F}_{\gamma\gamma} + \vec{F}_{QQ} + \vec{F}_{QC} + \vec{F}_{CC} + \\ &+ i\vec{F}_{MQ} + i\vec{F}_{MC} + i\vec{F}_{Q\gamma} + i\vec{F}_{C\gamma}. \end{aligned} \quad (14)$$

It is seen that the interaction between complex energies  $\vec{F}_{EE}$  is decoupled into the real-real energy interaction  $\vec{F}_{RR}$ , the imaginary-imaginary energy interaction  $\vec{F}_{II}$ , and the real-imaginary energy interaction  $i\vec{F}_{RI}$ . The real-real energy interaction  $\vec{F}_{RR}$  is decoupled into the mass-mass interaction  $\vec{F}_{MM}$ , the radiation-radiation interaction  $\vec{F}_{\gamma\gamma}$ , and the mass-radiation interaction  $\vec{F}_{M\gamma}$ . The imaginary-imaginary energy interaction  $\vec{F}_{II}$  is decoupled into the interaction between electric charges  $\vec{F}_{QQ}$ , the interaction between color charges  $\vec{F}_{CC}$ , and the interaction between electric and color charges  $\vec{F}_{QC}$ . The real-imaginary energy interaction  $i\vec{F}_{RI}$  is decoupled into the mass-electric charge interaction  $i\vec{F}_{MQ}$ , the mass-color charge interaction  $i\vec{F}_{MC}$ , the radiation-electric charge interaction  $i\vec{F}_{Q\gamma}$ , the radiation-color charge interaction  $i\vec{F}_{C\gamma}$ . All these interactions as shown in Eq. (14) can be represented by Figure 1 or Table 2.

	$M$	$\gamma$	iQ	iC
$M$	$\vec{F}_{MM}$	$\vec{F}_{M\gamma}$	$i\vec{F}_{MQ}$	$i\vec{F}_{MC}$
$\gamma$		$\vec{F}_{\gamma\gamma}$	$i\vec{F}_{Q\gamma}$	$i\vec{F}_{C\gamma}$
iQ			$\vec{F}_{QQ}$	$\vec{F}_{QC}$
iC				$\vec{F}_{CC}$

Table 2: Fundamental elements and interactions of nature.

### 3.1 Gravitational force

The force  $\vec{F}_{MM}$  represents Newton’s law for the gravitational interaction between two masses. This force governs the orbital motion of the solar system. The force  $\vec{F}_{M\gamma}$  is the gravitational interaction between mass and radiation. The force  $\vec{F}_{\gamma\gamma}$  is the gravitational interaction between radiation and radiation. These three types of gravitational interactions are categorized from the interaction between real energies (see Figure 3 of [1]).

Calculating the work done by this mass-radiation force on a photon, we can derive the Einsteinian gravitational redshift without using the Einsteinian general relativity

$$Z_G = \frac{\lambda_o - \lambda_e}{\lambda_e} = \exp\left(\frac{GM}{c^2 R}\right) - 1. \tag{15}$$

In the weak field approximation, it reduces

$$Z_G \approx \frac{GM}{c^2 R}. \tag{16}$$

Similarly, calculating the work done on a photon from an object by the radiation-radiation gravitation  $\vec{F}_{\gamma\gamma}$ , we obtain a radiation redshift,

$$Z_\gamma = \frac{4GM}{15c^5} \sigma AT_c^4 + \frac{G}{c^5} \sigma AT_s^4, \tag{17}$$

where  $\sigma$  is the Stepan-Boltzmann constant,  $A$  is the surface area,  $T_c$  is the temperature at the center,  $T_s$  is the temperature on the surface. Here we have assumed that the inside temperature linearly decreases from the center to the surface. The radiation redshift contains two parts. The first term is contributed by the inside radiation. The other is contributed by the outside radiation. The redshift contributed by the outside radiation is negligible because  $T_s \ll T_c$ .

The radiation redshift derived here is significantly small in comparison with the empirical expression of radiation redshift proposed by Finlay-Freundlich [18]. For the Sun with  $T_c = 1.5 \times 10^7$  K and  $T_s = 6 \times 10^3$  K, the radiation redshift is only about  $Z_\gamma = 1.3 \times 10^{-13}$ , which is much smaller than the gravitational redshift  $Z_G = 2.1 \times 10^{-6}$ .

### 3.2 Electromagnetic force

The force  $\vec{F}_{QQ}$  represents Coulomb’s law for the electromagnetic interaction between two electric charges. Electric charges have two varieties and thus three types of interactions: 1) repelling between positive electric charges  $\vec{F}_{++}$ ,

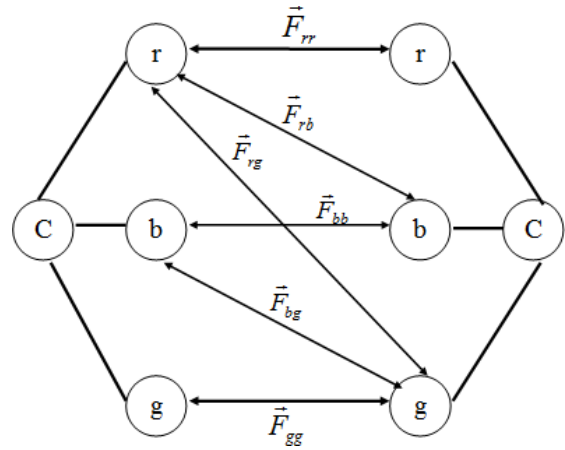


Fig. 2: Six types of strong interactions between color charges: red-red, green-green, blue-blue, red-green, red-blue, and green-blue interactions.

2) repelling between negative electric charges  $\vec{F}_{--}$ , and 3) attracting between positive and negative electric charges  $\vec{F}_{+-}$ . Figure 2 of [1] shows the three types of Coulomb interactions between two electric charges.

### 3.3 Strong force

The force  $\vec{F}_{CC}$  is the strong interaction between color and color charges. Color charges have three varieties: red, blue, and green and thus six types of interactions: 1) the red-red interaction  $\vec{F}_{rr}$ , 2) the blue-blue interaction  $\vec{F}_{bb}$ , 3) the green-green interaction  $\vec{F}_{gg}$ , 4) the red-blue interaction  $\vec{F}_{rb}$ , 5) the red-green interaction  $\vec{F}_{rg}$ , and 6) the blue-green interaction  $\vec{F}_{bg}$ . Figure 2 shows these six types of color interactions.

Considering the strong interaction to be asymptotically free [19], we replace the color charge by

$$C \rightarrow rC; \tag{18}$$

this assumption represents that the color charge becomes less colorful if it is closer to each other, i.e., asymptotically colorless. Then the strong interaction between color charges can be rewritten by

$$\vec{F}_{CC} = C_1 C_2 \hat{r}, \tag{19}$$

which is independent of the radial distance and consistent with measurement.

The strong interaction is the only one that can change the color of quarks in a hadron. A typical strong interaction is proton-neutron scattering,  $p + n \rightarrow n + p$ . This is an interaction between the color charge of one up quark in proton and the color charge of one down quark in neutron via exchanging a  $\pi^+$ ,  $u + d \rightarrow d + u$  (see Figure 2). In other words, during this proton-neutron scattering an up quark in the proton changes into a down quark by emitting a  $\pi^+$ , meanwhile a down quark in the neutron changes into an up quark by absorbing the  $\pi^+$ . Another typical strong interaction is delta decay,  $\Delta^0 \rightarrow p + \pi^-$ . This is an interaction between the color

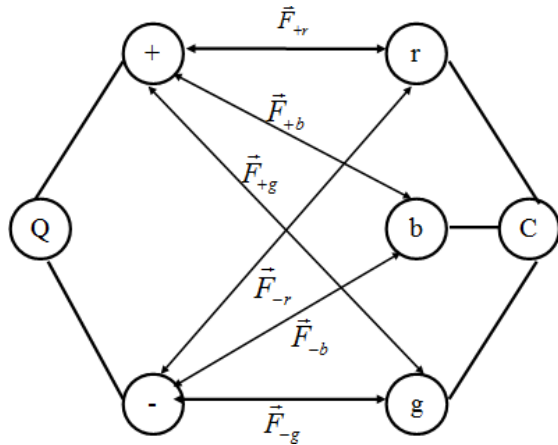


Fig. 3: Six types of weak interactions between electric and color charges: positive-red, positive-green, positive-blue, negative-red, negative-green, and negative-blue interactions.

charge of one down quark and the color charges of the other two quarks. In this interaction, a down quark emits a  $\pi^-$  and then becomes a up quark,  $d \rightarrow u + \pi^-$ .

### 3.4 Weak force

The force  $\vec{F}_{QC}$  is the weak interaction between electric and color charges. Considering electric charges with two varieties (positive and negative) and color charges with three varieties (red, blue, and green), we have also six types of weak interaction: 1) the positive-red interaction  $\vec{F}_{+r}$ , 2) the positive-blue interaction  $\vec{F}_{+b}$ , 3) the positive-green interaction  $\vec{F}_{+g}$ , 4) the negative-red interaction  $\vec{F}_{-r}$ , 5) the negative-blue interaction  $\vec{F}_{-b}$ , and 6) the negative-green interaction  $\vec{F}_{-g}$ . Figure 3 shows these six types of electric-color charge interactions.

Considering equation (18), we can represent the weak interaction by

$$\vec{F}_{QC} = \frac{QC}{r} \hat{r}, \quad (20)$$

which is inversely proportional to the radial distance and consistent with measurement.

The weak interaction is the only one that can change the flavors of quarks in a hadron. A typical weak interaction is the neutron decay,  $n \rightarrow p + e^- + \bar{\nu}_e$ . In this process, a down quark in the neutron changes into an up quark by emitting  $W^-$  boson, which lives about  $10^{-26}$  seconds and then breaks into a high-energy electron and an electron antineutrino, i.e.,  $d \rightarrow u + W^-$  and then  $W^- \rightarrow u + e^- + \bar{\nu}_e$ . There are actually two interactions involved in this neutron decay. One is the interaction between electric and color charges inside the down quark, which is changed into an up quark by emitting a  $W^-$  boson. Another is the interaction inside  $W^-$ , which is broken into an electron and an electron antineutrino. Since  $W^-$  is composed of an up antiquark and a down quark ( $\bar{u}d$ ), we suggest that the down quark changes into an up quark by emitting an electron and then the up antiquark and the up quark annihilate into an electron antineutrino. It should be noted that an

upper antiquark and an up quark usually forms an  $\eta$  particle, which may live about a few tens of nanoseconds and decay into other particles such as photons and pions, which further decay to nuons and nuon neutrinos and antineutrinos. The formation of  $\eta$  and decay to photons and pions may explain the solar neutrino missing problem and neutrino oscillations, the detail of which leaves for a next study.

### 3.5 Imaginary force

The other terms with the imaginary number in Eq. (14) are imaginary forces between real and imaginary energies. These imaginary forces should play essential roles in combining or separating imaginary energies with or from real energies. The physics of imaginary forces needs further investigations.

## 4 Summary

As a summary, we have appropriately suggested mass, radiation, electric charge, and color charge as the four fundamental elements of nature. Mass and radiation are two types of real energy, while electric and color charges are considered as two forms of imaginary energy. we have described the nature as a system of complex energy and classically unified all the fundamental interactions of nature into a single interaction between complex energies. Through this classical unification theory, we provide a more general understanding of nature fundamental elements and interactions, especially the weak interaction as an interaction between electric and color charges without assuming a weak charge. The interaction between real energies is the gravitational force, which has three types: mass-mass, mass-radiation, and radiation-radiation interactions. Calculating the work done by the mass-radiation gravitation on a photon derives the Einsteinian gravitational redshift. Calculating the work done on a photon from an object by the radiation-radiation gravitation derives a radiation redshift, which is much smaller than the gravitational redshift. The interaction between imaginary energies is the electromagnetic (between electric charges), weak (between electric and color charges), and strong (between color charges) interactions. In addition, we have four imaginary forces between real and imaginary energies, which are mass-electric charge, radiation-electric charge, mass-color charge, and radiation-color charge interactions. Therefore, among the four fundamental elements, we have in total ten (six real and four imaginary) fundamental interactions. In addition, we introduce a three-dimensional energy space to describe all types of matter or particles including quarks and antiquarks.

### Acknowledgement

This work was supported by the Title III program of Alabama A & M University, the NASA Alabama EPSCoR Seed grant (NNX07AL52A), and the National Natural Science Foundation of China (G40890161).

Submitted on January 21, 2010 / Accepted on January 25, 2010

**References**

1. Zhang T.X. Electric charge as a form of imaginary energy. *Progress in Phys.*, 2008, v.2, 79–83.
  2. Newton I. Mathematical principles of nature philosophy. Book III 1687.
  3. Hoskins L.M. Mass as quantity of matter. *Science*, 1915, v.42, 340–341.
  4. Mach E. The science of mechanics. Reprinted by Open Court Pub. Co., 1960.
  5. Einstein A. Ist die Trägheit eines Körpers von seinem Energieinhalt abhängig? *Ann. Phys.*, 1905, v.323, 639–641.
  6. Einstein A. Über einen die Erzeugung und Verwandlung des Lichtes betreffenden heuristischen Gesichtspunkt. *Ann. Phys.*, 1905, v.322, 132–148.
  7. Planck M. Ueber das Gesetz der Energieverteilung im Normalspectrum. *Ann. Phys.*, 1901, v.309, 553–563.
  8. Coulomb C. Theoretical research and experimentation on torsion and the elasticity of metal wire. *Ann. Phys.*, 1802, v.11, 254–257.
  9. Weinberg S. The first three minutes. Basic Books, New York, 1977.
  10. Kaluza T. On the problem of unity in physics. *Sitz. Preuss. Akad. Wiss. Berlin*, Berlin, 1921, 966–972.
  11. Klein O. Quantum theory and five dimensional theory of relativity. *Z. Phys.*, 1926a, v.37, 895–906.
  12. Klein O. The atomicity of electricity as a quantum theory law. *Nature*, 1926b, v.118, 516–520.
  13. Zhang T.X. Electric redshift and quasars. *Astrophys. J. Letters*, 2006, v.636, 61–64.
  14. Dirac P.A.M. The quantum theory of the electron. *Proc. R. Soc. London A*, 1928, v.117, 610–624.
  15. Anderson C.D. The positive electron. *Phys. Rev.*, 1933, v.43, 491–498.
  16. Zhang T.X. A new cosmological model: black hole universe. *Progress in Phys.*, 2009, v.3, 3–11.
  17. Veltman M. Facts and mysteries in elementary particle physics. World Scientific Pub. Co. Pte. Ltd., 2003.
  18. Finlay-Freundlich E. Red shift in the spectra of celestial bodies. *Phyl. Mag.*, 1954, v.45, 303–319.
  19. Gross D.J. and Wilczek F. Asymptotically free gauge theories I. *Phys. Rev. D*, 1973, v.8, 3633–3652.
-

## The Solar System According to General Relativity: The Sun's Space Breaking Meets the Asteroid Strip

Larissa Borissova

E-mail: borissova@ptep-online.com

This study deals with the exact solution of Einstein's field equations for a sphere of incompressible liquid without the additional limitation initially introduced in 1916 by Schwarzschild, by which the space-time metric must have no singularities. The obtained exact solution is then applied to the Universe, the Sun, and the planets, by the assumption that these objects can be approximated as spheres of incompressible liquid. It is shown that gravitational collapse of such a sphere is permitted for an object whose characteristics (mass, density, and size) are close to the Universe. Meanwhile, there is a spatial break associated with any of the mentioned stellar objects: the break is determined as the approaching to infinity of one of the spatial components of the metric tensor. In particular, the break of the Sun's space meets the Asteroid strip, while Jupiter's space break meets the Asteroid strip from the outer side. Also, the space breaks of Mercury, Venus, Earth, and Mars are located inside the Asteroid strip (inside the Sun's space break).

The main task of this paper is to study the possibilities of applying condensed matter models in astrophysics and cosmology. A cosmic object consisting of condensed matter has a constant volume and a constant density. A sphere of incompressible liquid, being in the weightless state (as any cosmic object), is a kind of condensed matter. Thus, assuming that a star is a sphere of incompressible liquid, we can study the gravitational field of the star inside and outside it.

The Sun orbiting the center of the Galaxy meets the weightless condition (see [1] for detail)

$$\frac{GM}{r} = v^2,$$

where  $G = 6.67 \times 10^{-8} \text{ cm}^3/\text{g} \times \text{sec}^2$  is the Newtonian gravitational constant,  $M$  is the mass of the Galaxy,  $r$  is the distance of the Sun from the center of the Galaxy, and  $v$  is the Sun's velocity in its orbit. The planets of the Solar System also satisfy the weightless condition. Assuming that the planets have a similar internal constitution as the Sun, we can consider these objects as spheres of incompressible liquid being in a weightless state.

I will consider the problems by means of the General Theory of Relativity. First, it is necessary to obtain the exact solution of the Einstein field equations for the space-time metric induced by the gravitational field of a sphere of incompressible liquid.

The regular field equations of Einstein, with the  $\lambda$ -field neglected, have the form

$$R_{\alpha\beta} - \frac{1}{2} g_{\alpha\beta} R = -\kappa T_{\alpha\beta}, \quad (1)$$

where  $R_{\alpha\beta}$  is the Ricci tensor,  $R$  is the Riemann curvature scalar,  $\kappa = \frac{8\pi G}{c^2} = 18.6 \times 10^{-28} \text{ cm/g}$  is the Einstein gravitational constant,  $T_{\alpha\beta}$  is the energy-momentum tensor, and  $\alpha, \beta =$

0, 1, 2, 3 are the space-time indices. The gravitational field of spherical island of substance should possess spherical symmetry. Thus, it is described by the metric of spherical kind

$$ds^2 = e^\nu c^2 dt^2 - e^\lambda dr^2 - r^2(d\theta^2 + \sin^2\theta d\varphi^2), \quad (2)$$

where  $e^\nu$  and  $e^\lambda$  are functions of  $r$  and  $t$ .

In the case under consideration the energy-momentum tensor is that of an ideal liquid (incompressible, with zero viscosity), by the condition that its density is constant, i.e.  $\rho = \rho_0 = \text{const}$ . As known, the energy-momentum tensor in this case is

$$T^{\alpha\beta} = \left(\rho_0 + \frac{p}{c^2}\right) b^\alpha b^\beta - \frac{p}{c^2} g^{\alpha\beta}, \quad (3)$$

where  $p$  is the pressure of the liquid, while

$$b^\alpha = \frac{dx^\alpha}{ds}, \quad b_\alpha b^\alpha = 1 \quad (4)$$

is the four-dimensional velocity vector, which determines the reference frame of the given observer. Also, the energy-momentum tensor should satisfy the conservation law

$$\nabla_\sigma T^{\alpha\sigma} = 0, \quad (5)$$

where  $\nabla_\sigma$  is the four-dimensional symbol of covariant differentiation.

Formally, the problem we are considering is a generalization of the Schwarzschild solution produced for an analogous case (a sphere of incompressible liquid). Karl Schwarzschild [2] solved the Einstein field equations for this case, by the condition that the solution must be regular. He assumed that the components of the fundamental metric tensor  $g_{\alpha\beta}$  must satisfy the signature conditions (the space-time metric must have no singularities). Thus, the Schwarzschild solution, according to his initial assumption, does not include space-time singularities.

This limitation of the space-time geometry, initially introduced in 1916 by Schwarzschild, will not be used by me in this study. Therefore, we will be able to study the singular properties of the space-time metric associated with a sphere of incompressible liquid. Then I will apply the obtained results to the cosmic objects such as the Sun and the planets.

The exact solution of the field equations (1) is obtained for the spherically symmetric metric (2) inside a sphere of incompressible liquid, which is described by the energy-momentum tensor (3). I consider here the reference frame which accompanies to the observer, consequently the components of his four-velocity vector are [3]

$$b^0 = \frac{1}{\sqrt{g_{00}}}, \quad b^i = 0, \quad i = 1, 2, 3, \quad (6)$$

while the physically observed components of the energy-momentum tensor  $T_{\alpha\beta}$  has the form

$$\rho = \frac{T_{00}}{g_{00}} = \rho_0, \quad J^i = \frac{c T_0^i}{\sqrt{g_{00}}} = 0, \quad U^{ik} = c^2 T^{ik} = p h^{ik}, \quad (7)$$

where  $\rho$  is the density of the medium,  $J^i$  is the density of the momentum in the medium,  $U^{ik}$  is the stress-tensor,  $h^{ik}$  is the observable three-dimensional fundamental metric tensor [3].

Because we do not limit the solution by that the metric must be regular, the obtained metric has two singularities: 1) collapse by  $g_{00} = 0$ , and 2) break of the space by  $g_{11} \rightarrow \infty$ . It will be shown then that these singularities are irremovable, because the strong signature condition is also violated in both cases.

In order to obtain the exact internal solution of the Einstein field equations with respect to a given distribution of matter, it is necessary to solve two systems of equations: the Einstein field equations (1), and the equations of the conservation law (5).

After algebra we obtain the Einstein field equations in the spherically symmetric space (2) inside a sphere of incompressible liquid. The obtained equations, in component notation, are

$$e^{-\nu} \left( \ddot{\lambda} - \frac{\dot{\lambda}\dot{\nu}}{2} + \frac{\dot{\lambda}^2}{2} \right) - c^2 e^{-\lambda} \left[ \nu'' - \frac{\lambda'\nu'}{2} + \frac{2\nu'}{r} + \frac{(\nu')^2}{2} \right] = -\kappa (\rho_0 c^2 + 3p), \quad (8)$$

$$\frac{\lambda}{r} e^{-\lambda-\frac{\nu}{2}} = \kappa J^1 = 0, \quad (9)$$

$$e^{\lambda-\nu} \left( \ddot{\lambda} - \frac{\dot{\lambda}\dot{\nu}}{2} + \frac{\dot{\lambda}^2}{2} \right) - c^2 \left[ \nu'' - \frac{\lambda'\nu'}{2} + \frac{(\nu')^2}{2} \right] + \frac{2c^2\lambda'}{r} = \kappa (\rho_0 c^2 - p) e^{\lambda}, \quad (10)$$

$$\frac{c^2 (\lambda' - \nu')}{r} e^{-\lambda} + \frac{2c^2}{r^2} (1 - e^{-\lambda}) = \kappa (\rho_0 c^2 - p). \quad (11)$$

The second equation manifests that  $\dot{\lambda} = 0$  in this case. Hence, the space inside the sphere of incompressible liquid

does not deform. Taking this circumstance into account, and also that the stationarity of  $\lambda$ , we reduce the field equations (8–11) to the final form

$$c^2 e^{-\lambda} \left[ \nu'' - \frac{\lambda'\nu'}{2} + \frac{2\nu'}{r} + \frac{(\nu')^2}{2} \right] = \kappa (\rho_0 c^2 + 3p) e^{\lambda}, \quad (12)$$

$$-c^2 \left[ \nu'' - \frac{\lambda'\nu'}{2} + \frac{(\nu')^2}{2} \right] + \frac{2c^2\lambda'}{r} = \kappa (\rho_0 c^2 - p) e^{\lambda}, \quad (13)$$

$$\frac{c^2 (\lambda' - \nu')}{r} e^{-\lambda} + \frac{2c^2}{r^2} (1 - e^{-\lambda}) = \kappa (\rho_0 c^2 - p) e^{\lambda}. \quad (14)$$

To solve the equations (12–14), a formula for the pressure  $p$  is necessary. To find the formula, we now deal with the conservation equations (5). Because, as was found,  $J^i = 0$  we obtain, this formula reduces to only a single nontrivial equation

$$p' e^{-\lambda} + (\rho_0 c^2 + p) \frac{\nu'}{2} e^{-\lambda} = 0, \quad (15)$$

where  $p' = \frac{dp}{dr}$ ,  $\nu' = \frac{d\nu}{dr}$ ,  $e^{\lambda} \neq 0$ . Dividing both parts of (15) by  $e^{-\lambda}$ , we arrive at

$$\frac{dp}{\rho_0 c^2 + p} = -\frac{d\nu}{2}, \quad (16)$$

which is a plain differential equation with separable variables. It can be easily integrated as

$$\rho_0 c^2 + p = B e^{-\frac{\nu}{2}}, \quad B = const. \quad (17)$$

Thus we have to express the pressure  $p$  as the function of the variable  $\nu$ ,

$$p = B e^{-\frac{\nu}{2}} - \rho_0 c^2. \quad (18)$$

In look for an  $r$ -dependent function  $p(r)$ , we integrate the field equations (12–14), taking into account (18). We find finally expressions for  $e^{\lambda}$  and  $e^{\nu}$

$$g_{00} = e^{\nu} = \frac{1}{4} \left( 3e^{\frac{\nu_0}{2}} - \sqrt{1 - \frac{\kappa\rho_0 r^2}{3}} \right)^2, \quad (19)$$

$$e^{\lambda} = -g_{11} = \frac{1}{1 - \frac{\kappa\rho_0 r^2}{3}}, \quad (20)$$

where  $e^{\frac{\nu_0}{2}} = \sqrt{1 - \frac{2GM}{c^2 a}} = \sqrt{1 - \frac{r_g}{r}}$  is obtained from the boundary conditions, while  $r_g$  is the Hilbert radius.

Thus the space-time metric of the gravitational field inside a sphere of incompressible liquid is, since the formulae of  $\nu$  and  $\lambda$  have already been obtained, as follows

$$ds^2 = \frac{1}{4} \left( 3e^{\frac{\nu_0}{2}} - \sqrt{1 - \frac{\kappa\rho_0 r^2}{3}} \right)^2 c^2 dt^2 - \frac{dr^2}{1 - \frac{\kappa\rho_0 r^2}{3}} - r^2 (d\theta^2 + \sin^2\theta d\varphi^2). \quad (21)$$

Taking into account that  $M = \frac{4\pi a^3 \rho_0}{3}$  and  $r_g = \frac{2GM}{c^2}$ , we rewrite (21) in the form

$$ds^2 = \frac{1}{4} \left( 3 \sqrt{1 - \frac{r_g}{a}} - \sqrt{1 - \frac{r^2 r_g}{a^3}} \right)^2 c^2 dt^2 - \frac{dr^2}{1 - \frac{r^2 r_g}{a^3}} - r^2 (d\theta^2 + \sin^2 \theta d\varphi^2). \quad (22)$$

It is therefore obvious that this “internal” metric completely coincides with the Schwarzschild metric in emptiness on the surface of the sphere of incompressible liquid ( $r = a$ ). This study is a generalization of the originally Schwarzschild solution for such a sphere [2], and means that Schwarzschild’s requirement to the metric to be free of singularities will not be used here. Naturally, the metric (22) allows singularities. This problem will be solved by analogy with the singular properties of the Schwarzschild solution in emptiness [4] (a mass-point’s field), which already gave black holes.

Consider the collapse condition for the space-time metric of the gravitational field inside a sphere of incompressible liquid (21). The collapse condition  $g_{00} = 0$  in this case is

$$3e^{\frac{v_a}{2}} = \sqrt{1 - \frac{\kappa \rho_0 r^2}{3}}, \quad (23)$$

or, in terms of the Hilbert radius, when the metric takes the form (22), the collapse condition is

$$3 \sqrt{1 - \frac{r_g}{a}} = \sqrt{1 - \frac{r_g r^2}{a^3}}. \quad (24)$$

We obtain that the numerical value of the radial coordinate  $r_c$ , by which the sphere’s surface meets the surface of collapse, is

$$r_c = a \sqrt{9 - \frac{8a}{r_g}}. \quad (25)$$

Because we keep in mind really cosmic objects, the numerical value of  $r_c$  should be real. This requirement is obviously satisfied by

$$a < 1.125 r_g. \quad (26)$$

If this condition holds not ( $a \geq r_g$ ), the sphere, which is a spherical liquid body, has not the state of collapse. It is obvious that the condition  $a = r_g$  satisfies to (26). It is obvious that  $r_c$  is imaginary for  $r_g \ll a$ , so collapse of such a sphere of incompressible liquid is impossible.

For example, consider the Universe as a sphere of incompressible liquid (the liquid model of the Universe). Assuming, according to the numerical value of the Hubble constant (17), that the Universe’s radius is  $a = 1.3 \times 10^{28}$  cm, we obtain the collapse condition, from (26),

$$r_g > 1.2 \times 10^{28} \text{ cm}, \quad (27)$$

and immediately arrive at the following conclusion:

The observable Universe as a whole, being represented in the framework of the liquid model, is completely located inside its gravitational radius. In other words, the observable Universe is a collapsar — a huge black hole.

In another representation, this result means that a sphere of incompressible liquid can be in the state of collapse only if its radius approaches the radius of the observable Universe.

Let’s obtain the condition of spatial singularity — space breaking. As is seen, the metric (21) or its equivalent form (22) has space breaking if its radial coordinate  $r$  equals to

$$r_{br} = \sqrt{\frac{3}{\kappa \rho_0}} = a \sqrt{\frac{a}{r_g}}. \quad (28)$$

For example, considering the Sun as a sphere of incompressible liquid, whose density is  $\rho_0 = 1.4 \text{ g/cm}^3$ , we obtain

$$r_{br} = 3.4 \times 10^{13} \text{ cm}, \quad (29)$$

while the radius of the Sun is  $a = 7 \times 10^{10}$  cm and its Hilert radius  $r_g = 3 \times 10^5$  cm. Therefore, the surface of the Sun’s space of breaking is located outside the surface of the Sun, far distant from it in the near cosmos.

Another example. Assume our Universe to be a sphere of incompressible liquid, whose density is  $\rho_0 = 10^{-31} \text{ g/cm}^3$ . The radius of its space breaking, according to (28), is

$$r_{br} = 1.3 \times 10^{29} \text{ cm}. \quad (30)$$

Observational astronomy provides the following numerical value of the Hubble constant

$$H = \frac{c}{a} = (2.3 \pm 0.3) \times 10^{18} \text{ sec}^{-1}, \quad (31)$$

where  $a$  is the observed radius of the Universe. It is easily obtain from here that

$$a = 1.3 \times 10^{28} \text{ cm}. \quad (32)$$

This value is comparable with (30), so the Universe’s radius may meet the surface of its space breaking by some conditions. We calculate the mass of the Universe by  $M = \frac{4\pi a^3 \rho_0}{3}$ , where  $a$  is (32). We have  $M = 5 \times 10^{54}$  g. Thus, for the liquid model of the Universe, we obtain  $r_g = 7.4 \times 10^{26}$  cm: the Hilbert radius (the radius of the surface of gravitational collapse) is located inside the liquid spherical body of the Universe.

A few words more on the singularities of the liquid sphere’s internal metric (21). In this case, the determinant of the fundamental metric tensor equals

$$g = -\frac{1}{4} \left( 3e^{\frac{v_a}{2}} - \sqrt{1 - \frac{\kappa \rho_0 r^2}{3}} \right)^2 \frac{r^4 \sin^2 \theta}{\sqrt{1 - \frac{\kappa \rho_0 r^2}{3}}}, \quad (33)$$

so the strong signature condition  $g < 0$  is always true for a sphere of incompressible liquid, except in two following

cases: 1) in the state of collapse ( $g_{00} = 0$ ), 2) by the breaking of space ( $g_{11} \rightarrow \infty$ ). These particular cases violate the weak signature conditions  $g_{00} > 0$  and  $g_{11} < 0$  correspondingly. If both weak signature conditions are violated,  $g$  has a singularity of the kind  $\frac{0}{0}$ . If collapse occurs in the absence of the space breaking, we have  $g = 0$ . If no collapse, while the space breaking is present, we have  $g \rightarrow \infty$ . In all the cases, the singularity is non-removable, because the strong singular condition  $g < 0$  is violated.

So, as was shown above, a spherical object consisting of incompressible liquid can be in the state of gravitational collapse only if it is as large and massive as the Universe. Meanwhile, the space breaking realizes itself in the fields of all cosmic objects, which can be approximated by spheres of incompressible liquid. Besides, since  $r_{br} \sim \frac{1}{\sqrt{\rho_0}}$ , the  $r_{br}$  is then greater while smaller is the  $\rho_0$ . Assuming all these, we arrive at the following conclusion:

A regular sphere of incompressible liquid, which can be observed in the cosmos or an Earth-bound laboratory, cannot collapse but has the space breaking — a singular surface, distantly located around the liquid sphere.

First, we are going to consider the Sun as a sphere of incompressible liquid. Schwarzschild [2] was the first person who considered the gravitational field of a sphere of incompressible liquid. He however limited this consideration by an additional condition that the space-time metric should not have singularities. In this study the metric (21) will be used. It allows singularities, in contrast to the limited case of Schwarzschild: 1) collapse of the space, and 2) the space breaking.

Calculating the radius of the space breaking by formula (28), where we substitute the Sun's density  $\rho_0 = 1.41 \text{ g/cm}^3$ , we obtain

$$r_{br} = 3.4 \times 10^{13} \text{ cm} = 2.3 \text{ AU}, \quad (34)$$

where  $1 \text{ AU} = 1.49 \times 10^{13} \text{ cm}$  (Astronomical Unit) is the average distance between the Sun and the Earth. So, we have obtained that the spherical surface of the Sun's space breaking is located inside the Asteroid strip, very close to the orbit of the maximal concentration of substance in it (as is known, the Asteroid strip is hold from 2.1 to 4.3 AU from the Sun). Thus we conclude that:

The space of the Sun (its gravitational field), as that of a sphere of incompressible liquid, has a breaking. The space breaking is distantly located from the Sun's body, in the space of the Solar System, and meets the Asteroid strip near the maximal concentration of the asteroids.

In addition to it, we conclude:

The Sun, approximated by a mass-point according to the Schwarzschild solution for a mass-point's field in emptiness, has a space breaking located inside

the Sun's body. This space breaking coincides with the Schwarzschild sphere — the sphere of collapse.

What is the Schwarzschild sphere? It is an imaginary spherical surface of the Hilbert radius  $r_g = \frac{2GM}{c^2}$ , which is not a radius of a physical body in a general case (despite it can be such one in the case of a black hole — a physical body whose radius meets the Hilbert radius calculated for its mass). The numerical value of  $r_g$  is determined only by the mass of the body, and does not depend on its other properties. The physical meaning of the Hilbert radius in a general case is as follows: this is the boundary of the region in the gravitational field of a mass-point  $M$ , where real particles exist; particles in the boundary (the Hilbert radius) bear the singular properties. In the region wherein  $r \leq r_g$ , real particles cannot exist.

Let us turn back to the Sun approximated by a sphere of incompressible liquid. The space-time metric is (21) in this case. Substituting into (25) the Sun's mass  $M = 2 \times 10^{33} \text{ g}$ , radius  $a = 7 \times 10^7 \text{ cm}$ , and the Hilbert radius  $r_g = 3 \times 10^5 \text{ cm}$  calculated for its mass, we obtain that the numerical value of the radial coordinate  $r_c$  by which the Sun's surface meets the surface of collapse of its mass is imaginary. Thus, we arrive at the conclusion that a sphere of incompressible liquid, whose parameters are the same as those of the Sun, cannot collapse.

Thus, we conclude:

A Schwarzschild sphere (collapsing space breaking) exists inside any physical body. The numerical value of its radius  $r_g$  is determined only by the body's mass  $M$ . We refer to the space-time inside the Schwarzschild sphere ( $r < r_g$ ) as a "black hole". This space-time does not satisfy the singular conditions of the space-time where real observers exist. Schwarzschild sphere (internal black hole) is an internal characteristic of any gravitating body, independent on its internal constitution.

One can ask: then what does the Hilbert radius  $r_g$  mean for the Sun, in this context? Here is the answer:  $r_g$  is the photometric distance in the radial direction, separating the "external" region inhabited with real particles and the "internal" region under the radius wherein all particles bear imaginary masses. Particles which inhabit the boundary surface (its radius is  $r_g$ ) bear singular physical properties. Note that no one real (external) observer can register events inside the singularity.

What is a sphere of incompressible liquid of the radius  $r = r_c$ ? This is a "collapsar" — the object in the state of gravitational collapse. As it was shown above, not any sphere of incompressible liquid can be collapsar: the possibility of its collapse is determined by the relation between its radius  $a$  and its Hilbert radius  $r_g$ , according to formula (25). It was shown above that the Universe considered as a sphere of incompressible liquid is a collapsar.

Now we apply this research method to the planets of the Solar System. Thus, we approximate the planets by spheres

of incompressible liquid. The numerical values of  $r_c$ , calculated for the planets according to the same formula (25) as that for the liquid model of the Sun, are imaginary. Therefore, the planets being approximated by spheres of incompressible liquid cannot collapse as well as the Sun.

The Hilbert radius  $r_g$  calculated for the planets is much smaller than the sizes of their physical bodies, and is in the order of 1 cm. This means that, given any of the planets of the Solar System, the singularity surface separating our world and the imaginary mass particles world in its gravitational field draws the sphere of the radius about one centimetre around its centre of gravity.

The numerical values of the radius of the space breaking are calculated for each of the planets through the average density of substance inside the planet according to the formula (28).

The results of the summarizing and substraction associated with the planets lead to the next conclusions:

1. The spheres of the singularity breaking of the spaces of Mercury, Venus, and the Earth are completely located inside the sphere of the singularity breaking of the Sun's space;
2. The spheres of the singularity breaking of the internal spaces of all planets intersect among themselves, when being in the state of a "parade of planets";
3. The spheres of the singularity breaking of the Earth's space and Mars' space reach the Asteroid strip;
4. The sphere of the singularity breaking of Mars' space intersects with the Asteroid strip near the orbit of Phaeton (the hypothetical planet which was orbiting the Sun, according to the Titius–Bode law, at  $r = 2.8$  AU, and whose distraction in the ancient time gave birth to the Asteroid strip).
5. Jupiter's singularity breaking surface intersects the Asteroid strip near Phaeton's orbit,  $r = 2.8$  AU, and meets Saturn's singularity breaking from the outer side;
6. The singularity breaking surface of Saturn's space is located between those of Jupiter and Uranus;
7. The singularity breaking surface of Uranus's space is located between those of Saturn and Neptune;
8. The singularity breaking surface of Neptune's space meets, from the outer side, the lower boundary of the Kuiper belt (the strip of the aphelia of the Solar System's comets);
9. The singularity breaking surface of Pluto is completely located inside the lower strip of the Kuiper belt.

Just two small notes in addition to these. The intersections of the space breakings of the planets, discussed here, take place for only that case where the planets themselves are in the state of a "parade of planets". However the conclusions concerning the location of the space breaking spheres, for instance — that

the space breaking spheres of the internal planets are located inside the sphere of the Sun's space breaking, while the space breaking spheres of the external planets are located outside it, — are true for any position of the planets.

The fact that the space breaking of the Sun meets the Asteroid strip, near Phaeton's orbit, allows us to say: yes, the space breaking considered in this study has a really physical meaning. As probable the Sun's space breaking did not permit the Asteroids to be joined into a common physical body, Phaeton. Alternatively, if Phaeton was an already existing planet of the Solar System, the common action of the space breaking of the Sun and that of another massive cosmic body, appeared near the Solar System in the ancient ages (for example, another star passing near it), has led to the distraction of Phaeton's body.

Thus the internal constitution of the Solar System was formed by the structure of the Sun's space (space-time) filled with its gravitational field, and according to the laws of the General Theory of Relativity.

These and related results will be published in necessary detail later [5]\*.

Submitted on October 31, 2009 / Accepted on January 27, 2010

## References

1. Rabounski D. and Borissova L. Particles Here and Beyond the Mirror. Svenska fysikarkivet, Stockholm, 2008.
2. Schwarzschild K. Über das Gravitationsfeld einer Kugel aus incompressibler Flüssigkeit nach der Einsteinschen Theorie. *Sitzungsberichte der Königlich Preussischen Akademie der Wissenschaften*, 1916, 424–435 (published in English as: Schwarzschild K. On the gravitational field of a sphere of incompressible liquid, according to Einstein's theory. *The Abraham Zelmanov Journal*, 2008, vol. 1, 20–32).
3. Zelmanov A. L. Chronometric invariants and accompanying frames of reference in the General Theory of Relativity. *Soviet Physics Doklady*, 1956, vol. 1, 227–230 (translated from *Doklady Akademii Nauk USSR*, 1956, vol. 107, no. 6, 815–818).
4. Schwarzschild K. Über das Gravitationsfeld eines Massenpunktes nach der Einsteinschen Theorie. *Sitzungsberichte der Königlich Preussischen Akademie der Wissenschaften*, 1916, 196–435 (published in English as: Schwarzschild K. On the gravitational field of a point mass according to Einstein's theory. *The Abraham Zelmanov Journal*, 2008, vol. 1, 10–19).
5. Borissova L. The gravitational field of a condensed matter model of the Sun: the space breaking meets the Asteroid strip. Accepted to publication in *The Abraham Zelmanov Journal*, 2009, v.2, 224–260.

\*The detailed presentation of the results [5] was already published at the moment when this short paper was accepted.

# The Matter-Antimatter Concept Revisited

Patrick Marquet

Postal address: 7, rue du 11 nov, 94350 Villiers/Marne, Paris, France  
Email: patrick.marquet6@wanadoo.fr

In this paper, we briefly review the theory elaborated by Louis de Broglie who showed that in some circumstances, a particle tunneling through a dispersive refracting material may reverse its velocity with respect to that of its associated wave (phase velocity): this is a consequence of Rayleigh's formula defining the group velocity. Within his "Double Solution Theory", de Broglie re-interprets Dirac's aether concept which was an early attempt to describe the matter-antimatter symmetry. In this new approach, de Broglie suggests that the (hidden) sub-quantum medium required by his theory be likened to the dispersive and refracting material with identical properties. A Riemannian generalization of this scheme restricted to a space-time section, and formulated within an holonomic frame is here considered. This procedure is shown to be founded and consistent if one refers to the extended formulation of General Relativity (EGR theory), wherein pre-exists a persistent field.

## 1 Introduction

The original wave function first predicted by Louis de Broglie [1] in his famous *Wave Mechanics Theory*, then was detected in 1927 by the American physicists Davisson and Germer in their famous experiment on electrons diffraction by a nickel crystal lattice.

In the late 1960's, Louis de Broglie improved on his first theory which he called *Double Solution Interpretation of Quantum Mechanics* [2, 3].

His successive papers actually described the massive particle as being much closely related to its physical wave and constantly in phase with it.

The theory which grants the wave function a true physical reality as it should be, necessarily requires the existence of an underlying medium that permanently exchanges energy and momentum with the guided particle [4].

The hypothesis of such a concealed "thermostat" was brought forward by D. Bohm and J. P. Vigié [5] who referred to it as the *sub-quantum medium*.

They introduced a hydrodynamical model in which the (real) wave amplitude is represented by a fluid endowed with some specific irregular fluctuations so that the quantum theory receives a causal interpretation.

Francis Fer [6] successfully extended the double solution theory by building a non-linear and covariant equation wherein the "fluid" is taken as a physical entity. In the recent paper [7], the author proposed to generalize this model to an extended formulation of General Relativity [8], which allows to provide a physical solution to the fluid random perturbation requirement.

Based on his late conceptions, Louis de Broglie then completed a subsequent theory [9] on the guided particle: under specific circumstances the particle tunneling through a dispersive refracting material is shown to reverse velocity with

respect to the associated wave phase velocity.

As a further assumption, Louis de Broglie identified the dispersive refracting material with the hidden medium [10] considered above.

In this case, the theoretical results obtained are describing the behavior of a pair particle-antiparticle which is close to the Stueckelberg-Feynmann picture [11], in which antiparticles are viewed as particles with negative energy that move backward in time.

Within this interpretation, the sub-quantum medium as derived from de Broglie's theories, appears to provide a deeper understanding of Dirac's aether theory [12], once popular before.

In this paper, we try to generalize this new concept by identifying the hidden medium with the persistent energy-momentum field tensor inherent to the EGR theory.

Such a generalization is here only restricted to a Riemannian space-time section ( $t = \text{const}$ ), where the integration is further performed over a spatial volume. By doing so, we are able to find back the essential formulas set forth by Louis de Broglie in the Special Relativity formulation.

We assumed here a limited extension without loss of generality: a fully generalized theory is desirable, as for example the attempt suggested by E. B. Gliner [13], who has defined a " $\mu$ -medium" entirely derived from General Relativity considerations.

## 2 Short overview of the Double Solution Theory within wave mechanics (Louis de Broglie)

### 2.1 The reasons for implementing the theory

As an essential contribution to quantum physics, Louis de Broglie's wave mechanics theory has successfully extended the wave-particle duality concepts to the whole physics.

Double solution theory which aimed at confirming the

true physical nature of the wave function is based on two striking observations: within the Special Theory of Relativity, the frequency  $\nu_0$  of a plane monochromatic wave is transformed as

$$\nu = \frac{\nu_0}{\sqrt{1 - \beta^2}},$$

whereas a clock's frequency  $\nu_0$  is transformed according to  $\nu_c = \nu_0 \sqrt{1 - \beta^2}$  with the phase velocity

$$\tilde{v} = \frac{c}{\beta} = \frac{c^2}{v}.$$

The 4-vector defined by the gradient of the plane monochromatic wave is linked to the energy-momentum 4-vector of a particle by introducing Planck's constant  $h$  as

$$W = h\nu, \quad \lambda = \frac{h}{p}, \quad (1)$$

where  $p$  is the particle's momentum and  $\lambda$  is the wave length.

If the particle is considered as that containing a rest energy  $M_0c^2 = h\nu_0$ , it is likened to a small clock of frequency  $\nu_0$  so that when moving with velocity  $v = \beta c$ , its frequency different from that of the wave is then

$$\nu = \nu_0 \sqrt{1 - \beta^2}.$$

In the spirit of the theory, the wave is a physical entity having a very small amplitude not arbitrarily normed and which is distinct from the  $\psi$ -wave reduced to a statistical quantity in the usual quantum mechanical formalism.

Let us call  $\vartheta$  the physical wave which is connected to the  $\psi$ -wave by the relation  $\psi = C\vartheta$ , where  $C$  is a normalizing factor.

The  $\psi$ -wave has then nature of a subjective probability representation formulated by means of the objective  $\vartheta$ -wave.

Therefore wave mechanics is complemented by the double solution theory, for  $\psi$  and  $\vartheta$  are two solutions of the same equation.

If the complete solution of the equation representing the  $\vartheta$ -wave (or, if preferred, the  $\psi$ -wave, since both waves are equivalent according to  $\psi = C\vartheta$ ), is written as

$$\vartheta = a(x, y, z, t) \exp\left[\frac{i}{\hbar} \phi(x, y, z, t)\right], \quad \hbar = \frac{h}{2\pi}, \quad (2)$$

where  $a$  and  $\phi$  are real functions, while the energy  $W$  and the momentum  $p$  of the particle localized at point  $(x, y, z)$ , at time  $t$  are given by

$$W = \partial_t \phi, \quad p = -\text{grad } \phi, \quad (3)$$

which in the case of a plane monochromatic wave, where one has

$$\phi = h \left[ \nu - \frac{(\alpha x + \beta y + \gamma z)}{\lambda} \right]$$

yields equation (1) for  $W$  and  $p$ .

## 2.2 The guidance formula and the quantum potential

Taking Schrodinger's equation for the scalar wave  $\vartheta$ , and  $U$  being the external potential, we get

$$\partial_t \vartheta = \frac{\hbar}{2im} \Delta \vartheta + \frac{i}{\hbar} U \vartheta. \quad (4)$$

This complex equation implies that  $\vartheta$  be represented by two real functions linked by these two real equations which leads to

$$\vartheta = a \exp\left(\frac{i\phi}{\hbar}\right), \quad (5)$$

where  $a$  the wave's amplitude, and  $\phi$  its phase, both are real. Substituting this value into equation (4), it gives two important equations

$$\left. \begin{aligned} \partial_t \phi - U - \frac{1}{2m} (\text{grad } \phi)^2 &= -\frac{\hbar^2}{2m} \frac{\Delta a}{a} \\ \partial_t (a^2) - \frac{1}{m} \text{div} (a^2 \text{ grad } \phi) &= 0 \end{aligned} \right\}. \quad (6)$$

If terms involving Planck's constant  $\hbar$  in equation (6) are neglected (which amounts to disregard quanta), and if we set  $\phi = S$ , this equation becomes

$$\partial_t S - U = \frac{1}{2m} (\text{grad } S)^2.$$

As  $S$  is the Jacobi function, this equation is the Jacobi equation of Classical Mechanics.

Only the term containing  $\hbar^2$  is responsible for the particle's motion being different from the classical motion.

The extra term in (6) can be interpreted as another potential  $Q$  distinct from the classical  $U$  potential

$$Q = -\frac{\hbar^2}{2m} \frac{\Delta a}{a}. \quad (7)$$

One has thus a variable proper mass

$$M_0 = m_0 + \frac{Q_0}{c^2}, \quad (8)$$

where, in the particle's rest frame,  $Q_0$  is a positive or negative variation of this rest mass and it represents the "quantum potential" which causes the wave function's amplitude to vary.

By analogy with the classical formula  $\partial_t S = E$ , and  $p = -\text{grad } S$ ,  $E$  and  $p$  being the classical energy and momentum, one may write

$$\partial_t \phi = E, \quad -\text{grad } \phi = p. \quad (9)$$

As in non-relativistic mechanics, where  $p$  is expressed as a function of velocity by the relation  $p = mv$ , one eventually finds the following results

$$v = \frac{p}{m} = -\frac{1}{m} \text{ grad } \phi, \quad (10)$$

which is the *guidance formula*.

It gives the particle's velocity, at position  $(x, y, z)$  and time  $t$  as a function of the local phase variation at this point.

Inspection shows that relativistic dynamics applied to the variable proper mass  $M_0$  eventually leads to the following result

$$W = \frac{M_0 c^2}{\sqrt{1-\beta^2}} = M_0 c^2 \sqrt{1-\beta^2} + \frac{M_0 v^2}{\sqrt{1-\beta^2}} \quad (11)$$

known as the Planck-Laue formula.

Here, the quantum force results from the variation of  $M_0 c^2$  as the particle moves.

### 2.3 Particles with internal vibration and the hidden thermodynamics

The idea of considering the particle as a small clock is of central importance here.

Let us look at the self energy  $M_0 c^2$  as the hidden heat content of a particle. One easily conceives that such a small clock has (in its proper system) an internal periodic energy of agitation which does not contribute to the whole momentum. This energy is similar to that of a heat containing body in the state of thermal equilibrium.

Let  $Q_0$  be the heat content of the particle in its rest frame, and viewed in a frame where the body has a velocity  $\beta c$ , the contained heat will be

$$Q = Q_0 \sqrt{1-\beta^2} = M_0 c^2 \sqrt{1-\beta^2} = h\nu_0 \sqrt{1-\beta^2}. \quad (12)$$

The particle thus appears as being at the same time a small clock of frequency

$$\nu = \nu_0 \sqrt{1-\beta^2}$$

and a small reservoir of heat

$$Q = Q_0 \sqrt{1-\beta^2}$$

moving with velocity  $\beta c$ . If  $\phi$  is the wave phase  $a \exp(\frac{i\phi}{\hbar})$ , where  $a$  and  $\phi$  are real, the guidance theory states that

$$\partial_t \phi = \frac{M_0 c^2}{\sqrt{1-\beta^2}}, \quad -\text{grad } \phi = \frac{M_0 v}{\sqrt{1-\beta^2}}. \quad (13)$$

The Planck-Laue equation may be written

$$Q = M_0 c^2 \sqrt{1-\beta^2} = \frac{M_0 c^2}{\sqrt{1-\beta^2}} - v p. \quad (14)$$

Combining (13) and (14) results in

$$M_0 c^2 \sqrt{1-\beta^2} = \partial_t \phi + v \text{grad } \phi = \frac{d\phi}{dt}.$$

Since the particle is regarded as a clock of proper frequency  $M_0 \frac{c^2}{\hbar}$ , the phase of its internal vibration expressed with  $a_i \exp(\frac{i\phi_i}{\hbar})$  and  $a_i$  and  $\phi_i$  real will be

$$\phi_i = h\nu_0 \sqrt{1-\beta^2} t = M_0 c^2 \sqrt{1-\beta^2} t,$$

thus we obtain

$$d(\phi_i - \phi) = 0. \quad (15)$$

This fundamental result agrees with the assumption according to which the particle as it moves in its wave, remains constantly in phase with it.

## 3 Propagation in a dispersive refracting material

### 3.1 Group velocity

The classical wave is written as

$$a \exp[2\pi i(\nu t - kr)]; \quad (16)$$

it propagates along the direction given by the unit vector  $n$ .

We next introduce the phase velocity  $\tilde{v}$  of the wave, which determines the velocity between two "phases" of the wave.

Consider now the superposition of two stationary waves having each a very close frequency: along the  $x$ -axis, they have distinct energies

$$E_1 = A \sin 2\pi(\nu + d\nu) \left[ t - \frac{x}{\nu + d\nu} \right],$$

$$E_2 = A \sin 2\pi(\nu - d\nu) \left[ t - \frac{x}{\nu - d\nu} \right],$$

thus next we have

$$\frac{\nu + d\nu}{\nu + d\nu} = \frac{\nu}{\nu} + d\left(\frac{\nu}{\nu}\right), \quad \frac{\nu - d\nu}{\nu - d\nu} = \frac{\nu}{\nu} - d\left(\frac{\nu}{\nu}\right),$$

and by adding both waves

$$E = 2A \cos 2\pi d\nu \left[ t - x \left( \frac{d}{d\nu} \right) \left( \frac{\nu}{\nu} \right) \right] \sin 2\pi \nu \left( t - \frac{x}{\nu} \right). \quad (17)$$

The term

$$2A \cos 2\pi d\nu \left[ t - x \left( \frac{d}{d\nu} \right) \left( \frac{\nu}{\nu} \right) \right] \quad (18)$$

may be regarded as the resulting amplitude that varies along with the so-called "group velocity"  $[v]_g$  and such that

$$\frac{1}{[v]_g} = \left( \frac{d}{d\nu} \right) \left( \frac{\nu}{\nu} \right). \quad (19)$$

Recalling the relation between the wave length  $\lambda$  and the material refracting index  $n$

$$\lambda = \frac{\tilde{v}}{\nu} = \frac{v_0}{n\nu} \quad (20)$$

where  $v_0$  is the wave velocity in a given reference material ( $c$  in vacuum), we see that

$$n = \frac{v_0}{\tilde{v}}, \quad \text{i.e. in vacuum } n = \frac{c}{\tilde{v}}. \quad (21)$$

Now, we have the Rayleigh formulae

$$\frac{1}{[v]_g} = \frac{d}{d\nu} \left( \frac{\nu}{\nu} \right) = \frac{1}{\nu_0} \left( \frac{\partial}{\partial \nu} \right) n \nu = \left( \frac{\partial}{\partial \nu} \right) \left( \frac{1}{\lambda} \right). \quad (22)$$

It is then easy to show that  $[v]_g$  coincides with the velocity  $v$  of the particle, which is also expressed in term of the wave energy  $W$  as

$$[v]_g = \frac{\partial W}{\partial k}.$$

The velocity of the particle  $v$  may be directed either in the propagating orientation of the wave in which case

$$p = k = \left(\frac{h}{\lambda}\right) n,$$

or in the opposite direction  $p = -k = -\left(\frac{h}{\lambda}\right) n$ .

When the particle's velocity  $v > 0$ , and  $p = k$ , we have the Hamiltonian form

$$v = \frac{\partial W}{\partial p}.$$

### 3.2 Influence of the refracting material

Let us recall the relativistic form of the Doppler's formulae:

$$\nu_0 = \frac{\nu \left(1 - \frac{v}{\tilde{v}}\right)}{\sqrt{1 - \beta^2}}, \quad (23)$$

where as usual  $\nu_0$  is the wave's frequency in the frame attached to the particle.

Considering the classical relation  $W = h\nu$  connecting the particle energy and its wave frequency, and taking into account (23), we have

$$W = W_0 \sqrt{1 - \beta^2} \left(1 - \frac{v}{\tilde{v}}\right).$$

However, inspection shows that the usual formula

$$W = \frac{W_0}{\sqrt{1 - \beta^2}}$$

holds only if

$$1 - \frac{v}{\tilde{v}} = 1 - \beta^2,$$

which implies

$$\tilde{v} = c^2$$

and this latter relation is satisfied provided we set

$$W = \frac{M_0 c^2}{\sqrt{1 - \beta^2}}, \quad p = \frac{M_0 v}{\sqrt{1 - \beta^2}},$$

where  $M_0$  is the particle's proper mass which includes an extra term  $\delta M_0$  resulting from the quantum potential  $Q$  contribution.

When the particle whose internal frequency is  $\nu_0 = \frac{M_0 c^2}{h}$  has travelled a distance  $dn$  during  $dt$ , its internal phase  $\phi_i$  has changed by

$$d\phi_i = M_0 c^2 \sqrt{1 - \beta^2} dt = d\phi,$$

where  $n$  is the unit vector normal to the phase surface.

The identity of the corresponding wave phase variation

$$d\phi = \partial_t \phi dt + \partial_n \phi dn = (\partial_t \phi + v \text{grad } \phi) dt$$

is also expressed by

$$\partial_t \phi + \partial_n \phi dn = d_t \phi_i, \quad (24)$$

and it leads to

$$\frac{M_0 c^2}{\sqrt{1 - \beta^2}} - \frac{M_0 v^2}{\sqrt{1 - \beta^2}} = M_0 c^2 \sqrt{1 - \beta^2}.$$

The situation is different in a refracting material which is likened to a "potential"  $P$  acting on the particle so that we write

$$W = \frac{M_0 c^2}{\sqrt{1 - \beta^2}} + P, \quad (25)$$

$$p = \frac{M_0 v}{\sqrt{1 - \beta^2}} = v \frac{W - P}{c^2}. \quad (26)$$

Now taking into account equation (23), the equation (24) reads (re-instating  $\hbar$ )

$$\frac{1}{\hbar} d_t \phi_i = \nu_0 \sqrt{1 - \beta^2} = \nu \left(1 - \frac{v}{\tilde{v}}\right)$$

yielding

$$W - v^2 \frac{W - P}{c^2} = W \left(1 - \frac{v}{\tilde{v}}\right) \quad (27)$$

from which we infer the expression of the potential  $P$

$$P = W \left(1 - \frac{c^2}{\tilde{v}} \frac{v}{c}\right) = h\nu \left(1 - \frac{c^2}{\tilde{v}} \frac{v}{c}\right) \quad (28)$$

and with the Rayleigh formulae (22)

$$P = W \left[1 - n \frac{\partial(n\nu)}{\partial \nu}\right] \quad (29)$$

(we assume  $\nu_0 = c$ ), for the phase  $\phi$  of the wave along the  $x$ -axis we find  $d\phi = Wdt - kdx$  with

$$k = v \frac{W - P}{c^2} = \frac{h}{\lambda}. \quad (30)$$

The phase concordance  $hd\phi_i = hd\phi$  readily implies

$$(W - kv) dt = \left(W - v^2 \frac{W - P}{c^2}\right) dt \quad (31)$$

and taking into account (28),

$$d\phi_i = \frac{W}{h} \left(1 - \frac{v}{\tilde{v}}\right) dt = 2\pi\nu \left(1 - \frac{v}{\tilde{v}}\right) dt. \quad (32)$$

Now applying the Doppler formulae (23), and bearing in mind the transformation  $dt_0 = dt \sqrt{1 - \beta^2}$ , we can write

$$d\phi = 2\pi\nu_0 dt_0 = 2\pi\nu \left(1 - \frac{v}{\tilde{v}}\right) dt. \quad (33)$$

One easily sees that the equivalence of (32) and (33) fully justifies the form of the "potential"  $P$ .

## 4 The particle-antiparticle state

### 4.1 Reduction of the EGR tensor to the Riemannian scheme

#### 4.1.1 Massive tensor in the EGR formulation

Setting the 4-unit velocity  $u^a = \frac{dx^a}{ds}$  which obeys here

$$g_{ab} u^a u^b = g^{ab} u_a u_b = 1.$$

Expressed in mixed indices, the usual Riemannian massive tensor is well known

$$(T_a^b)_{\text{Riem}} = \rho_0 c^2 u^b u_a, \quad (34)$$

where  $\rho_0$  is the proper density of the mass.

In the EGR formulation, the massive tensor is given by

$$(T_a^b)_{\text{EGR}} = (\rho_0)_{\text{EGR}} c^2 (u^b)_{\text{EGR}} (u_a)_{\text{EGR}} + (T_a^b)_{\text{field}}. \quad (35)$$

The EGR world velocity is not explicitly written but it carries a small correction w.r.t. to the regular Riemannian velocity  $u^a$ .

The EGR density  $\rho_0$  is also modified, as was shown in our paper [8] which explains the random perturbation of the fluid.

Let us now express  $(T_a^b)_{\text{EGR}}$  in terms of the Riemannian representation

$$(T_a^b)_{\text{EGR}} = (T_a^b)_{\text{Riem}}^*. \quad (36)$$

With respect to  $(T_a^b)_{\text{Riem}}$ , the tensor  $(T_a^b)_{\text{Riem}}^*$  is obviously only modified through the Riemannian proper density  $\rho$  we denote  $\rho^*$  since now.

Having said that, we come across a difficulty since the quantity  $(T_a^b)_{\text{EGR}}$  is antisymmetric whereas  $(T_a^b)_{\text{Riem}}^*$  is symmetric.

In order to avoid this ambiguity, we restrict ourselves to a space-time section  $x^4 = \text{const}$ . In this case, we consider the tensor  $(T_a^b)_{\text{EGR}}$  which we split up into

$$(T_4^\alpha)_{\text{EGR}} = (T_4^\alpha)_{\text{Riem}}^*, \quad (37)$$

$$(T_4^4)_{\text{EGR}} = (T_4^4)_{\text{Riem}}^*. \quad (38)$$

Inspection shows that each of the EGR tensors components when considered separately in (37) and (38) is now symmetric.

#### 4.1.2 The modified proper mass

We write down the above components

$$(T_4^\alpha)_{\text{Riem}}^* = \rho_0^* c^2 u^\alpha u_4, \quad (39)$$

$$(T_4^4)_{\text{Riem}}^* = \rho_0^* c^2 u^4 u_4. \quad (40)$$

This amounts to state that the proper density  $\rho_0$  is modified by absorbing the EGR free field component  $(T_a^b)_{\text{field}}$  tensor.

By the modification, we do not necessarily mean an ‘‘increase’’, as will be seen in the next sections.

## 4.2 Refracting material

### 4.2.1 Energy-momentum tensor

We now consider a dispersive refracting material which is characterized by a given (variable) index denoted by  $n$ .

Unlike a propagation in vacuum, a particle progressing through this material will be subject to a specific ‘‘influence’’ which is acting upon the tensor  $(T_4^b)_{\text{Riem}}^*$ . Thus, the energy-momentum tensor of the system will thus be chosen to be

$$(T_4^b)_{\text{Riem}}^* = \rho_0^* c^2 u^b u_4 - \delta_4^b b(n), \quad (41)$$

where  $b(n)$  is a scalar term representing the magnitude of the influence and which is depending on the refracting index  $n$ .

The tensor  $\delta_4^b b(n)$  is reminiscent of a ‘‘pressure term’’ which appears in the perfect fluid solution except that no equation of state exists.

Equation (41) yields

$$(T_4^\alpha)_{\text{Riem}}^* = \rho_0^* c^2 u^\alpha u_4, \quad (42)$$

$$(T_4^4)_{\text{Riem}}^* = \rho_0^* c^2 + b(n), \quad (43)$$

Applying the relation  $u^\alpha c = v^\alpha u^4$ , equation (42) becomes

$$(T_4^\alpha)_{\text{Riem}}^* = \rho_0^* c v^\alpha. \quad (44)$$

### 4.2.2 Integration over the hypersurface $x^4 = \text{const}$

Integration of (43) over the spatial volume  $V$  yields

$$(P^4)_{\text{Riem}}^* = \frac{1}{c} \int \rho_0^* c^2 \sqrt{-g} dV + \frac{1}{c} \int b(n) \sqrt{-g} dV, \quad (45)$$

$$c (P^4)_{\text{Riem}}^* = m_0^* c^2 + B(n), \quad (46)$$

while integrating (44), we get a 3-momentum vector

$$(P^\alpha)_{\text{Riem}}^* = \frac{1}{c} \int \rho_0^* c v^\alpha \sqrt{-g} dV, \quad (47)$$

$$(P^\alpha)_{\text{Riem}}^* = m_0^* v^\alpha. \quad (48)$$

### 4.2.3 Matching the formulas of de Broglie

Let us multiply, respectively, (46) and (48) by  $u^4$

$$u^4 c (P^4)_{\text{Riem}}^* = u^4 m_0^* c^2 + u^4 B(n); \quad (49)$$

if we set  $P = u^4 B(n)$ , we retrieve de Broglie’s first formula (25)

$$u^4 c (P^4)_{\text{Riem}}^* = W = \frac{m_0^* c^2}{\sqrt{1 - \beta^2}} + P(n) \quad (50)$$

as well as the second formula (26)

$$u^4 (P^\alpha)_{\text{Riem}}^* = p = \frac{m_0^* v^\alpha}{\sqrt{1 - \beta^2}}. \quad (51)$$

## 5 A new aspect of the antiparticle concept

### 5.1 Proper mass

In §4.1.2 we have considered the modified proper density  $\rho_0^*$ , resulted from the EGR persistent free field “absorbed” by the tensor in the Riemannian scheme.

Having established the required generalization, we now revert to the classical formulation as suggested by de Broglie.

The corresponding modified proper mass  $m_0^*$  should always be positive, therefore we are bound to set

$$p = k \text{ if } v > 0, \quad p = -k \text{ if } v < 0. \quad (52)$$

With these, we infer

$$\frac{m_0^*}{\sqrt{1-\beta^2}} = \pm \frac{W-P}{c^2} \quad (53)$$

that is

$$m_0^* = \pm \frac{W}{\tilde{v}} \sqrt{1-\beta^2}. \quad (54)$$

For propagation in vacuum we have  $P = 0$ ,  $v = v_0 = c^2/\tilde{v}$ , and  $W = m_0c^2/\sqrt{1-\beta^2}$  which implies, a expected,

$$m_0^* = m_0.$$

### 5.2 Antiparticles state

The early theory of antiparticles is due to P. A. M. Dirac after he derived his famous relativistic equation revealing the electron-positon symmetric state. In order to explain the production of a pair “electron-positon”, Dirac postulated the presence of an underlying medium filled with electrons  $e$  bearing a negative energy  $-m_0c^2$ .

An external energy input  $2m_0c^2$  would cause an negative energy electron to emerge from the medium as a positive energy one, thus become observable. The resulting “hole” would constitute, in this picture, an “observable” particle, positon, bearing a positive charge.

With Louis de Broglie, we follow this postulate: we consider that the hidden medium should also be filled with particles bearing a negative proper energy. Therefore the proper mass “modification” discussed above is expressed by

$$m_0^* = -m_0 \quad (55)$$

and is true in the medium.

At this point, two fundamental situations are to be considered as follows:

- a) The “normal” situation where  $P = 0$ ,  $m_0^*$ , and  $v = v_0$ ;
- b) The “singular” situation where  $P = 2W$ , in which case, according to (28) and (29), the following relations are obtained

$$n \frac{\partial(nv)}{\partial v} = -1.$$

Hence, in the “singular” situation b),

$$\frac{1}{[v]_g} = \frac{\partial\left(\frac{1}{\lambda}\right)}{\partial v} = -\frac{\tilde{v}}{c^2} = -\frac{1}{v_0},$$

from which is inferred

$$W = \frac{m_0^*c^2}{\sqrt{1-\beta^2}} + P = -\frac{m_0^*c^2}{\sqrt{1-\beta^2}}, \quad W = \frac{m_0^*c^2}{\sqrt{1-\beta^2}}. \quad (56)$$

On the other hand

$$\left. \begin{aligned} k = v_0 \frac{(W-P)}{c^2} &= \frac{m_0^*v_0}{\sqrt{1-\beta^2}}, & k &= \frac{m_0v_0}{\sqrt{1-\beta^2}} \\ p = -k &= -\frac{m_0v_0}{\sqrt{1-\beta^2}} \end{aligned} \right\}. \quad (57)$$

Within this interpretation, the *observed* antiparticle has an opposite charge, a positive rest mass  $m_0$  and a reversed velocity  $v_0$  with respect to the phase wave propagation.

The state of electron-positon requires negative energies *bounded* to the sub-quantum medium which can be now further explicited.

The external energy input  $2m_0c^2$  causes a positive (observable) energy of the electron to emerge from the medium according to

$$-m_0c^2 + 2m_0c^2 = m_0c^2. \quad (58)$$

However, the charge conservation law requires the simultaneous emergence of an electron with positive rest energy  $m_0c^2$  implying for the hidden medium to supply a *total* energy of  $2m_0c^2$ . In other words, we should have

$$Q = 2m_0c^2. \quad (59)$$

### 5.3 Introducing the quantum potential

Following the same pattern as above, the quantum potential  $Q$  is now assumed to act as a dispersive refracting material.

This means that  $Q = P$  where the definition (8) holds now, for  $m_0^*$ ,

$$Q = M_0c^2 - m_0^*c^2. \quad (60)$$

Since  $m_0^*c^2 = -m_0c^2$ , we have with (59)

$$M_0 = m_0.$$

The energy and the momentum of the antiparticle are now given by

$$W = \frac{M_0c^2}{\sqrt{1-\beta^2}} = \frac{m_0c^2}{\sqrt{1-\beta^2}}, \quad (61)$$

$$p = \frac{M_0v}{\sqrt{1-\beta^2}} = -\frac{m_0v_0}{\sqrt{1-\beta^2}} = -k. \quad (62)$$

Clearly, the value obtained here for  $p$  characterizes a particle whose velocity direction  $v$  is opposite to that of the associated wave  $-v_0$ .

This result perfectly matches the equation (57), which is physically satisfied.

## 6 Concluding remarks

According to the double solution theory, there exists a close relationship between the guidance formula, and the relativistic thermodynamics.

Following this argument, it is interesting to try to connect the entropy with the particle/antiparticle production process as it is derived above.

We first recall the classical action integral for the free particle :

$$\alpha = \int L dt = - \int M_0 c^2 \sqrt{1 - \beta^2} dt. \quad (63)$$

If we choose a period  $T_i$  of the particle's internal vibration (its proper mass is  $M_0$ ) as the intergration interval, from (12) we have

$$\frac{1}{T_i} = \frac{m_0 c^2}{h} \sqrt{1 - \beta^2} \quad (64)$$

so that a "cyclic" action integral be defined as

$$\frac{\alpha}{h} = - \int_0^{T_i} M_0 c^2 \sqrt{1 - \beta^2} dt = - \frac{M_0 c^2}{m_0 c^2} \quad (65)$$

( $T_i$  is assumed to be always short so that  $M_0$  and  $\beta^2 = \frac{v^2}{c^2}$  can be considered as constants over the integration interval).

Denoting the hidden thermostat's entropy by  $s$ , we set

$$\frac{s}{\mathfrak{R}} = \frac{\alpha}{h}, \quad (66)$$

where  $\mathfrak{R}$  is Boltzmann's constant.

Since

$$\delta Q_0 = \delta m_0 c^2,$$

we obtain

$$\delta s = -\mathfrak{R} \frac{\delta Q_0}{m_0 c^2}. \quad (67)$$

An entropy has thus been determined for the single particle surrounded by its guiding wave. According to Boltzmann's relation

$$s = \mathfrak{R} \ln \mathcal{P},$$

where  $\mathcal{P} = \exp\left(\frac{s}{\mathfrak{R}}\right)$  is the probability characterizing the system.

In this view, the prevailing plane monochromatic wave representing the quantized (stable) stationary states corresponds to an entropy maxima, whereas the other states also exist but with a much reduced probability.

Now, we revert to the hidden sub-quantum medium which thus supplies the equivalent heat quantity

$$Q_0 = Q. \quad (68)$$

The definition (8) can be re-written as

$$Q_0 = M_0 c^2 - m_0 c^2. \quad (69)$$

Therefore, according to the formula (67), the medium is needed to supply an energy of  $2m_0 c^2$  that is characterized by an entropy decrease of  $2\mathfrak{R}$ .

Its probability being reduced, this explains why an antiparticle is *unstable*.

So, the thermodynamics approach, which could at first glance seem strange in quantum theory, eventually finds here a consistent ground. It is linked to "probability" situations which fit in the physical processes involving wave "packet" propagations within the guidance of the single particle.

We have tried here to provide a physical interpretation of the sub-quantum medium from which the particle-antiparticle symmetry originates within the double solution theory elaborated by Louis de Broglie. In the Riemannian approximation which we have presented above, the introduction of a term generalizing the quantum potential would appear as that having a somewhat degree of arbitrariness. However, if one refers to our extended general relativity theory (EGR theory), the introduction of this term is no longer arbitrary as it naturally arises from its main feature.

Submitted on January 22, 2010 / Accepted on January 29, 2010

## References

1. De Broglie L. *Eléments de la théorie des quantas et de mécanique ondulatoire*. Gauthier-Villars, Paris, 1959.
2. De Broglie L. *Une interprétation causale et non linéaire de la mécanique ondulatoire: la théorie de la double solution*. Gauthier-Villars, Paris, 1960.
3. De Broglie L. *La réinterprétation de la mécanique ondulatoire*. Gauthier-Villars, Paris, 1971.
4. De Broglie L. *Thermodynamique relativiste et mécanique ondulatoire*. *Ann. Inst. Henri Poincaré*, 1968, v.IX, no.2, 89–108.
5. Bohm D. and Vigier J.P. Model of the causal interpretation of quantum theory in terms of a fluid with irregular fluctuations. *Physical Review*, 1954, v.96, no.1, 208–216.
6. Fer F. Construction d'une équation non linéaire en théorie de la double solution. *Séminaire Louis de Broglie*, Faculté des Sciences de Paris, 1955, exposé no.3.
7. Marquet P. The EGR theory: an extended formulation of General Relativity. *The Abraham Zelmanov Journal*, 2009, v.2, 148–170.
8. Marquet P. On the physical nature of the wave function: a new approach through the EGR theory. *The Abraham Zelmanov Journal*, 2009, 195–207.
9. De Broglie L. Etude du mouvement des particules dans un milieu réfringent. *Ann. Inst. Henri Poincaré*, 1973, v.XVIII, no.2, 89–98.
10. De Broglie L. La dynamique du guidage dans un milieu réfringent et dispersif et la théorie des antiparticules. *Le Journal de Physique*, 1967, tome 28, no.5–6, 481–486.
11. Greiner W. and Reinhardt J. *Field quantization*. Springer, Berlin, 1996, p.108–109.
12. Dirac P.A.M. Is there an aether? *Nature*, 1951, v.168, 906–907.
13. Gliner E.B. Algebraic properties of the energy-momentum tensor and vacuum like state of matter. *Soviet Physics JETP*, 1966, v.22, no.2, 378–383.

# A Derivation of $\pi(n)$ Based on a Stability Analysis of the Riemann-Zeta Function

Michael Harney\* and Ioannis Iraklis Haranas†

\*841 North 700 West, Pleasant Cove, Utah, 84062, USA. E-mail: michael.harney@signaldisplay.com

†Department of Physics and Astronomy, York University, 314 A Pertie Science Building North York, Ontario, M3J-1P3, Canada. E-mail: ioannis@yorku.ca

The prime-number counting function  $\pi(n)$ , which is significant in the prime number theorem, is derived by analyzing the region of convergence of the real-part of the Riemann-Zeta function using the unilateral  $z$ -transform. In order to satisfy the stability criteria of the  $z$ -transform, it is found that the real part of the Riemann-Zeta function must converge to the prime-counting function.

## 1 Introduction

The Riemann-Zeta function, which is an infinite series in a complex variable  $s$ , has been shown to be useful in analyzing nuclear energy levels [1] and the filling of  $s_1$ -shell electrons in the periodic table [2]. The following analysis of the Riemann-Zeta function with a  $z$ -transform shows the stability zones and requirements for the real and complex variables.

## 2 Stability with the $z$ -transform

The Riemann-Zeta function is defined as

$$\Gamma(s) = \sum_{n=1}^{\infty} n^{-s}. \tag{1}$$

We start by setting the following equality

$$\Gamma(s) = \sum_{n=1}^{\infty} n^{-s} = \sum_{n=1}^{\infty} e^{-as}. \tag{2}$$

Then by simplifying

$$n^{-s} = e^{-as} = e^{-a(r+j\omega)} \tag{3}$$

and taking natural logarithm of both sides we obtain

$$-s \ln(n) = -as. \tag{4}$$

We then find the constant  $a$  such that

$$a = \ln(n). \tag{5}$$

We then apply the unilateral  $z$ -transform on (1):

$$\Gamma(s) = \sum_{n=1}^{\infty} n^{-s} z^{-n} = \sum_{n=1}^{\infty} e^{-as} z^{-n} = \sum_{n=1}^{\infty} e^{-a(r+j\omega)} z^{-n}. \tag{6}$$

Substituting (5), the real part of (6) becomes:

$$\text{Re} [\Gamma(s)] = \sum_{n=1}^{\infty} e^{-ar} z^{-n} = \sum_{n=1}^{\infty} e^{-r \ln(n)} z^{-n}. \tag{7}$$

In order to find the region of convergence (ROC) of (7), we have to factor (7) to the common exponent  $-n$ , which requires

$$r = n / \ln(n), \tag{8}$$

which is the same as saying that the real part of  $\Gamma(s)$  must converge to the prime-number counting function  $\pi(n)$ . With (8) satisfied, (7) becomes

$$\text{Re} [\Gamma(s)] = \sum_{n=1}^{\infty} (ez)^{-n}. \tag{9}$$

which has a region of convergence (ROC)

$$\text{ROC} = \frac{1}{1 - \frac{1}{ez}}. \tag{10}$$

To be within the region of convergence,  $z$  must satisfy the following relation

$$|z| > e^{-1} \quad \text{or} \quad |z| > 0.368. \tag{11}$$

which, places  $z$  within the critical strip. It can also be shown that the imaginary part of (6)

$$\text{Im} [\Gamma(s)] = \sum_{n=1}^{\infty} e^{-aj\omega} z^{-n} = \sum_{n=1}^{\infty} e^{-j\omega \ln(n)} z^{-n}. \tag{12}$$

converges based on the Fourier series of  $\sum e^{-j\omega \ln(n)}$ .

## 3 Conclusions

The prime number-counting function  $\pi(n)$  has been derived from a stability analysis of the Riemann-Zeta function using the  $z$ -transform. It is found that the real part of the roots of the zeta function correspond to  $\pi(n)$  under the conditions of stability dictated by the unit-circle of the  $z$ -transform. The distribution of prime numbers has been found to be useful in analyzing electron and nuclear energy levels.

Submitted on November 11, 2009 / Accepted on December 16, 2009

## References

1. Dyson F. Statistical theory of the energy levels of complex systems. III. *Journal of Mathematical Physics*, 1962, v. 3, 166–175.
2. Harney M. The stability of electron orbital shells based on a model of the Riemann-Zeta function. *Progress in Physics*, 2008, v. 1, 1–5.

# On the Significance of the Upcoming Large Hadron Collider Proton-Proton Cross Section Data

Eliahu Comay

Charactell Ltd., PO Box 39019, Tel-Aviv, 61390, Israel. E-mail: elicomay@post.tau.ac.il

The relevance of the Regular Charge-Monopole Theory to the proton structure is described. The discussion relies on classical electrodynamics and its associated quantum mechanics. Few experimental data are used as a clue to the specific structure of baryons. This basis provides an explanation for the shape of the graph of the pre-LHC proton-proton cross section data. These data also enable a description of the significance of the expected LHC cross section measurements which will be known soon. Problematic QCD issues are pointed out.

## 1 Introduction

Scattering experiments are used as a primary tool for investigating the structure of physical objects. These experiments can be divided into several classes, depending on the kind of colliding particles. The energy involved in scattering experiments has increased dramatically during the previous century since the celebrated Rutherford experiment was carried out (1909). Now, the meaningful value of scattering energy is the quantity measured in the rest frame of the projectile-target center of energy. Therefore, devices that use colliding beams enable measurements of very high energy processes. The new Large Hadron Collider (LHC) facility at CERN, which is designed to produce 14 TeV proton-proton ( $pp$ ) collisions, will make a great leap forward.

This work examines the presently available  $pp$  elastic and total cross section data (denoted by ECS and TCS, respectively) and discusses the meaning of two possible alternatives for the LHC  $pp$  ECS values which will be known soon. The discussion relies on the Regular Charge-Monopole Theory (RCMT) [1,2] and its relevance to strong interactions [3,4].

Section 2 contains a continuation of the discussion presented in [4]. It explains the meaning of two possible LHC results of the  $pp$  ECS. Inherent QCD difficulties to provide an explanation for the data are discussed in section 3. The last section contains concluding remarks.

## 2 The proton-proton elastic cross section

The discussion carried out below is a continuation of [4]. Here it aims to examine possible LHC's ECS results and their implications for the proton structure. Thus, for the reader's convenience, the relevant points of [4] are presented briefly in the following lines.

RCMT is the theoretical basis of the discussion and strong interactions are regarded as interactions between magnetic monopoles which obey the laws derived from RCMT. Two important results of RCMT are described here:

1. Charges do not interact with bound fields of monopoles and monopoles do not interact with bound fields of charges. Charges interact with all fields of charges and

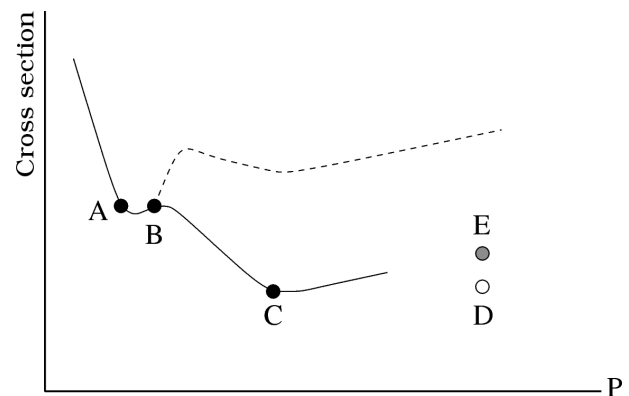


Fig. 1: A qualitative description of the pre-LHC proton-proton cross section versus the laboratory momentum  $P$ . Axes are drawn in a logarithmic scale. The solid line denotes elastic cross section and the broken line denotes total cross section. (The accurate figure can be found in [5]). Points A-E help the discussion (see text).

with radiation fields emitted from monopoles. Analogously, monopoles interact with all fields of monopoles and with radiation fields emitted from charges.

2. The unit of the elementary magnetic charge  $g$  is a free parameter. However, hadronic data indicate that this unit is much larger than that of the electric charge:  $g^2 \gg e^2 \approx 1/137$ . (Probably  $g^2 \approx 1$ .)

The application of RCMT to strong interactions regards quarks as spin-1/2 Dirac particles that carry a unit of magnetic monopole. A proton has three valence quarks and a core that carries three monopole units of the opposite sign. Thus, a proton is a magnetic monopole analogue of a nonionized atom. By virtue of the first RCMT result, one understands why electrons (namely, pure charges) do not participate in strong interactions whereas photons do that [6]. Referring to the pre-LHC data, it is shown in [4] that, beside the three valence quarks, a proton has a core that contains inner closed shells of quarks.

Applying the correspondence between a nonionized atom and a proton, one infers the validity of screening effects and of an analogue of the Franck-Hertz effect that takes place for the

proton's quarks. Thus, quarks of closed shells of the proton's core behave like inert objects for cases where the projectile's energy is smaller than the appropriate threshold.

The pre-LHC  $pp$  scattering data is depicted in Fig. 1. Let  $ep$  denote both electron-proton and positron-proton interaction. Comparing the  $ep$  scattering data with those of  $pp$ , one finds a dramatic difference between both the ECS and the TCS characteristics of these experiments. Thus, the deep inelastic and the Rosenbluth  $ep$  formulas respectively show that TCS *decreases* together with an increase of the collision energy and that at the high energy region, ECS decreases even faster and takes a negligible part of the entire TCS events (see [7], p. 266). The  $pp$  data of Fig. 1 show a completely different picture. Indeed, for high energy, both the TCS and the ECS  $pp$  graphs *go up* with collision energy and ECS takes about 15% of the total events.

The last property proves that a proton contains a quite solid component that can take the heavy blow of a high energy  $pp$  collision and leave each of the two colliding protons intact. Valence quarks certainly cannot do this, because in the case of a high energy  $ep$  scattering, an electron collides with a valence quark. Now, in this case, deep inelastic scattering dominates and elastic events are very rare. The fact that the quite solid component is undetected in an  $ep$  scattering experiment, proves that it is a spinless electrically neutral component. This outcome provides a very strong support for the RCMT interpretation of hadrons, where baryons have a core [3,4].

The foregoing points enable one to interpret the shape of the  $pp$  ECS graph of Fig. 1. Thus, for energies smaller than that of point A of the figure, the wave length is long and effects of large distance between the colliding protons dominate the process. Here the ordinary Coulomb potential,  $1/r$ , holds and the associated  $1/p^2$  decrease of the graph is in accordance with the Rutherford and Mott formulas (see [7], p. 192)

$$\left(\frac{d\sigma}{d\Omega}\right)_{\text{Mott}} = \frac{\alpha^2 \cos^2\left(\frac{\theta}{2}\right)}{4p^2 \sin^4\left(\frac{\theta}{2}\right) \left[1 + \frac{2p}{M} \sin^2\left(\frac{\theta}{2}\right)\right]}. \quad (1)$$

At the region of points A-B, the rapidly varying nuclear force makes the undulating shape of the graph. Results of screening effects of the valence quarks are seen for momentum values belonging to the region of points B-C. Indeed, a correspondence holds for electrons in an atom and quarks (that carry a monopole unit) in a proton. Hence, for a core-core interaction, the screening associated with the valence quarks weakens as the distance from the proton's center becomes smaller. It means that the strength of the core's monopole potential arises faster than the Coulomb  $1/r$  formula. For this reason, the decreasing slope of the graph between points B-C is smaller than that which is seen on the left hand side of point A.

The ECS graph stops decreasing and begins to increase on the right hand side of point C. This change of the graph's

slope indicates that for this energy a new effect shows up. Indeed, assume that the proton consists of just valence quarks and an elementary pointlike core which is charged with three monopole units of the opposite sign. Then, as the energy increases and the wave length decreases, the contribution of the inner proton region becomes more significant. Now, at inner regions, the valence quarks' screening effect fades away and the potential tends to the Coulomb formula  $1/r$ . Hence, in this case, the steepness of the decreasing graph between points B-C *should increase* near point C and tend to the Coulomb-like steepness of the graph on the left hand side of point A. The data negate this expectation. Thus, the increase of the graph on the right hand side of point C indicates the existence of inner closed shells of quarks at the proton. It is concluded that at these shells, a new screening effect becomes effective.

It is interesting to note that at the same momentum region also the TCS graph begins to increase and that on the right hand side of point C, the vertical distance between the two graphs is uniform. The logarithmic scale of the figure proves that, at this region, the ratio ECS to TCS practically does not change. The additional TCS events are related to an analogue of the Franck-Hertz effect. Here a quark of the closed shells is struck out of its shell. This effect corresponds to the  $ep$  deep inelastic process and it is likely to produce an inelastic event.

The main problem to be discussed here is *the specific structure of the proton's closed shells of quarks*. One may expect that the situation takes the simplest case and that the core's closed shells consist of just two  $u$  quarks and two  $d$  quarks that occupy an S shell. The other extreme is the case where the proton is analogous to a very heavy atom and the proton's core contains many closed shells of quarks. Thus, the energy of the higher group of the core's shells takes quite similar value and their radial wave functions partially overlap. (Below, finding the actual structure of the proton's core is called Problem A.) The presently known  $pp$  ECS data which is depicted in Fig. 1 is used for describing the relevance of the LHC future data to Problem A.

The rise of the  $pp$  ECS graph on the right hand side of point C is related to a screening effect of the proton's inner closed shells that takes a repulsive form. An additional contribution is the repulsive phenomenological force that stems from Pauli's exclusion principle which holds for quarks of the inner shells of the two colliding protons. Now, if the simplest case which is described above holds then, for higher energies, this effect should diminish and the graph is expected to stop rising and pass near the open circle of Fig. 1, which is marked by the letter D. On the other hand, if the proton's core contains several closed shells having a similar energy and a similar radial distribution, then before the screening contribution of the uppermost closed shell fades away another shell is expected to enter the dynamics. In this case, the graph is expected to continue rising up to the full LHC energy and pass near the gray circle of Fig. 1, which is marked by the letter E [8].

The foregoing discussion shows one example explaining how the LHC data will improve our understanding of the proton's structure.

### 3 Inherent QCD difficulties

Claims stating that QCD is unable to provide an explanation for the  $pp$  cross section data have been published in the last decade [9]. Few specific reasons justifying these claims are listed below. The examples rely on QCD's main property where baryons consist of three valence quarks, gluons and possible pairs of quark-antiquark:

- Deep inelastic  $ep$  scattering proves that for a very high energy, elastic events are very rare (see [7], p. 266). It means that an inelastic event is found for nearly every case where a quark is struck violently by an electron. On the other hand, Fig. 1 proves that for high energy, elastic  $pp$  events take about 15% of the total events. Therefore, one wonders what is the proton's component that takes the heavy blow of a high energy  $pp$  collision and is able to leave the two colliding protons intact? Moreover, why this component is not observed in the corresponding  $ep$  scattering?
- A QCD property called Asymptotic Freedom (see [10], p. 397) states that the interaction strength tends to zero at a very small vicinity of a QCD particle. Thus, at this region, a QCD interaction is certainly much weaker than the corresponding Coulomb-like interaction. Now, the general expression for the elastic scattering amplitude is (see [7], p. 186)

$$M_{if} = \int \psi_f^* V \psi_i d^3x, \quad (2)$$

where  $V$  represents the interaction. Evidently, for very high energy, the contribution of a very short distance between the colliding particles dominates the process. Therefore, if asymptotic freedom holds then the  $pp$  ECS line is expected to show a *steeper decrease* than that of the Coulomb interaction, which is seen on the left hand side of point A of Fig. 1. The data of Fig. 1 proves that for an energy which is greater than that of point C of Fig. 1, the  $pp$  ECS line *increases*. Hence, the data completely contradict this QCD property.

- A general argument. At point C of Fig. 1, the ECS graph changes its inclination. Here it stops decreasing and begins to increase. This effect proves that for this energy value, *something new shows up in the proton*. Now, QCD states that quarks and gluons are elementary particles that move quite freely inside the proton's volume. Therefore, one wonders how can QCD explain why a new effect shows up for this energy?

Each of these specific points illustrates the general statement of [9], concerning QCD's failure to describe the high energy  $pp$  cross section data.

### 4 Concluding remarks

The following lines describe the logical structure of this work and thereby help the reader to evaluate its significance.

A construction of a physical theory must assume the validity of some properties of the physical world. For example, one can hardly imagine how can a person construct the Minkowski space with *three* spatial dimensions, if he is not allowed to use experimental data. Referring to the validity of a physical theory, it is well known that unlike a mathematical theory which is evaluated just by pure logics, a physical theory must also be consistent with well established experimental data that belong to its domain of validity. The Occam's razor principle examines another aspect of a theory and prefers a theory that relies on a minimal number of assumptions. Thus, the Occam's razor can be regarded as a "soft" acceptability criterion for a theory.

Following these principles, the assumptions used for the construction of RCMT and of its application to strong interactions are described below. The first point has a theoretical character and the rest rely on experimental results that serve as a clue for understanding the specific structure of baryons:

- A classical regular charge-monopole theory is built on the basis of duality relations which hold between ordinary Maxwellian theory of charges together with their fields and a monopole system together with its associated fields [2]. (In [1], it is also required that the theory be derived from a regular Lagrangian density.) Like ordinary electrodynamics, this theory is derived from the variational principle where regular expressions are used. Therefore, the route to quantum mechanics is straightforward.
- In RCMT, the value of the elementary monopole unit  $g$  is a free parameter. Like the case of the electric charge, it is assumed that  $g$  is quantized. It is also assumed that its elementary value  $g^2 \gg e^2 \approx 1/137$ . (Probably,  $g^2 \approx 1$ .)
- It is assumed that strong interactions are interactions between monopoles. The following points describe the specific systems that carry monopoles.
- It is assumed that quarks are spin 1/2 Dirac particles that carry a unit of magnetic monopole. (As a matter of fact, it can be *proved* that an elementary massive quantum mechanical particle is a spin-1/2 Dirac particle [11].)
- It is assumed that baryons contain *three* valence quarks. It follows that baryons must have a core that carries three monopole units of the opposite sign.
- It is assumed that the baryonic core contains closed shells of quarks.

The discussion carried out in [4] and in section 2 of this work explains how RCMT can be used for providing a qualitative interpretation of the shape of the graph that describes

the elastic  $pp$  scattering data. In particular, an explanation is provided for the relation between the pre-LHC  $pp$  elastic cross section data and the existence of closed shells of quarks at the baryonic core. It is also explained how the upcoming LHC data will enrich our understanding of the structure of baryonic closed shells of quarks by providing information on whether there are just two active closed shells of  $u$  and  $d$  quarks or there are many shells having a quite similar energy value and radial distribution.

QCD's inherent difficulties to provide an explanation for the high energy pre-LHC  $pp$  scattering data are discussed in the third section. Screening effects of proton's quarks are used in the Regular Charge-monopole Theory's interpretation of the elastic cross section  $pp$  scattering. It is interesting to note that this kind of screening also provides an automatic explanation for the first EMC effect [12]. This effect compares the quarks' Fermi motion in deuteron and iron (as well as other heavy nuclei). The data show that the Fermi motion is smaller in heavier nuclei. This experimental data and the Heisenberg uncertainty relations prove that the quarks' self-volume increases in heavier nuclei. In spite of the quite long time elapsed, QCD supporters have not yet provided an adequate explanation for the first EMC effect [13].

Submitted on January 23, 2010 / Accepted on February 09, 2010

## References

1. Comay E. Axiomatic deduction of equations of motion in Classical Electrodynamics. *Nuovo Cimento B*, 1984, v. 80, 159–168.
2. Comay E. Charges, monopoles and duality relations. *Nuovo Cimento B*, 1995, v. 110, 1347–1356.
3. Comay E. A regular theory of magnetic monopoles and its implications. In: *Has the Last Word Been Said on Classical Electrodynamics?* ed. A. Chubykalo, V. Onochin, A. Espinoza and R. Smirnov-Rueda. Rinton Press, Paramus, NJ, 2004.
4. Comay E. Remarks on the proton structure. *Apeiron*, 2009, v. 16, 1–21.
5. Amsler C. et al. (Particle Data Group) Review of particle properties. *Phys. Lett. B*, 2008, v. 667, 1–1340. (See p. 364).
6. Bauer T. H., Spital R. D., Yennie D. R. and Pipkin F. M. The hadronic properties of the photon in high-energy interactions. *Rev. Mod. Phys.*, 1978, v. 50, 261–436.
7. Perkins D. H. Introduction to high energy physics. Addison-Wesley, Menlo Park, CA, 1987.
8. This possibility has been overlooked in [4].
9. Arkhipov A. A. On global structure of hadronic total cross-sections. arXiv: hep-ph/9911533.
10. Frauenfelder H. and Henley E. M. Subatomic physics. Prentice Hall, Englewood Cliffs, 1991. (see pp. 296–304.)
11. Comay E. Physical consequences of mathematical principles. *Progress in Physics*, 2009, v. 4, 91–98.
12. Arrington J. et al. New measurements of the EMC effect in few-body nuclei. *J. Phys. Conference Series*, 2007, v. 69, 012024, 1–9.

# The Intensity of the Light Diffraction by Supersonic Longitudinal Waves in Solid

Vahan Minasyan and Valentin Samoïlov

Scientific Center of Applied Research, JINR, Dubna, 141980, Russia

E-mails: mvahan@scar.jinr.ru; scar@off-serv.jinr.ru

First, we predict existence of transverse electromagnetic field created by supersonic longitudinal waves in solid. This electromagnetic wave with frequency of ultrasonic field is moved by velocity of supersonic field toward of direction propagation of one. The average Poynting vector of superposition field is calculated by presence of the transverse electromagnetic and the optical fields which in turn provides appearance the diffraction of light.

## 1 Introduction

In 1921 Brillouin have predicted that supersonic wave in ideal liquid acts as diffraction gratings for optical light [1]. His result justify were confirmed by Debay and Sears [2]. Further, Schaefer and Bergmann had shown that supersonic waves in crystal leads to light diffraction [3]. The description of latter experiment is that the diffraction pattern is formed by passing a monochromatic light beam through solid perpendicular to direction of ultrasonic wave propagation. Furthermore, the out-coming light is directed on diffraction pattern. As results of these experiment, a diffraction maximums of light intensity represent as a sources of light with own intensities. Each intensity of light source depends on the amplitude of acoustical power because at certain value of power ultrasound wave there is vanishing of certain diffraction maxima. Other important result is that the intensity of the first positive diffraction maximum is not equal to the intensity of the first negative minimum, due to distortion of the waveform in crystals by the departures from Hooke's law as suggested [4]. For theoretical explanation of experimental results, connected with interaction ultrasonic and optical waves in isotropy homogeneous medium, were used of so called the Raman-Nath theory [5] and theory of photo-elastic linear effect [6] which were based on a concept that acoustic wave generates a periodical distribution of refractive index in the coordinate-time space. For improving of the theory photo-elastic effect, the theories were proposed by Fues and Ludloff [7], Mueller [8] as well as Melngailis, Maradudin and Seeger [9]. In this letter, we predict existence of transverse electromagnetic radiation due to strains created by supersonic longitudinal waves in solid. The presence of this electromagnetic field together with optical one provides appearance of superposition wave which forms diffracted light with it's maxima.

## 2 Creation of an electromagnetic field

A model of solid is considered as lattice of ions and gas of free electrons. Each ion coupled with a point of lattice knot by spring, creating of ion dipole. The knots of lattice define a position equilibrium of each ion which is vibrated by own frequency  $\Omega_0$ .

The electron with negative charge  $-e$  and ion with positive charge  $e$  are linked by a spring which in turn defines the frequency  $\omega_0$  of electron oscillation in the electron-ion dipole. Obviously, such dipoles are discussed within elementary dispersion theory [10]. Hence, we suggest that property of springs of ion dipole and ion-electron one is the same.

Now we attempt to investigate an acoustic property of solid. By under action of longitudinal acoustic wave which is excited into solid, there is an appearance of vector displacement  $\vec{u}$  of each ions.

Consider the propagation of an ultrasonic plane traveling wave in cubic crystal. Due to laws of elastic field for solid [11], the vector displacement  $\vec{u}$  satisfies to condition which defines a longitudinal supersonic field

$$\text{curl } \vec{u} = 0 \quad (1)$$

and is defined by wave-equation

$$\nabla^2 \vec{u} - \frac{1}{c_l^2} \frac{d^2 \vec{u}}{dt^2} = 0, \quad (2)$$

where  $c_l$  is the velocity of a longitudinal ultrasonic wave which is determined by elastic coefficients.

The simple solution of (2) in respect to  $\vec{u}$  has a following form

$$\vec{u} = \vec{u}_0 \vec{e}_x \sin(Kx + \Omega t), \quad (3)$$

where  $u_0$  is the amplitude of vector displacement;  $\vec{e}_x$  is the unit vector determining the direction of axis OX in the coordinate system XYZ.

The appearance of the vector displacement for ions implies that each ion acquires the dipole moment  $\vec{p} = e\vec{u}$  in of ion dipole. Consequently, we may argue that there is a presence of the electromagnetic field which may find by using of a moving equation for ion in the ion dipole

$$M \frac{d^2 \vec{u}}{dt^2} + q\vec{u} = e\vec{E}_l, \quad (4)$$

where  $\vec{E}_l$  is the vector electric field which is induced by longitudinal ultrasonic wave;  $M$  is the mass of ion; the second term  $q\vec{u}$  in left part represents as changing of quasi-elastic force which acts on ion in ion dipole, in this respect

$\Omega_0 = \sqrt{\frac{q}{M}} = \omega_0 \sqrt{\frac{m}{M}}$  which is the resonance frequency or own frequency of ion determined via a resonance frequency  $\omega_0$  of electron into electron-ion dipole [10].

Using of the operation *rot* of the both part of (4) together with (1), we obtain a condition for longitudinal electromagnetic wave

$$\text{curl } \vec{E}_l = 0. \tag{5}$$

Now, substituting solution  $\vec{u}$  from (3) in (4), we find the vector longitudinal electric field of longitudinal electromagnetic wave

$$\vec{E}_l = E_{0,l} \vec{e}_x \sin(Kx + \Omega t), \tag{6}$$

where

$$E_{0,l} = \frac{M(\Omega_0^2 - \Omega^2)u_0}{e} \tag{7}$$

is the amplitude of longitudinal electric field.

On other hand, the ion dipole acquires a polarizability  $\alpha$ , which is determined by following form

$$\vec{p} = \alpha \vec{E}_l = \frac{M(\Omega_0^2 - \Omega^2) \alpha \vec{u}}{e}. \tag{8}$$

The latter is compared with  $\vec{p} = e\vec{u}$ , and then, we find a polarizability  $\alpha$  for ion dipole as it was made in the case of electron-ion one presented in [10]

$$\alpha = \frac{e^2}{M(\Omega_0^2 - \Omega^2)}. \tag{9}$$

Thus, the dielectric respond  $\varepsilon$  of ion medium takes a following form

$$\varepsilon = 1 + 4\pi N_0 \alpha = 1 + \frac{4\pi N_0 e^2}{M(\Omega_0^2 - \Omega^2)}, \tag{10}$$

where  $N_0$  is the concentration of ions.

The dielectric respond  $\varepsilon$  of acoustic medium likes to optical one, therefore,

$$\sqrt{\varepsilon} = \frac{c}{c_l}, \tag{11}$$

where  $c$  is the velocity of electromagnetic wave in vacuum.

We note herein that a longitudinal electric wave with frequency  $\Omega$  is propagated by velocity  $c_l$  of ultrasonic wave in the direction OX. In the presented theory, the vector electric induction  $\vec{D}_l$  is determined as

$$\vec{D}_l = 4\pi \vec{P}_l + \vec{E}_l, \tag{12}$$

and

$$\vec{D}_l = \varepsilon \vec{E}_l, \tag{13}$$

where  $\vec{P}_l = N_0 \vec{p}$  is the total polarization created by ion dipoles in acoustic medium.

Furthermore, the Maxwell equations for electromagnetic field in acoustic medium with a magnetic penetration  $\mu = 1$  take following form

$$\text{curl } \vec{E} + \frac{1}{c} \frac{d\vec{H}}{dt} = 0, \tag{14}$$

$$\text{curl } \vec{H} - \frac{1}{c} \frac{d\vec{D}}{dt} = 0, \tag{15}$$

$$\text{div } \vec{H} = 0, \tag{16}$$

$$\text{div } \vec{D} = 0 \tag{17}$$

with

$$\vec{D} = \varepsilon \vec{E}, \tag{18}$$

where  $\vec{E} = \vec{E}(\vec{r}, t)$  and  $\vec{H} = \vec{H}(\vec{r}, t)$  is the vectors of local electric and magnetic fields in acoustic medium;  $\vec{D} = \vec{D}(\vec{r}, t)$  is the local electric induction in the coordinate-time space;  $\vec{r}$  is the coordinate;  $t$  is the current time in space-time coordinate system.

As we see in above, due to action of ultrasonic wave on the solid there is changed a polarization of ion dipole by creation electric field  $\vec{E}_l$  and electric induction  $\vec{D}_l$ . Therefore, we search a solution of Maxwell equations by introducing the vector electric field by following form

$$\vec{E} = \vec{E}_t + \vec{E}_l - \text{grad } \phi \tag{19}$$

and

$$\vec{H} = \text{curl } \vec{A}, \tag{20}$$

where

$$\vec{E}_t = -\frac{d\vec{A}}{cdt}, \tag{21}$$

where  $\phi$  and  $\vec{A}$  are, respectively, the scalar and vector potential of electromagnetic wave.

As result, the solution of Maxwell equations leads to following expression

$$\text{grad } \phi = \vec{E}_l. \tag{22}$$

In turn, using of (6) we find a scalar potential

$$\phi = \phi_0 \cos(Kx + \Omega t), \tag{23}$$

where  $\phi_0 = -\frac{E_{0,l}}{K}$ .

As we see the gradient of scalar potential  $\text{grad } \phi$  of electromagnetic wave neutralizes the longitudinal electric field  $\vec{E}_l$ .

After simple calculation, we obtain a following equations for vector potential  $\vec{A}$  of transverse electromagnetic field

$$\nabla^2 \vec{A} - \frac{\varepsilon}{c^2} \frac{d^2 \vec{A}}{dt^2} = 0 \tag{24}$$

with condition of plane transverse wave

$$\text{div } \vec{A} = 0. \tag{25}$$

The solution of (24) and (25) may present by plane transverse wave with frequency  $\Omega$  which is moved by velocity  $c_l$  along of direction of unit vector  $\vec{s}$

$$\vec{A} = \vec{A}_0 \sin(K\vec{s}\vec{r} + \Omega t) \tag{26}$$

and

$$\vec{A} \cdot \vec{s} = 0, \tag{27}$$

where  $K = \frac{\Omega\sqrt{\varepsilon}}{c}$  is the wave number of transverse electromagnetic wave;  $\vec{s}$  is the unit vector in direction of wave normal;  $\vec{A}_0$  is the vector amplitude of vector potential. In turn, the vector electric transverse wave  $\vec{E}_t$  takes a following form

$$\vec{E}_t = \vec{E}_0 \cos(K\vec{s}\vec{r} + \Omega t), \quad (28)$$

where the vector amplitude  $\vec{E}_0$  of vector electric wave equals to

$$\vec{E}_0 = -\frac{\Omega\vec{A}_0}{c}.$$

Consequently, we found a transverse electromagnetic radiation which is induced by longitudinal ultrasonic wave. To find the vector amplitude  $\vec{E}_0$ , we using of the law conservation energy. In turn, the energy  $W_a$  of ultrasonic wave is transformed by energy  $W_t$  of transverse electromagnetic radiation, namely, there is a condition  $W_a = W_t$  because there is absence the longitudinal electric field  $\vec{E}_l$  which was neutralized by the gradient of scalar potential  $\text{grad } \phi$  of electromagnetic wave as it was shown in above

$$W_a = \frac{M}{2} \left[ \left( \frac{d\vec{u}}{dt} \right)^2 + \frac{1}{c_l^2} \left( \frac{d\vec{u}}{dx} \right)^2 \right] = M \Omega^2 u_0^2 \cos^2(Kx + \Omega t), \quad (29)$$

$$W_t = \frac{\varepsilon}{4\pi} E_0^2 \cos^2(K\vec{s}\vec{r} + \Omega t). \quad (30)$$

At comparing of (29) and (30), we may argue that vector of wave normal  $\vec{s}$  is directed along of axis OX or  $\vec{s} = \vec{e}_x$ , and then, we arrive to finally form of

$$\vec{E}_t = \vec{E}_0 \cos(Kx + \Omega t) \quad (31)$$

with condition

$$\frac{\varepsilon}{4\pi} E_0^2 = M \Omega^2 u_0^2. \quad (32)$$

Obviously, the law conservation energy plays an important role for determination of the transverse traveling plane wave.

### 3 Diffraction of light

First step, we consider an incident optical light into solid which is directed along of axis OZ in the coordinate space XYZ with electric vector  $\vec{E}_e$

$$\vec{E}_e = \vec{E}_{0,e} \cos(kz + \omega t), \quad (33)$$

where  $k = \frac{\omega\sqrt{\varepsilon_0}}{c}$  is the wave number;  $\omega$  is the frequency of light;  $\varepsilon_0$  is the dielectric respond of optical medium created by electron dipoles [10]

$$\frac{\varepsilon_0 - 1}{\varepsilon_0 + 2} = \frac{4\pi N_0 e^2}{3m(\omega_0^2 - \omega^2)}, \quad (34)$$

where  $\omega_0$  is the own frequency of electron in electron-ion dipole;  $m$  is the mass of electron.

The interaction of ultrasonic waves with incident optical light in a crystal involves the relation between intensity of out coming light from solid and the strain created by ultrasonic wave.

Consequently, the superposition vector electric  $\vec{E}_s$  field in acoustic-optical medium is determined by sum of vectors of electric transverse  $\vec{E}_t$  and optical  $\vec{E}_e$  waves

$$\vec{E}_s = \vec{E}_0 \cos(Kx + \Omega t) + \vec{E}_{0,e} \cos(kz + \omega t). \quad (35)$$

The average Poynting vector of superposition field  $\langle \vec{S} \rangle$  in acoustic-optical medium is expressed via the average Poynting vectors of  $\langle \vec{S}_e \rangle$  and  $\langle \vec{S}_t \rangle$  corresponding to the optical and the transverse electromagnetic waves

$$\langle \vec{S} \rangle = \frac{c}{\sqrt{\varepsilon_0}} w_e \vec{e}_z + \frac{c}{\sqrt{\varepsilon}} w_t \vec{e}_x, \quad (36)$$

where  $w_e$  and  $w_t$  are, respectively, the average density energies of the optical and the transverse electromagnetic waves

$$w_e = \frac{\varepsilon_0 E_{0,e}^2}{4\pi} \cdot \lim_{T \rightarrow \infty} \frac{1}{2T} \int_{-T}^T \cos^2(kz + \omega t) dt = \frac{\varepsilon_0 E_{0,e}^2}{8\pi} \quad (37)$$

and

$$w_t = \frac{\varepsilon E_0^2}{4\pi} \cdot \lim_{T \rightarrow \infty} \frac{1}{2T} \int_{-T}^T \cos^2(Kx + \Omega t) dt = \frac{M \Omega^2 u_0^2}{2} \quad (38)$$

by using of condition (32).

Thus, the average Poynting vector of superposition field  $\langle \vec{S} \rangle$  is presented via intensities of the optical  $I_e$  and the transverse electromagnetic wave  $I_t$

$$\langle \vec{S} \rangle = I_e \vec{e}_z + I_t \vec{e}_x, \quad (39)$$

where

$$I_e = \frac{E_{0,e}^2 c \sqrt{\varepsilon_0}}{8\pi} \quad (40)$$

and

$$I_t = \frac{M \Omega^2 u_0^2 c_l}{2}. \quad (41)$$

This result shows that the intensity of transverse electromagnetic wave  $I_t$  represents as amplitude of acoustic field.

Obviously, we may rewrite down (39) by complex form within theory function of the complex variables

$$\langle \vec{S} \rangle = I_e + iI_t = \sqrt{I_e^2 + I_t^2} \exp(i\theta), \quad (42)$$

where  $\theta$  is the angle propagation of observation light in the coordinate system XYZ in regard to OZ

$$\theta = \text{arccctg} \left( \frac{I_e}{I_t} \right), \quad (43)$$

which is chosen by the condition  $0 \leq \text{arccctg} \left( \frac{I_e}{I_t} \right) \leq \pi$ .

Using of identity

$$\exp(iz \cos \psi) = \sum_{m=-\infty}^{m=\infty} J_m(z) i^m \exp(im\psi), \quad (44)$$

where  $\psi = \arccos \theta$ .

The average Poynting vector of superposition field  $\langle \vec{S} \rangle$  is explicated on the spectrum of number  $m$  light sources with intensity  $I_m$

$$\langle \vec{S} \rangle = \sum_{m=-\infty}^{m=\infty} I_m, \quad (45)$$

where

$$I_m = \sqrt{I_t^2 + I_e^2} J_m \left( \text{arcctg} \left( \frac{I_e}{I_t} \right) \right) i^m \exp(im\psi), \quad (46)$$

but  $J_m(z)$  is the Bessel function of  $m$  order.

Thus, there is a diffraction of light by action of ultrasonic wave. In this respect, the central diffraction maximum point corresponds to  $m = 0$  with intensity  $I_{m=0}$

$$I_{m=0} = \sqrt{I_t^2 + I_e^2} J_0 \left( \text{arcctg} \left( \frac{I_e}{I_t} \right) \right). \quad (47)$$

In the case, when  $\text{arcctg} \frac{I_e}{I_t} = 2.4$  (at  $z = 2.4$ , the Bessel function equals zero  $J_0(z) = 0$ , that implies  $I_{m=0} = 0$ . In this respect, there is observed a vanishing of central diffraction maximum at certainly value of amplitude  $I_t$  acoustic field.

The main result of above-mentioned experiment [4,9] is that the intensity of the first positive diffraction maximum  $I_{m=1}$  is not equal to the intensity of the first negative minimum  $I_{m=-1}$ . Due to presented herein theory, the intensity of the first positive diffraction maximum is

$$I_{m=1} = i \sqrt{I_t^2 + I_e^2} J_1 \left( \text{arcctg} \left( \frac{I_e}{I_t} \right) \right) \exp(\psi), \quad (48)$$

but the intensity of the first negative diffraction maximum is

$$I_{m=-1} = -i \sqrt{I_t^2 + I_e^2} J_{-1} \left( \text{arcctg} \left( \frac{I_e}{I_t} \right) \right) \exp(-\psi). \quad (49)$$

It is easy to show that  $I_{m=1} \neq I_{m=-1}$ . Indeed, at comparing  $I_{m=1}$  and  $I_{m=-1}$ , we have

$$J_{-1} = -J_1$$

and

$$\exp(\psi) \neq \exp(-\psi),$$

which is fulfilled always because the there is a condition for observation angle  $\theta \neq \frac{\pi}{2}$ . Consequently, we proved that evidence  $I_{m=1} \neq I_{m=-1}$  confirms the experimental data.

Thus, as we have been seen the longitudinal ultrasonic wave induces the traveling transverse electromagnetic field which together with optical light provides an appearance diffraction of light.

Submitted on February 04, 2010 / Accepted on February 09, 2010

## References

1. Brillouin L. *Ann. de Physique*, 1921, v. 17, 102.
2. Debay P. and Sears F.W. Scattering of light by supersonic waves. *Proc. Nat. Acad. Sci. Wash.*, 1932, v. 18, 409.
3. Schaefer C. and Bergmann L. *Naturwiss.*, 1935, v. 23, 799.
4. Seeger A. and Buck O. Z. *Natureforsch.*, 1960, v. 15a, 1057.
5. Raman C.V., Nath N.S.N. *Proc. Indian. Acad. Sci.*, 1935, v. 2, 406.
6. Estermann R. and Wannier G. *Helv. Phys. Acta*, 1936, v. 9, 520; Pockels F. *Lehrbuch der Kristallographic*. Leipzig, 1906.
7. Fues E. and Ludloff H. *Sitzungsber. d. press. Akad. Math. phys. Kl.*, 1935, v. 14, 222.
8. Mueller M. *Physical Review*, 1937, v. 52, 223.
9. Melngailis J., Maradudin A.A., and Seeger A. *Physical Review*, 1963, v. 131, 1972.
10. Born M. and Wolf E. *Principles of optics*. Pergamon press, Oxford, 1964.
11. Landau L.D. and Lifshiz E.M. *Theory of elasticity*. (Course of Theoretical Physics, v. 11.) Moscow, 2003.

# Oscillations of the Chromatic States and Accelerated Expansion of the Universe

Gunn Quznetsov

Chelyabinsk State University, Chelyabinsk, Ural, Russia  
E-mail: gunn@mail.ru, quznets@yahoo.com

It is known (Quznetsov G. Higgsless Glashow's and quark-gluon theories and gravity without superstrings. *Progress in Physics*, 2009, v. 3, 32–40) that probabilities of point-like events are defined by some generalization of Dirac's equation. One part of such generalized equation corresponds to the Dirac's leptonic equation, and the other part corresponds to the Dirac's quark equation. The quark part of this equation is invariant under the oscillations of chromatic states. And it turns out that these oscillations bend space-time so that at large distances the space expands with acceleration according to Hubble's law.

## 1 Introduction

In 1998 observations of Type Ia supernovae suggested that the expansion of the universe is accelerating [1]. In the past few years, these observations have been corroborated by several independent sources [2]. This expansion is defined by the Hubble rule [3]

$$V(r) = Hr, \tag{1}$$

where  $V(r)$  is the velocity of expansion on the distance  $r$ ,  $H$  is the Hubble's constant ( $H \approx 2.3 \times 10^{-18} c^{-1}$  [4]).

It is known that Dirac's equation contains four anticommutative complex  $4 \times 4$  matrices. And this equation is not invariant under electroweak transformations. But it turns out that there is another such matrix anticommutative with all these four matrices. If additional mass term with this matrix will be added to Dirac's equation then the resulting equation shall be invariant under these transformations [5]. I call these five of anticommutative complex  $4 \times 4$  matrices *Clifford pentade*. There exist only six Clifford pentads [7, 8]. I call one of them the light pentad, three — the chromatic pentads, and two — the gustatory pentads.

The light pentad contains three matrices corresponding to the coordinates of 3-dimensional space, and two matrices relevant to mass terms — one for the lepton and one for the neutrino of this lepton.

Each chromatic pentad also contains three matrices corresponding to three coordinates and two mass matrices — one for top quark and another — for bottom quark.

Each gustatory pentad contains one coordinate matrix and two pairs of mass matrices [9] — these pentads are not needed yet.

It is proven [6] that probabilities of pointlike events are defined by some generalization of Dirac's equation with additional gauge members. This generalization is the sum of products of the coordinate matrices of the light pentad and covariant derivatives of the corresponding coordinates plus product of all the eight mass matrices (two of light and six of chromatic) and the corresponding mass numbers.

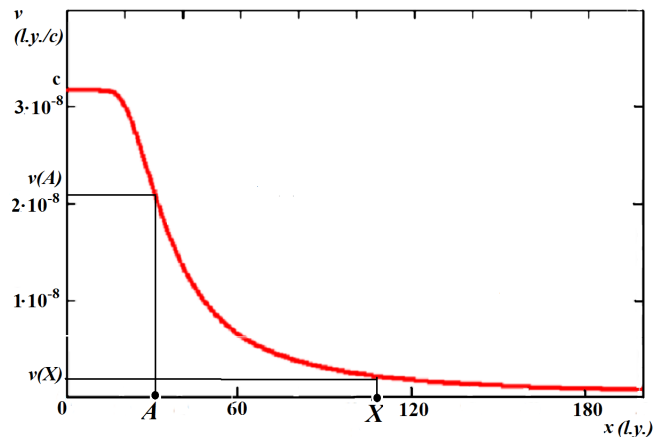


Fig. 1: Dependence of  $v(t, x)$  from  $x$  [8].

If lepton's and neutrino's mass terms are equal to zero in this equation then we obtain the Dirac's equation with gauge members similar to eight gluon's fields [8]. And oscillations of chromatic states of this equation bend space-time.

## 2 Chromatic oscillations and the Hubble's law

Some oscillations of chromatic states bend space-time as follows [8]

$$\left. \begin{aligned} \frac{\partial t}{\partial t'} &= \cosh 2\sigma \\ \frac{\partial x}{\partial t'} &= c \sinh 2\sigma \end{aligned} \right\}. \tag{2}$$

Hence, if  $v$  is the velocity of a coordinate system  $\{t', x'\}$  in the coordinate system  $\{t, x\}$  then

$$\sinh 2\sigma = \frac{\left(\frac{v}{c}\right)}{\sqrt{1 - \frac{v^2}{c^2}}}, \quad \cosh 2\sigma = \frac{1}{\sqrt{1 - \frac{v^2}{c^2}}}.$$

Therefore,

$$v = c \tanh 2\sigma. \tag{3}$$

Let

$$2\sigma := \omega(x) \frac{t}{x}$$

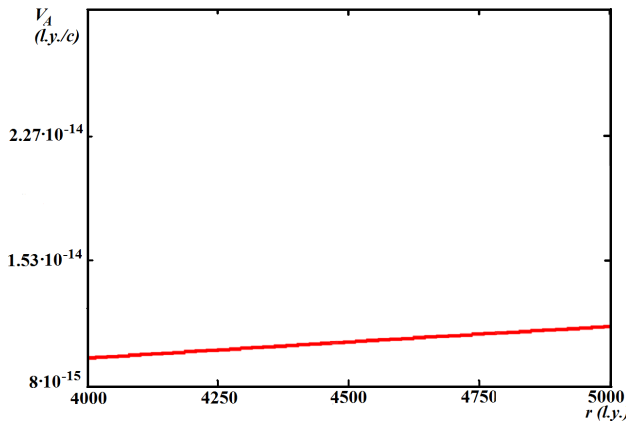


Fig. 2: Dependence of  $V_A(r)$  on  $r$  with  $x_A = 25 \times 10^3$  l.y.

with

$$\omega(x) = \frac{\lambda}{|x|},$$

where  $\lambda$  is a real constant with positive numerical value.

In that case

$$v(t, x) = c \tanh\left(\frac{\lambda t}{|x| x}\right). \quad (4)$$

Let a black hole be placed in a point  $O$ . Then a tremendous number of quarks oscillate in this point. These oscillations bend time-space and if  $t$  has some fixed volume,  $x > 0$ , and  $\Lambda := \lambda t$  then

$$v(x) = c \tanh\left(\frac{\Lambda}{x^2}\right). \quad (5)$$

A dependency of  $v(x)$  (light years/c) from  $x$  (light years) with  $\Lambda = 741.907$  is shown in Fig. 1.

Let a placed in a point  $A$  observer be stationary in the coordinate system  $\{t, x\}$ . Hence, in the coordinate system  $\{t', x'\}$  this observer is flying to the left to the point  $O$  with velocity  $-v(x_A)$ . And point  $X$  is flying to the left to the point  $O$  with velocity  $-v(x)$ .

Consequently, the observer  $A$  sees that the point  $X$  flies away from him to the right with velocity

$$V_A(x) = c \tanh\left(\frac{\Lambda}{x_A^2} - \frac{\Lambda}{x^2}\right) \quad (6)$$

in accordance with the relativistic rule of addition of velocities.

Let  $r := x - x_A$  (i.e.  $r$  is distance from  $A$  to  $X$ ), and

$$V_A(r) := c \tanh\left(\frac{\Lambda}{x_A^2} - \frac{\Lambda}{(x_A + r)^2}\right). \quad (7)$$

In that case Fig. 2 demonstrates the dependence of  $V_A(r)$  on  $r$  with  $x_A = 25 \times 10^3$  l.y.

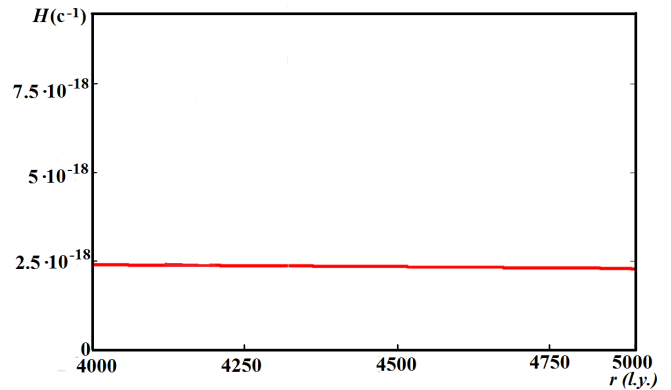


Fig. 3: Dependence of  $H$  on  $r$ .

Hence,  $X$  runs from  $A$  with almost constant acceleration

$$\frac{V_A(r)}{r} = H. \quad (8)$$

Fig. 3 demonstrates the dependence of  $H$  on  $r$  (the Hubble constant).

### 3 Conclusion

Therefore, the phenomenon of the accelerated expansion of Universe is explained by oscillations of chromatic states.

Submitted on February, 12, 2009 / Accepted on February 16, 2009

### References

1. Riess A. et al. *Astronomical Journal*, 1998, v. 116, 1009–1038.
2. Spergel D.N., et al. *The Astrophysical Journal Supplement Series*, 2003, September, v. 148, 175–194; Chaboyer B. and Krauss L.M. *Astrophys. J. Lett.*, 2002, v. 567, L45; Astier P., et al. *Astronomy and Astrophysics*, 2006, v. 447, 31–48; Wood-Vasey W.M., et al. *The Astrophysical Journal*, 2007, v. 666, no. 2, 694–715.
3. Coles P., ed. *Routledge critical dictionary of the new cosmology*. Routledge, 2001, 202.
4. Chandra confirms the Hubble constant. Retrieved on 2007-03-07. <http://www.universetoday.com/2006/08/08/chandra-confirms-the-hubble-constant/>
5. Quznetsov G. Probabilistic treatment of gauge theories. In series: *Contemporary Fundamental Physics*, ed. V.Dvoeglazov, Nova Sci. Publ., NY, 2007, 95–131.
6. Quznetsov G. Higgsless Glashow's and quark-gluon theories and gravity without superstrings. *Progress in Physics*, 2009, v. 3, 32–40.
7. Madelung E. *Die Mathematischen Hilfsmittel des Physikers*. Springer Verlag, 1957, 29.
8. Quznetsov G. 4x1-marix functions and Dirac's equation. *Progress in Physics*, v. 2, 2009, 96–106.
9. Quznetsov G. *Logical foundation of theoretical physics*. Nova Sci. Publ., NY, 2006, 143–144.

LETTERS TO  
PROGRESS IN PHYSICS

LETTERS TO PROGRESS IN PHYSICS**Smarandache Spaces as a New Extension of the Basic Space-Time of General Relativity**

Dmitri Rabounski

E-mail: rabounski@ptep-online.com

This short letter manifests how Smarandache geometries can be employed in order to extend the “classical” basis of the General Theory of Relativity (Riemannian geometry) through joining the properties of two or more (different) geometries in the same single space. Perspectives in this way seem much profitable: the basic space-time of General Relativity can be extended to not only metric geometries, but even to non-metric ones (where no distances can be measured), or to spaces of the mixed kind which possess the properties of both metric and non-metric spaces (the latter should be referred to as “semi-metric spaces”). If both metric and non-metric properties possessed at the same (at least one) point of a space, it is one of Smarandache geometries, and should be referred to as “Smarandache semi-metric space”. Such spaces can be introduced according to the mathematical apparatus of physically observable quantities (chronometric invariants), if we consider a breaking of the observable space metric in the continuous background of the fundamental metric tensor.

When I was first acquainted with Smarandache geometries many years ago, I immediately started applying them, in order to extend the basic geometry of Einstein’s General Theory of Relativity.

Naturally, once the General Theory of Relativity was established already in the 1910’s, Albert Einstein stated that Riemannian geometry, as advised to him by Marcel Grossmann, was not the peak of excellence. The main advantage of Riemannian geometry was the invariance of the space metric and also the well-developed mathematical apparatus which allowed Einstein to calculate numerous specific effects, unknown or unexplained before (now, they are known as the effects of General Relativity). Thus, Einstein concluded, the basic spacetime of General Relativity would necessarily be extended in the future, when new experiments would overcome all the possibilities provided by the geometry of Riemannian spaces. Many theoretical physicists and mathematicians tried to extend the basic space-time of General Relativity during the last century, commencing in the 1910’s. I do not survey all the results obtained by them (this would be impossible in so short a letter), but only note that they all tried to get another basic space, unnecessary Riemannian one, then see that effects manifest themselves in the new geometry. No one person (at least according to my information on this subject, perhaps incomplete) did consider the “mixed” geometries which could possess the properties of two or more (different in principle) geometries at the same point.

This is natural, because a theoretical physicist looks for a complete mathematical engine which could drive the applications to physical phenomena. What would have happened had there been no Bernhard Riemann, Erwin Christoffel, Tullio Levi-Civita, and the others; could Einstein have been enforced to develop Riemannian geometry in solitude

from scratch? I think this would have been a “dead duck” after all. Einstein followed a very correct way when he took the well-approved mathematical apparatus of Riemannian geometry. Thus, a theoretical physicist needs a solid mathematical ground for further theoretical developments. This is why some people, when trying to extend the basis of General Relativity, merely took another space instead the four-dimensional pseudo-Riemannian space initially used by Einstein.

Another gate is open due to Smarandache geometries, which can be derived from any of the known geometries by the condition that one (or numerous, or even all) of its axioms is both true and violated in the space. This gives a possibility to create a sort of “mixed” geometries possessing the properties of two or more geometries in one. Concerning the extensions of General Relativity, this means that we can not refuse the four-dimensional pseudo-Riemannian space in place of another single geometry, but we may create a geometry which is common to the basic one, as well as one or numerous other geometries in addition to it. As a simplest example, we can create a space possessing the properties of both the curved Riemannian and the flat Euclidean geometries. So forth, we can create a space, every point of which possesses the common properties of Riemannian geometry and another geometry which is non-Riemannian.

Even more, we can extend the space geometry in such a way that the space will be particularly metric and particularly non-metric. In the future, I suggest we should refer to such spaces as semi-metric spaces. Not all semi-metric spaces manifest particular cases of Smarandache geometries. For example, a space wherein each pair of points is segregated from the others by a pierced point, i.e. distances can be determined only within differential fragments of the space segregated by pierced points. This is undoubtedly a semi-metric space, but is

not a kind of Smarandache geometries. Contrarily, a space wherein at least one pair of points possesses both metric and non-metric properties at the same time is definitely that of Smarandache geometries. In the future, I suggest, we should refer to such spaces as *Smarandache semi-metric spaces*, or *ssm-spaces* in short.

Despite the seeming impossibility of joining metric and non-metric properties in “one package”, Smarandache semi-metric spaces can easily be introduced even by means of “classical” General Relativity. The following is just one example of how to do it. Regularly, theoretical physicists are aware of the cases where the signature conditions of the space are violated. They argue that, because the violations produce a breaking of the space, the cases have not a physical meaning in the real world and, hence, should not be considered. Thus, when considering a problem of General Relativity, most theoretical physicists artificially neglect, from consideration, those solutions leading to the violated signature conditions and, hence, to the breaking of the space. On the other hand, we could consider these problems by means of the mathematical apparatus of chronometric invariants, which are physically observable quantities in General Relativity. In this way, we have to consider the observable (chronometrically invariant) metric tensor on the background of the fundamental (general covariant) metric tensor of the space. The signature conditions of the metrics are determined by different physical requirements. So, in most cases, the violated signature conditions of the observable metric tensor, i.e. breaking of the observable space, can appear in the continuous background of the fundamental metric tensor (and vice versa). This is definitely a case of Smarandache geometries. If a distance (i.e. a metric, even if non-Riemannian) can be determined on the surface of the space breaking, this is a metric space of Smarandache geometry. I suggest we should refer to such spaces as *Smarandache metric spaces*. However, if the space breaking is incapable of determining a distance inside it, this is a Smarandache semi-metric space: the space possesses both metric and non-metric properties at all points of the surface of the space breaking.

A particular case of this tricky situation can be observed in Schwarzschild spaces. There are two kinds of these: a space filled with the spherically symmetric gravitational field produced by a mass-point (the center of gravity of a spherical solid body), and a space filled with the spherically symmetric gravitational field produced by a sphere of incompressible liquid. Both cases manifest the most apparent metrics in the Universe: obviously, almost all cosmic bodies can be approximated by either a sphere of solid or a sphere of liquid. Such a metric space has a breaking along the spherical surface of gravitational collapse, surrounding the center of the gravitating mass (a sphere of solid or liquid). This space breaking originates in the singularity of the fundamental metric tensor. In the case of regular cosmic bodies, the radius of the space breaking surface (known as the gravita-

tional radius, it is determined by the body’s mass) is many orders smaller than the radius of such a body itself: it is 3 km for the Sun, and only 0.9 cm for the Earth. Obviously, only an extremely dense cosmic body can completely be located under its gravitational radius, thus consisting a gravitational collapsar (black hole). Meanwhile, the space breaking at the gravitational radius really exists inside any continuous body, close to its center of gravity. Contrary, the space breaking due to the singularity of the observable metric tensor is far distant from the body; the sphere of the space breaking is huge, and is like a planetary orbit. Anyhow, in the subspace inside the Schwarzschild space breaking, distances can be determined between any two points (but they are not those of the Schwarzschild space distances). Thus, when considering a Schwarzschild space without any breaking, as most theoretical physicists do, it is merely a kind of the basic space-time of General Relativity. Contrarily, being a Schwarzschild space considered commonly with the space breaking in it, as a single space, it is a kind of Smarandache metric spaces — a *Schwarzschild-Smarandache metric space*, which generalizes the basic space-time of General Relativity. Moreover, one can consider such a space breaking that no distance (metric) can be determined inside it. In this case, the common space of the Schwarzschild metric and the non-metric space breaking in it is a kind of Smarandache semi-metric spaces — a *Schwarzschild-Smarandache semi-metric space*, and is an actual semi-metric extension of the basic space-time of General Relativity.

So, we see how Smarandache geometries (both metric and semi-metric ones) can be a very productive engine for further developments in the General Theory of Relativity. Because the Schwarzschild metrics lead to consideration of the state of gravitational collapse, we may suppose that not only regular gravitational collapsars can be considered (the surface of a regular black hole possesses metric properties), but even a much more exotic sort of collapsed objects — a collapsar whose surface cannot be presented with metric geometries. Because of the absence of metricity, the surface cannot be inhabited by particles (particles, a sort of discrete matter, imply the presence of coordinates). Only waves can exist there. These are standing waves: in the metric theory, time cannot be introduced on the surface of gravitational collapse due to the collapse condition  $g_{00} = 0$ ; the non-metric case manifests the state of collapse by the asymptotic conditions from each side of the surface, while time is not determined in the non-metric region of collapse as well. In other words, the non-metric surface of such a collapsar is filled with a system of standing waves, i.e. holograms. Thus, we should refer to such objects — the collapsars of a Schwarzschild-Smarandache semi-metric space — as *holographic black holes*. All these are in the very course of the paradoxist mathematics, whose motto is “impossible is possible”.

Submitted on February 12, 2010 / Accepted on February 18, 2010

*Progress in Physics* is an American scientific journal on advanced studies in physics, registered with the Library of Congress (DC, USA): ISSN 1555-5534 (print version) and ISSN 1555-5615 (online version). The journal is peer reviewed and listed in the abstracting and indexing coverage of: Mathematical Reviews of the AMS (USA), DOAJ of Lund University (Sweden), Zentralblatt MATH (Germany), Scientific Commons of the University of St. Gallen (Switzerland), Open-J-Gate (India), Referential Journal of VINITI (Russia), etc. *Progress in Physics* is an open-access journal published and distributed in accordance with the Budapest Open Initiative: this means that the electronic copies of both full-size version of the journal and the individual papers published therein will always be accessed for reading, download, and copying for any user free of charge. The journal is issued quarterly (four volumes per year).

Electronic version of this journal:  
<http://www.ptep-online.com>

**Editorial board:**

Dmitri Rabounski (Editor-in-Chief)  
Florentin Smarandache  
Larissa Borissova

**Postal address for correspondence:**

Department of Mathematics and Science  
University of New Mexico  
200 College Road, Gallup, NM 87301, USA

**Printed in the United States of America**

